

Dipl. Ing. Thomas Bergner

# Characterisation of two microbial flavin dependent monooxygenases

DISSERTATION

zur Erlangung der akademischen Grades  
Doktor der technischen Wissenschaften (Dr. *techn.*)

erreicht an der  
**Technischen Universität Graz**

Betreuer: Univ.-Prof. Mag. *rer nat.* Dr. *rer. nat.* Peter Macheroux  
Institut für Biochemie  
Technische Universität Graz

**Graz, 2014**

---

# Danksagung

Es ist noch gar nicht so lange her, dass ich das Projekt Dissertation in Angriff genommen habe und wie es so oft im Leben ist, verging die Zeit wie im Flug und das Ende meiner Zeit auf der Technischen Universität Graz ist in greifbare Nähe gerückt. Bevor es heißt, Abschied zu nehmen, möchte ich mich bei den Personen bedanke, die mich während dieser Zeit unterstützt, mir den nötigen Rückhalt und die benötigte Motivation gegeben haben.

Besonderer Dank gebührt meinem Betreuer Prof. Peter Macheroux für die Möglichkeit meine Arbeit in seiner Arbeitsgruppe an zwei so unterschiedlichen, wie auch interessanten Projekten durchzuführen. Während der gesamten Zeit konnte ich immer auf seine Unterstützung und seinen wissenschaftlichen Input bauen, ohne den die Projekte nie so weit vorangeschritten wären. Sehr zu schätzen weiß ich auch die Freiheiten, die mir im Rahmen der Projekte und der Erreichung der geforderten Ziele gewährt wurde.

Ich möchte mich auf diesen Weg auch bei der gesamten Arbeitsgruppe Macheroux für die schöne Zeit bedanken in der ich Teil dieser Gemeinschaft sein durfte. Insbesondere bei Tanja Knaus, Silvia Wallner und Rosemarie Trenker, mit denen ich mir ein Labor geteilt habe und die immer für mich da waren, egal wo der Schuh gedrückt hat.

Dank gebührt auch den von mir betreuten Master-, Bachelor- und Projektstudenten, durch deren tatkräftige Unterstützung und Aufopferung vieles innerhalb von kürzester Zeit erreichbar wurde, sowie jenen Personen, mit denen ich im Rahmen der Projekte zusammen gearbeitet habe, zu erwähnen wäre hier Jakov Ivkovic, Tea Pavkov-Keller und Michael Uhl.

An dieser Stelle möchte ich mich auch bei Chaitanya Tabib für die Zusammenarbeit und den Gedankenaustausch im Rahmen des Biolumineszenz-Projektes bedanken und ihm viel Erfolg bei der Fortsetzung der Arbeit wünschen.

Zu erwähnen wären auch die Mitglieder meines Thesis Committee, Prof. Rolf Breinbauer, Prof. Karl Gruber und Frau Prof. Ellen Zechner, die durch das Einbringen ihrer Fachkenntnis Wege eröffnet haben, die sonst sehr wahrscheinlich verborgen geblieben wären.

Zu guter Letzt möchte ich mich bei meinen Freunden und meiner Familie bedanken, die immer für mich da waren, mich unterstützt, motiviert und auch zum richtigen Zeitpunkt abgelenkt haben. Besonderer Dank gebührt hier meiner Mutter, durch deren Unterstützung es mir erst möglich war diesen Weg zu gehen und meiner kleinen Schwester, die es immer wieder geschafft hat ihren großen Bruder zu motivieren.

## Abstract

Flavin dependent monooxygenases are the largest subgroup of the known flavin dependent proteins. They catalyse chemo-, regio- and enantioselective reactions and play a key role in several biological processes, like metabolite biosynthesis, degradation of toxic compounds and defence mechanisms.

However, all reactions catalysed by this class of enzymes with molecular oxygen show the same overall reaction, *i.e.* the incorporation of one atom of molecular oxygen into the substrate, while the other one is reduced to water. To facilitate such a reaction, the molecular oxygen has to be activated. This is mediated by an enzyme catalysed reaction between reduced flavin and oxygen, leading to C(4a)-hydroperoxyflavin, which then facilitates the incorporation of one oxygen atom into the substrate. There are two different ways how C(4a)-hydroperoxyflavin can interact with the substrate either by a nucleophilic or an electrophilic attack, depending on its protonation state.

This work was initiated to get deeper insight into the characteristics of two different microbial flavin dependent monooxygenases, bacterial luciferase and anthranoyl-CoA monooxygenase/reductase (ACMR).

The main project focused on the luciferase from *Photobacterium leiognathi* (S1). This enzyme catalyses light emission. A part from the characterisation of the enzyme, I tackled the mystery revealing around the formation of 6-(3'-(*R*)-myristyl)-FMN (myrFMN), an unusual flavin derivative, solely found in marine bioluminescent bacteria. In some strains of the genera *Photobacteria* an additional gene could be found in the *lux*-operon, the dimeric protein encoded by this gene (LuxF), has four of this unusual flavin molecules bound. Due to the fact that myrFMN can be assembled by the products of the luciferase reaction, it is assumed that it is a side product of the luciferase reaction. To elucidate the formation of myrFMN, different bioluminescent bacteria were analysed regarding myrFMN content and a possible correlation between myrFMN production and light emission was deduced. Furthermore *in-vitro* assays were established to demonstrate the formation of myrFMN, thereby a new substrate for bacterial luciferase was found.

In a side project an enzyme involved in an unusual degradation pathway for aromatic compounds was characterised. Therefore the enzyme anthranoyl-CoA monooxygenase/reductase (ACMR) from *Azoarcus evansii* was recombinantly expressed, purified and characterised. In contrast to previous findings, the presence of both FMN and FAD could be demonstrated and the cofactors could be assigned to the subunits. Furthermore it was possible to demonstrate the presence of two different substrate binding pockets and their spatial interaction.

## Kurzfassung

Flavin enthaltende Monooxygenasen repräsentieren die größte Gruppe der bis jetzt bekannten Flavoproteine. Sie katalysieren chemo-, regio- und enantioselektive Reaktionen und spielen eine wichtige Rolle in vielen biologischen Prozessen, wie der Metabolitbiosynthese, dem Abbau schädlicher Substanzen und in Verteidigungsmechanismen.

Obwohl die von dieser Enzymklasse katalysierten Reaktionen sehr vielseitig sind, haben sie dennoch eine Gemeinsamkeit, den Einbau von einem Molekül Sauerstoff in ihr Substrat unter gleichzeitiger Bildung von Wasser. Um eine solche Reaktion überhaupt erst möglich zu machen, bedarf es der Aktivierung des Sauerstoffs. Im Fall der Flavin abhängigen Monooxygenasen, geschieht das durch die Bildung eines C(4a)-Hydroperoxyflavins, wobei ein reduziertes Flavin und Sauerstoff miteinander reagieren. Ausgehend vom C(4a)-Hydroperoxyflavin gibt es zwei mögliche Wege, wie der Einbau des Sauerstoffs ins Substrat erfolgen kann. Entweder durch einen nukleophilen oder elektrophilen Angriff, welcher der beiden Wege gewählt wird, hängt vom Protonierungsstatus ab.

Hauptziel dieser Arbeit war es, tiefere Einblicke in die Funktion zweier aus Mikroorganismen stammenden Flavin-abhängigen Monooxygenasen zu bekommen, zum Einen der bakteriellen Luciferase und zum Anderen der ACMR aus *Azoarcus Evansii*.

Das Hauptprojekt beschäftigte sich mit der Luciferase aus dem Organismus *Photobacterium leiognathi* S1. Dieses Enzym ist für die Entstehung von Licht in diesem Meeresbakterium verantwortlich. Neben der Charakterisierung dieses Enzymes, wurde versucht, Klarheit in die bis jetzt nicht bekannte Entstehung von 6-(3'-(*R*)-myristyl)-FMN (myrFMN) zu bringen. In manchen Stämmen der Gattung *Photobacterium* findet man ein zusätzliches Gen im *Lux*-Operon. Das kodierte dimere Protein (LuxF), hat vier Moleküle dieses untypischen Flavins gebunden. Aufgrund der Tatsache, dass myrFMN sich aus den Produkten der Luciferase-Reaktion zusammensetzen lässt, liegt die Vermutung nahe, dass es sich dabei um ein Nebenprodukt von dieser handelt. Um die Bildung von myrFMN zu verstehen, wurden verschiedene biolumineszente Bakterien hinsichtlich der Anwesenheit von myrFMN und einer möglichen Korrelation zwischen dem Gehalt an myrFMN und der Lichtemission untersucht. In *in-vitro* Versuchen die Bildung von myrFMN gezeigt werden, wobei dies nur durch die Entdeckung eines neuen Substrates der Luciferase möglich war.

Daneben wurde außerdem ein Enzym, das in einem für Aromaten untypischen Abbauweg involviert ist untersucht. Dafür wurde das Enzym, Anthranoyl-CoA Monooxygenase/reductase (ACMR) rekombinant hergestellt, gereinigt und charakterisiert. Dabei konnte die Anwesenheit von FMN und FAD im Enzym bestätigt, sowie deren Verteilung auf die einzelnen Untereinheiten bestimmt werden. Des Weiteren war es möglich die Anwesenheit zweier unterschiedlicher Substratbindungstaschen und deren räumliche Interaktionen zu bestätigen.

---

### **Eidesstattliche Erklärung**

Ich erkläre an Eides statt, dass ich die vorliegende Arbeit selbstständig verfasst, andere als die angegebenen Quellen / Hilfsmittel nicht benutzt, und die den benutzen Quellen wörtlich oder inhaltlich entnommenen Stellen als solche kenntlich gemacht habe. Das in TUGRAZonline hochgeladene Textdokument ist mit der vorliegenden Dissertation identisch.

### **Statutory Declaration**

I declare that I have authored this thesis independently, that I have not used other than the declared sources / resources, and that I have explicitly indicated all material which has been quoted either literally or by content from the used sources. The text document uploaded to TUGRAZonline is identical to the present doctoral dissertation.

Graz, am ..... ..

---

# Table of Contents

<b>Danksagung</b> .....	<b>II</b>
<b>Abstract</b> .....	<b>III</b>
<b>Kurzfassung</b> .....	<b>IV</b>
<b>Table of Contents</b> .....	<b>VI</b>
<b>Abbreviations</b> .....	<b>IX</b>
<b>1 Introduction into flavin dependent monooxygenases</b> .....	<b>1</b>
<b>Flavoproteins</b> .....	<b>2</b>
<b>Flavin dependent monooxygenases</b> .....	<b>4</b>
<b>Classification of flavin dependent monooxygenases</b> .....	<b>6</b>
Classification of flavin dependent monooxygenases into eight groups .....	6
Alternative classifications for flavin dependent monooxygenases .....	8
<b>Anthranoyl-CoA monooxygenase/reductase (ACMR), an enzyme with a group A monooxygenase domain</b> .....	<b>11</b>
Structural features of Anthranoyl-CoA monooxygenase/reductase.....	11
Reaction catalysed by ACMR.....	12
Reaction catalysed in the monooxygenase subunit.....	13
Reaction catalysed in the reductase subunit.....	14
<b>Bacterial luciferase a class C monooxygenase</b> .....	<b>15</b>
Bacterial Bioluminescence.....	15
The lux-operon .....	15
The luciferase (LuxAB) .....	20
<b>References</b> .....	<b>26</b>

---

**2.1 Bioluminescence / The bacterial luciferase..... 30**

<b>A luciferous surprise: a new natural aldehyde substrate in bacterial bioluminescence .....</b>	<b>31</b>
Abstract .....	32
Introduction.....	32
Experimental procedures .....	35
Results .....	37
Discussion .....	43
Conclusion.....	45
Outlook.....	45
References .....	46

**2.2 Bioluminescence / The mystery of myrFMN..... 48**

<b>Distribution of 6-(3'-(<i>R</i>)-myristyl)-FMN among bioluminescent marine bacteria and its binding properties to luciferase and LuxF .....</b>	<b>49</b>
Abstract .....	50
Introduction .....	50
Experimental procedures.....	52
Results .....	57
Discussion .....	67
References .....	69
Supplementary Figures.....	71

---

<b>3 Antranoyl-CoA monooxygenase/reductase.....</b>	<b>74</b>
<b>Anthranoyl-CoA monooxygenase/reductase from <i>Azoarcus evansii</i> possesses two distinct active sites .....</b>	<b>75</b>
Abstract .....	76
Introduction .....	76
Experimental Procedures.....	77
Results .....	81
Discussion .....	88
References .....	89
Supplementary Figures.....	91
Supplementary Tables .....	94
<b>Curriculum vitae.....</b>	<b>95</b>

## Abbreviations

AbCoA	Antranoyl-CoA
ACM	Monooxygenase subdomain of ACMR
ACMR	Antranoyl-CoA monooxygenase/reductase
ACR	Reductase subdomain of ACMR
BVMO	Baeyer-Villiger monooxygenase
CIEEL	Chemically initiated electron exchange luminescence
ITC	Isothermal titration calorimetry
$K_d$	Dissociation constant
$K_i$	Inhibition constant
$K_m$	Michaelis-Menten constant
MM	Molecular mass
myrFMN	6-(3'-( <i>R</i> )-myristyl)-FMN
pHB	<i>p</i> -hydroxybenzaldehyde
SAX	Small-angle X-ray scattering

---

# **CHAPTER 1**

## **1 Introduction into flavin dependent monooxygenases**

---

## Flavoproteins

Since the first flavin containing protein was discovered by Otto Wartburg in the 1930s<sup>1</sup>, the knowledge about this class of proteins has increased steadily. A possible reason therefore might be the biological relevance of these enzymes and their distribution among different organisms. Depending on the organism, the flavoprotein content varies between 0.1% and 3.5%<sup>2</sup>. These enzymes participate in various reactions; a graphical representation of reactions with flavin involvement is shown in Figure 1.

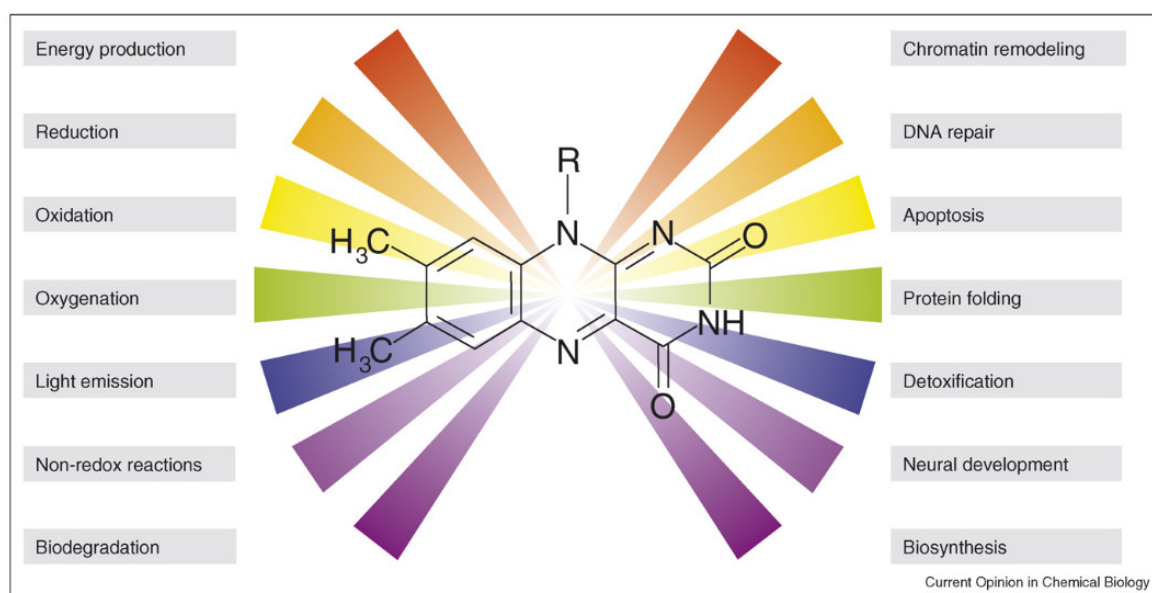


**Figure 1:** Reactions catalysed by flavin dependent proteins<sup>3</sup>

Already mentioned by the name flavoprotein, they have one common structural feature, the flavin cofactor. They contain a vitamin B<sub>2</sub> derivative, which is non-covalently bound to the apo-protein<sup>4</sup>. Vitamin B<sub>2</sub> also called riboflavin, the precursor for FMN and FAD (structures shown in Figure 2), is synthesized in bacteria and plants<sup>5,6</sup>.

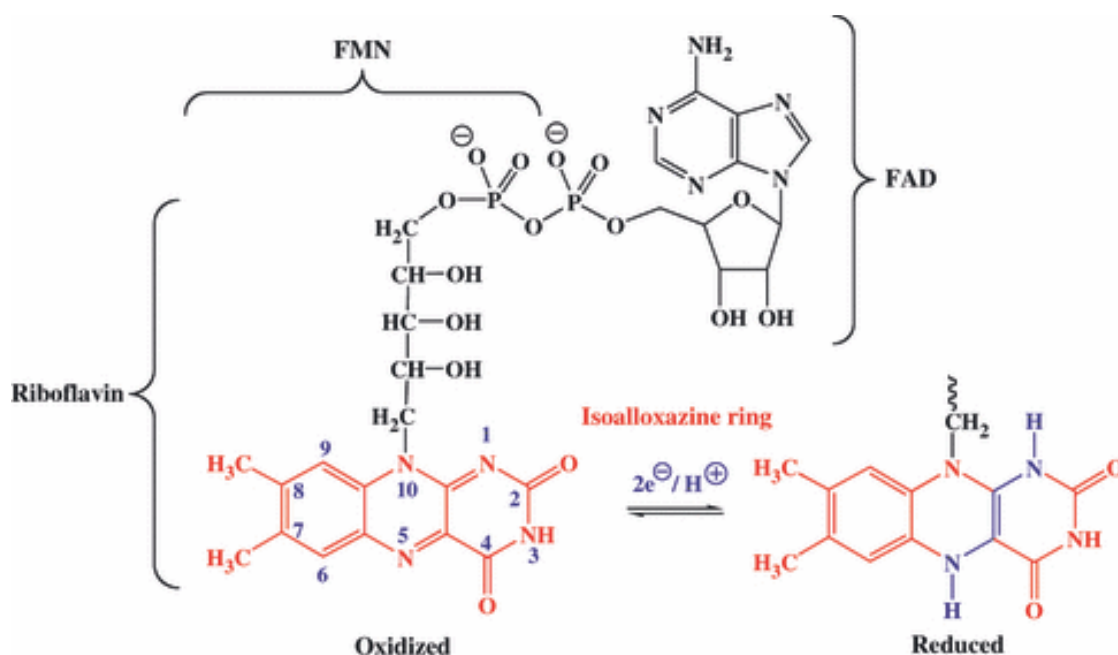


**Figure 2:** Structure of riboflavin and its derivatives FMN and FAD. The numbering of the redox-active isoalloxazine ring and the corresponding oxidised and fully reduced form of the ring system is shown<sup>2</sup>.

In a recently published review, 374 characterised flavin dependent proteins were analysed, regarding their structure and function. The distribution of FAD and FMN is, 75% and 25%, respectively, no enzyme using riboflavin as cofactor is known till today<sup>2</sup>.

About 11% of the known flavoproteins contain a cofactor, which is covalently attached to the protein, in nearly all cases, the attached cofactor is FAD. In 5 recently described enzymes even a bivalent linkage of the flavin to the apo-protein was discovered<sup>2</sup>.

In contrast to other cofactors flavins can catalyse one-electron and two-electron transfer reactions; this feature gives them the possibility to play a key role in the aerobic metabolism<sup>3</sup>. Furthermore some flavoenzymes have the outstanding property that they can activate molecular oxygen and use it for catalysis<sup>7</sup>.

The majority of flavin-dependent enzymes catalyse redox reactions and only ~10% of the characterised flavoproteins participate in non-redox reactions. Therefore it is not surprising that more than 90% of the characterised flavin dependent-enzymes belong to the protein family of the oxidoreductases. Beside oxidoreductases, flavoproteins can be classified as transferases, lyases, isomerases and ligases<sup>2</sup>. A pie chart of flavoprotein distribution among the different enzyme classes is shown in Figure 3.

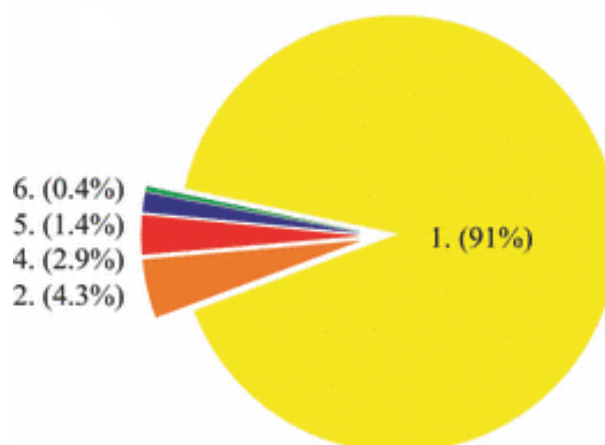


**Figure 3:** Distribution of flavoproteins; oxidoreductases (class 1); transferases (class 2); lyases (class 4); isomerases (class 5) and ligases (class 6)<sup>2</sup>

## Flavin dependent monooxygenases

Within the oxidoreductase family, the monooxygenases/hydrolases (EC 1.14 and 1.13) represent the largest subfamily<sup>2, 8</sup>. Flavin dependent monooxygenases can be described as chemo-, regio- and enantioselective enzymes, which participate in oxygenation reactions<sup>8, 9</sup>.

There are several biological processes, where this class of enzymes can be found. Typical examples are the biosynthesis of hormones, vitamins and antibiotics. Other members of this family catalyse key steps in the catabolism of natural and anthropogenic compounds or participate in defence strategies<sup>8</sup>.

The overall reaction of the monooxygenases can be described as the incorporation of one atom of molecular oxygen into the substrate, while the other one is reduced to water<sup>8</sup>. To react with molecular oxygen, the oxygen has to be activated. Therefore the flavin cofactor of the enzyme must be reduced; this electron rich compound can then use oxygen as a substrate<sup>7</sup>. The first step of the reaction of reduced flavin with molecular oxygen is the transfer of one electron from the flavin to the oxygen, resulting in the formation of a superoxide and a flavin radical. To come to the reduced form of oxygen a spin conversion has to take place subsequently<sup>10</sup>. In flavin monooxygenases, molecular oxygen is linked covalently to the C(4a) of the isoalloxazine ring resulting in the formation of a C(4a)-

hydroperoxyflavin. Under normal circumstances this peroxyflavin is unstable, deprotonation of the flavin at position N5 would result in the decay into hydrogen peroxide and reduced flavin. Flavin dependent monooxygenases have somehow managed to overcome this problem, stabilize this unstable flavin species and use it for catalysis<sup>11</sup>.

C(4a)-hydroperoxyflavin can interact with the substrates by two different ways, either by a nucleophilic or an electrophilic attack. The mode of reaction depends on the protonation state of the peroxyflavin, the outcome in both cases is the same, the incorporation of one atom of molecular oxygen into the substrate and the formation of water<sup>9</sup>. A graphical overview of the reaction between flavin and molecular oxygen is shown in Figure 4.

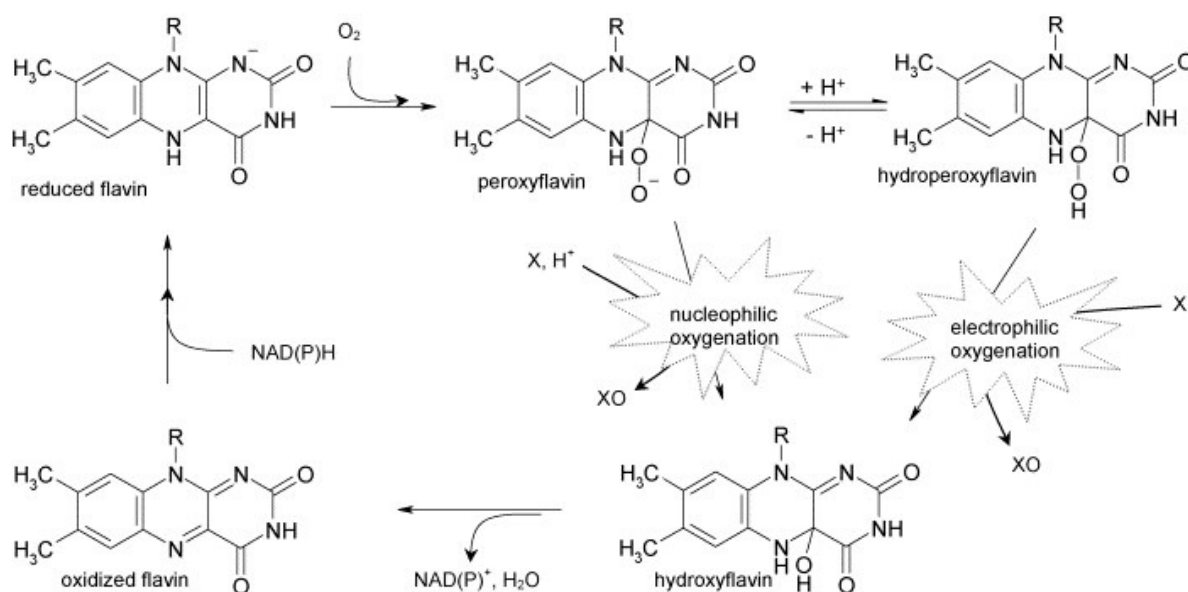


**Figure 4:** Reaction-cycle of the flavin cofactor with molecular oxygen found in flavin dependent monooxygenases. Shown are the possible intermediates and the reactions catalysed by these flavin species<sup>9</sup>.

## Classification of flavin dependent monooxygenases

There are several ways to classify this diverse class of enzymes.

### **Classification of flavin dependent monooxygenases into eight groups**

Van Berkel and co-workers have developed a method to classify flavin dependent monooxygenases based on their structural features, contained protein sequence motifs, their electron donor and the type of the oxygenation reaction. From the first review in 2006<sup>9</sup> to the latest review published in the year 2014<sup>8</sup> the number of classes has increased by two, resulting in eight distinguishable groups:

#### ***Group A***

The most popular member of this family is *p*-hydroxybenzoate hydroxylase<sup>12</sup>, however beside this enzyme about 60 other members are known. All of them are encoded by a single gene, in which the encoded protein contains a Rossmann fold with a tightly bound FAD. For reduction of FAD, NAD(P)H is required as cofactor. After the reduction of the FAD, the oxidised pyridine nucleotide is immediately released<sup>8,9</sup>.

Enzymes of this group play a key role in the degradation of aromatic compounds. The catalysed reaction can be described as electrophilic aromatic substitution, resulting in a regioselective ortho- or para-hydroxylation of the activated aromatic ring. Typical activating groups are the hydroxyl or the amino group. It was demonstrated that the reduction rate of the flavin is enhanced in the presence of the bound substrate<sup>8</sup>.

#### ***Group B***

This group consists of four sequence related groups, which can catalyse several different reactions and participate in the formation, degradation or detoxification of biological relevant substances. The four subgroups are the Baeyer-Villiger monooxygenases

(BVMOs), the Flavoprotein monooxygenases (FMOs), the *N*-hydroxylating monooxygenases and the Yuccas<sup>8</sup>.

Although the catalysed reactions are so different, they have some common features. All members of this group are encoded by a single gene. They contain a tightly bound FAD cofactor, which is reduced by NADPH. In contrast to members of group A, they do not release the oxidised NADP<sup>+</sup> after reduction of the flavin, instead of this it remains bound in one of the two  $\alpha/\beta$  Rossmann fold like domains<sup>8,9</sup>.

### ***Group C***

This is the first group where so called two component monooxygenases, composed of a reductase and a monooxygenase are found. The reduction of FMN is NAD(P)H dependent and takes place in the reductase, the reduced flavin is then passed over to the monooxygenases. A common structural feature from monooxygenases of this group is that they contain a TIM-barrel<sup>8,9</sup>.

Typical representatives of this family are the bacterial luciferases and several BVOMs<sup>9</sup>.

### ***Group D***

This small group has currently 13 members, they participate in the hydroxylation of aromatic compounds and *N*-hydroxylation reactions. The most popular member of this class is the 4-hydroxyphenylacetate 3-hydroxylase. They depend on a NAD(P)H-dependent flavin reductase for the reduction of the flavin. Monooxygenases of this group share an acyl-CoA dehydrogenase fold as structural similarity<sup>8,9</sup>.

### ***Group E***

Group E contains further two-component monooxygenases; they use reduced FAD as a coenzyme. The monooxygenase binds the reduced flavin in a Rossmann fold and it is proposed that there is an evolutionary link to group A flavin dependent monooxygenases. All members of this group are styrene monooxygenases<sup>9</sup>.

### ***Group F***

The 13 enzymes of this group participate in the biosynthesis of antibiotics and antitumor agents, where they catalyse halogenation reactions. The monooxygenase depends on a flavin reductase, to reduce the FAD cofactor and contains a Rossmann fold for FAD binding. Furthermore these enzymes contain a helical domain which is required for substrate binding. As prototype of this group the tryptophan 7-halogenase can be mentioned<sup>8,9</sup>.

### ***Group G***

Four members of this group are known presently, with tryptophan 2-monooxygenase as most prominent member. They are FAD dependent and contain a monoamine oxidase fold, typical substrates are amino acids, which are initially converted to an imino acid, thereby FAD gets reduced. Subsequently the imino acid is turned over to an amid and completes the reaction cycle<sup>8</sup>.

### ***Group H***

The known members of Group H are the lactate 2-monooxygenase and the nitronate monooxygenase, both enzymes contain FMN bound in a TIM-barrel fold. For the reduction of FMN no coenzyme is needed, instead of this the flavin is reduced by substrate oxidation<sup>8</sup>.

## **Alternative classifications for flavin dependent monooxygenases**

### ***“Cautious” and “bold” monooxygenases***

In the case of “cautious” monooxygenases, a hydroxylatable substrate has to be bound to allow the rapid reduction of the flavin and formation of the C(4a)-hydroperoxyflavin. Monooxygenases using this kind of mechanism stabilize the hydroperoxide only moderately<sup>13</sup>. A well characterised example regarding the reaction mechanism found in

this class of monooxygenases is the *p*-hydroxybenzoate hydroxylase. During the reaction the flavin adopts two different conformations, in the “in” conformation the N5 position of the isoalloxazine ring is inaccessible to solvent and NADPH, only a conformational change including a swing of the ring-system by 30° allows the flavin to adopt the “out” conformation where reduction is possible. The movement from the “in” to the “out” conformation is triggered by the binding of NADPH in the presence of the substrate<sup>14-16</sup>.

In “bold” monooxygenases the substrate is not necessary to be present for FMN reduction and subsequent formation of the C(4a)-hydroperoxyflavin. In turn the hydroperoxide is protected until the substrate is bound. Well known members of this group of enzymes are Baeyer-Villiger monooxygenases and FMOs, key enzymes in the detoxification of many xenobiotics and drugs<sup>13</sup>.

### ***Internal and external monooxygenases***

There are only a few examples for internal monooxygenases, one of them is lactate monooxygenase. This enzyme oxidizes lactate to pyruvate, with concomitant reduction of the flavin, which then reacts with molecular oxygen and converts pyruvate into carbon dioxide and acetate<sup>9</sup>.

In contrast to this, external monooxygenases require coenzymes to reduce the flavin, typically the electrons are provided from NAD(P)H<sup>9</sup>.

### ***Two-component monooxygenase systems***

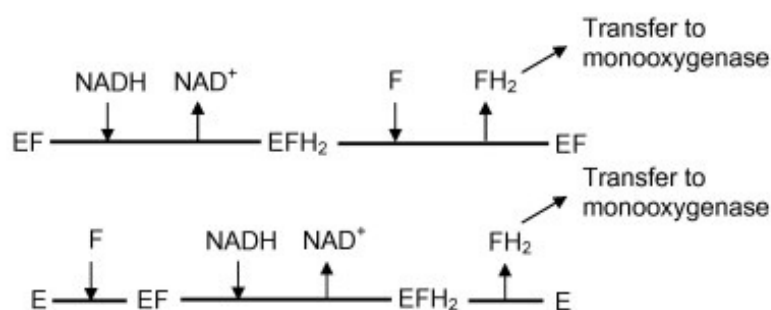
Several monooxygenases, which cannot reduce FMN on their own, depend on externally reduced flavins. These systems typically contain two enzymes, one which catalyses the reduction of FMN and another monooxygenase<sup>17</sup>.

A further subdivision of the two component systems can be done based on the mechanism of the reductase and the subsequent transfer of the reduced flavin to the monooxygenase. For reductases with a bound FMN cofactor two reaction mechanisms are proposed. The first reaction follows a ping-pong mechanism for the reductase, *i.e.* a second FMN binds and is reduced by an already present reduced flavin bound to the reductase, the reduced

FMN is subsequently transferred to the monooxygenase. The second observed mechanism, do not require a second flavin, but the already present reduced flavin is directly transferred to the monooxygenase (Figure 5A).

There are also reductases, which do not contain a bound cofactor. Reductases of this group catalyse flavin reduction following a sequential mechanism. Here the reduced flavin is transferred to the monooxygenase after it was reduced by the pyridine nucleotide (Figure 5B)<sup>17</sup>.

#### A. Mechanisms of FMN-bound reductases



#### B. Mechanism of FMN reductases without bound flavins

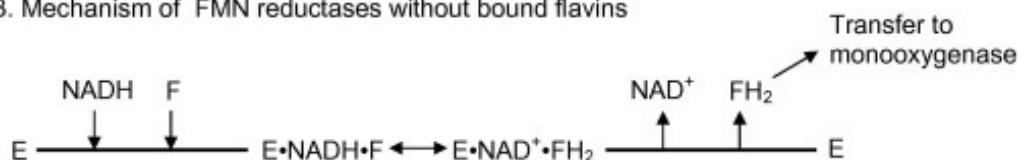


**Figure 5:** Possible mechanism of FMN reductases: (A) Mechanisms found in reductases with bound flavin-cofactor. Upper pathway, representing the ping-pong mechanism. Lower pathway shows the direct transfer of the flavin to the monooxygenasae. (B) Mechanism found in reductases without bound flavin, following a sequential mechanism<sup>17</sup>.

## Anthranoyl-CoA monooxygenase/reductase (ACMR), an enzyme with a group A monooxygenase domain

Anthranoyl-CoA monooxygenase/reductase (EC 1.14.13.40), is an enzyme found in *Azoarcus evansii*<sup>18</sup>, former *Pseudomonas* KB740<sup>19</sup>. ACMR participates in the degradation of anthranilate, an important intermediate in the synthesis and degradation of many N-heterocyclic compounds such as tryptophan. In *Azoarcus evansii*, the degradation pathway is coded by eight genes, which are clustered in form of an operon, beside ACMR, aminobenzoate-CoA ligase and three enzymes involved in  $\beta$ -oxidation were identified. Two copies of this gene cluster are present in the genome which are similar but not identical. Both coded ACMR variants are expressed simultaneously, when *Azoarcus* is grown under aerobic conditions<sup>18</sup>.

### Structural features of Anthranoyl-CoA monooxygenase/reductase

Anthranoyl-CoA monooxygenase/reductase is a homodimeric protein with a molecular mass ~170 kDa. Based on the fact that two operons are found, three dimeric forms of the protein are possible<sup>18, 20</sup>. As already indicated by the name, the protein is composed of two different subdomains. An N-terminal monooxygenase domain and a C-terminal reductase domain, the subdomains are separated by a 41 amino acid linker (shown in Figure 6). It is assumed that both subunits were initially separate, but a mutation within the stop-codon of the monooxygenase resulted in the formation of a fusion protein<sup>18</sup>. Originally it was assumed that the enzyme contains two FAD molecules<sup>21</sup>. Recent unpublished studies (for information see Chapter 3) performed with the recombinantly expressed protein revealed the presence of one FAD (in the monooxygenase domain) and one FMN (in the reductase domain).

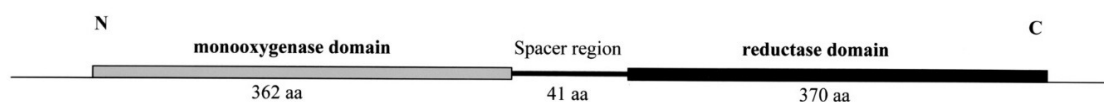


**Figure 6:** Structure of the ACMR: showing monooxygenase-, reductase domain and the linker region<sup>18</sup>

## Reaction catalysed by ACMR

The degradation pathway for 2-aminobenzoate found in *Azoarcus evansii* is unusual, in that typical degradation intermediates like catechol or gentisate could not be observed. In this organism the substrate is initially activated by the linkage of the substrate to coenzyme A, the CoA-thioesters are later converted to a non-aromatic product (see Figure 7). The first step in the degradation pathway is catalysed by the aminobenzoate-CoA ligase and the product is then converted by ACMR to a nonaromatic intermediate (2-amino-5-oxo-cyclohex-1-ene-1 carbonyl-CoA). The entire reduction catalysed by the ACMR requires two molecules of NADH and one molecule of oxygen. Based on the other enzymes coded by the operon it is proposed that the intermediate is further degraded by  $\beta$ -oxidation<sup>18</sup>.

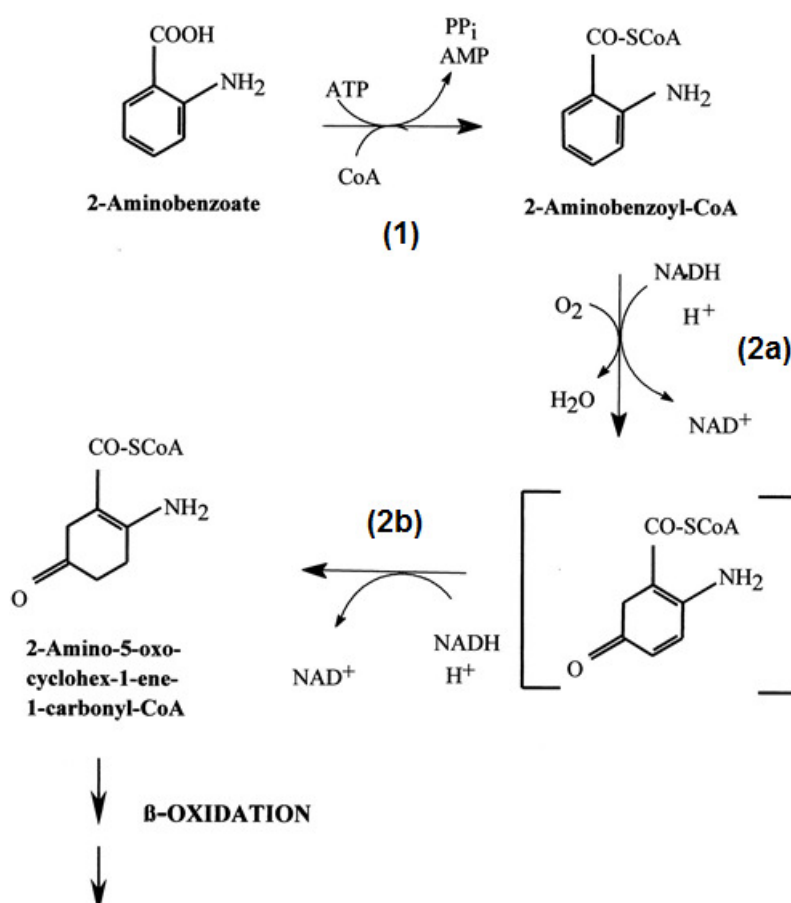


**Figure 7:** Primary steps of the degradation pathway found in *Azoarcus evansii*: (1) Activation of the substrate by aminobenzoate-CoA ligase; (2) Reactions catalysed by the enzyme ACMR: (2a) Reaction catalysed in the monooxygenase domain; (2b) Reaction occurring in the reductase domain<sup>18</sup>.

## Reaction catalysed in the monooxygenase subunit

The reaction catalysed by this Group A monooxygenase, requires one molecule of NADH and molecular oxygen. It can be described as a nucleophilic attack of the C(4a)-hydroperoxyflavin, thereby one atom of oxygen is transferred to the C5 of the activated substrate. After oxygen transfer migration of a hydrogen from C5 to C6 is observed. This hydrogen rearrangement can be described as a NIH shift<sup>22</sup>. *Ab initio* studies have demonstrated that the observed hydrogen transfer from C5 to C6 is energetically favoured over the possible 5,4-shift and results in a more stable product<sup>23</sup>. The reaction found in the monooxygenase domain is shown in Figure 8.

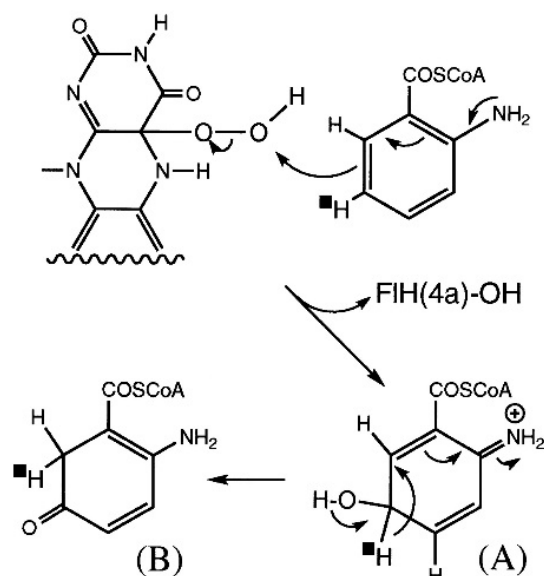


**Figure 8:** Reaction catalysed in the monooxygenase domain, indicating electron migration, the intermediate (A) and the final product observed after hydrogen migration (B)<sup>22</sup>.

## Reaction catalysed in the reductase subunit

Depending on the present NADH concentration, different products were observed. Under NADH limitation rearomatisation occurs, resulting in the formation of 2-amino-5-hydroxybenzoyl-CoA (Figure 9, route B). When NADH is supplied in excess, 5-oxo-2-aminocyclohexadiene is converted by the reductase. It is assumed that hydride transfer via the flavin cofactor is stereoselective from the *pro-R* site of the nicotinamide cofactor. The reduction results in the formation of 2-amino-5-oxocyclohex-1-enecarboxyl-CoA (Figure 9, route A)<sup>21, 22, 24</sup>.

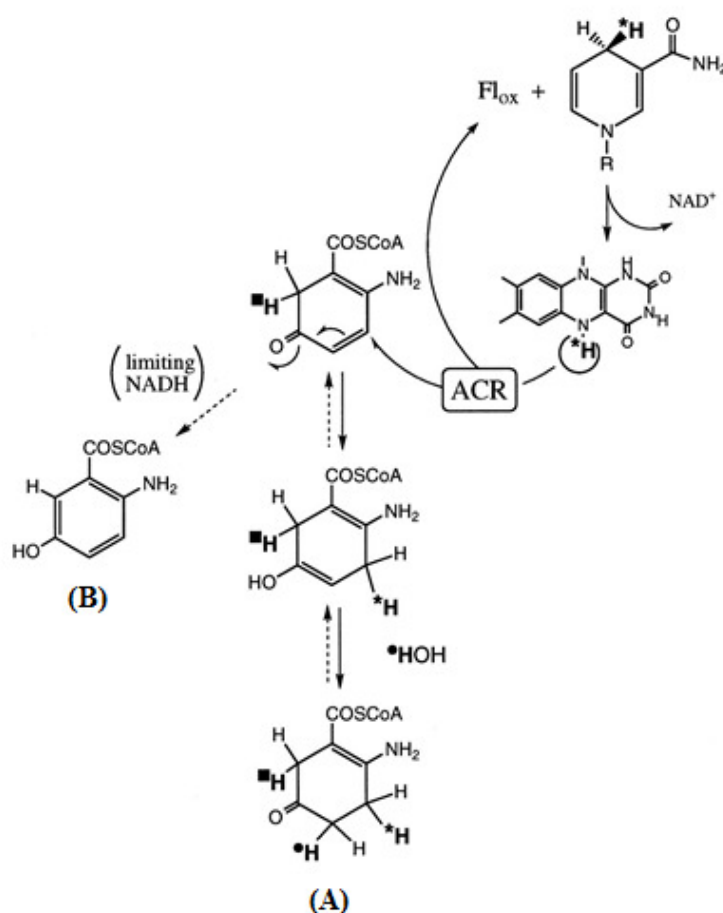


**Figure 9:** Reaction taking place in the reductase domain: (A) reaction found under NADH excess, leading to the formation of the 2-amino-5-oxocyclohex-1-enecarboxyl-CoA. Protons transferred from solvent and NADH are marked; (B) reaction under NADH limitation, resulting in rearomatisation<sup>22</sup>.

## Bacterial luciferase a class C monooxygenase

Bioluminescence is a long known fascinating phenomenon in nature. Light emitting organisms can be found among bacteria, fungi, dinoflagellates, fish, insects and squid. In all cases light emission is catalysed by an enzyme called luciferase. Substrates of this enzyme are usually known as luciferins. Different bioluminescent organisms have developed different reactions as well as luciferases and use different luciferins. Nevertheless beside the light emission, they all share a common feature, the requirement of oxygen for the bioluminescent reaction<sup>25</sup>.

### **Bacterial Bioluminescence**

Luminescent bacteria can either be found free living in the ocean, as saprophytes living on dead organisms, or in symbiosis as inhabitants of light organs from various organisms<sup>25</sup>. There are 19 bioluminescent bacterial species known, all of these are gram negative. They could be assigned to the three families *Vibrionaceae*, *Shewanellaceae* and *Enterobacteriaceae*. Most species are members of the *Vibrionaceae*, the most prominent genera are *Vibrio*, *Photobacterium* and *Aliivibrio*<sup>26</sup>.

### **The lux-operon**

In bioluminescent bacteria the genes responsible for the light emission are present in the form of an operon. The typical organisation within this operon is *luxCDAB(F)E* (Figure 10). Downstream of the *lux*-operon other genes responsible for the regulation of bioluminescence and involved in biosynthesis of flavins are found. Light emission is strongly dependent on the cell concentration, which is regulated by an autoinducer. For autoinduction a small metabolite is produced and released into the environment, with increasing cell concentration the level of the autoinducer is rising. When a critical concentration is reached, the autoinducer binds to a regulatory protein (LuxR) and thereby activates expression of the proteins encoded by *lux*-operon<sup>27</sup>. There is not much known

about the chemical structure of quorum sensing molecules, they differ among the species. In case of *Vibrio fischeri*,  $\beta$ -ketocaproyl-*N*-homoserine lactone was identified as quorum sensing molecule<sup>28, 29</sup>.

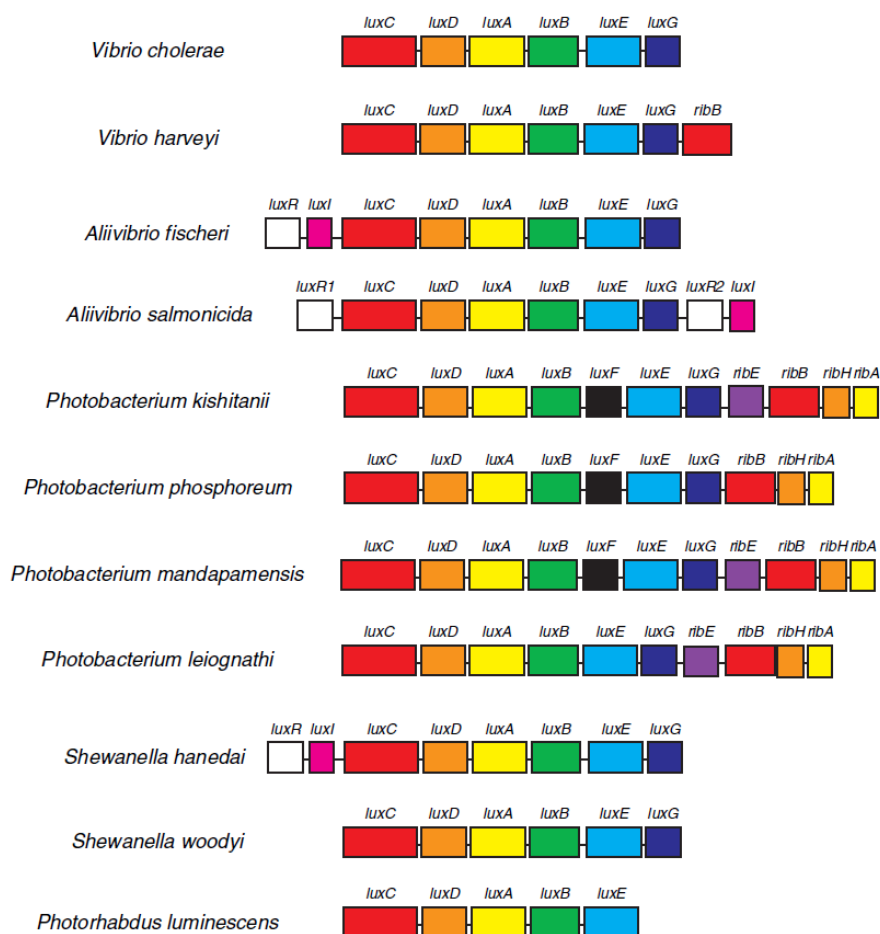


**Figure 10:** Organisation of the genes of the *lux*-operon found in different bioluminescent bacteria, as indicated the typical organisation is *luxC**D**A**B*(*F*)*E*. *luxA**B* encode the bacterial luciferase, *luxC**D**E* encode proteins involved in aldehyde synthesis, *luxG* encodes a FMN reductase, *luxF* encodes a protein on unknown function. Downstream an additional operon (*rib*-operon) could be found, containing genes responsible for riboflavin biosynthesis<sup>26</sup>.

The bacterial luciferase will be described in more detail later, however in the following selection other proteins of the *lux*-operon important for the understanding of the current thesis, are described.

### *Proteins involved in aldehyde synthesis*

Genes responsible for the synthesis of the long chain aldehyde are flanking the genes of the luciferase. There are three enzymes involved in the conversion of the long chain fatty acid into the final substrate, an aldehyde most likely tetradecanal. This multi-enzyme complex consists of a reductase (LuxC), a transferase (LuxD) and a synthetase (LuxE). In *Photobacterium phosphoreum* they form a 500 kDa complex with the stoichiometry  $r_{4s_4t_{2-4}}$ . This complex captures fatty acids from the fatty acid synthase complex and converts them to the substrate for luciferase<sup>25, 27</sup>.

### *LuxF*

Among bioluminescent bacteria some have an additional gene inserted between *luxB* and *luxE*. This gene known as *luxF* was only found in species of the genera *Photobacterium* (Figure 11)<sup>30</sup>.

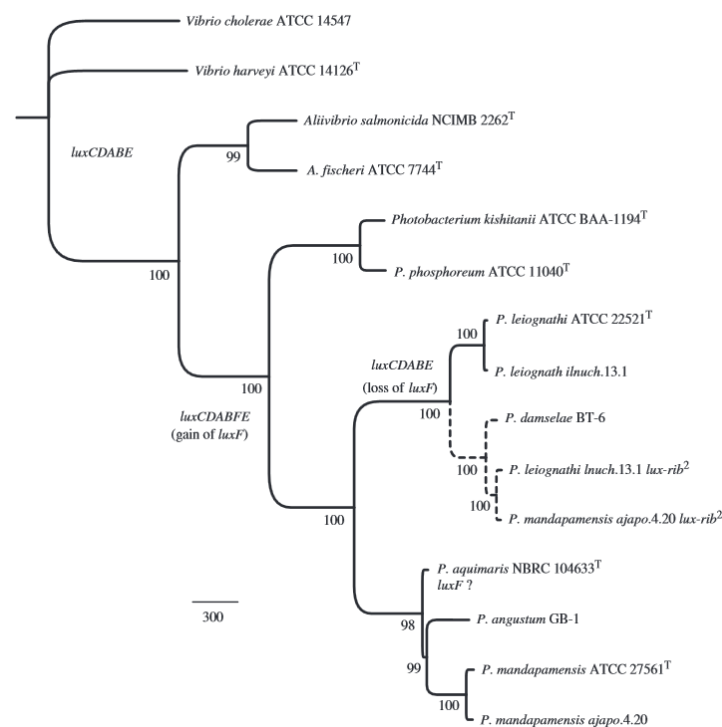


**Figure 11:** Phylogenetic tree of the bacterial *lux*-operon, indicating the evolutionary distribution of *luxF* within the luminescent genera<sup>30</sup>.

In older publications different nomenclatures like LuxN<sup>31</sup> or non-fluorescent protein (NFP)<sup>32</sup> could be found. In bacteria containing *luxF*, large quantities of the protein could be isolated from the cells. LuxF shows a high similarity to the subunits of the bacterial luciferase, which leads to the assumption that it has arisen by gene duplication of *luxB*. LuxF exists as a homodimer and shows  $\alpha/\beta$  barrel fold. The protein was originally isolated with two unusual flavin derivatives per subunit. Apparently, this derivate (3'-(*R*)-myristyl)-FMN was formed by a fatty acid linked via the  $\beta$ -carbon to the C-6 position of FMN (see Figure 12). Based on the stereoselectivity and the fact that FMN and fatty acid are products of the luciferase reaction, it was hypothesized that myrFMN is a side product of the bioluminescent reaction<sup>32-35</sup>.

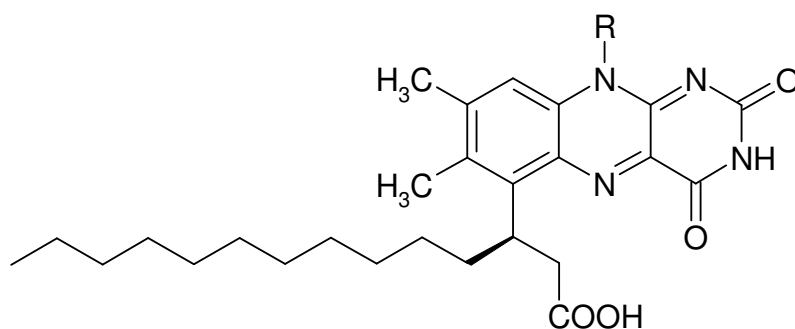


**Figure 12:** Structure of (3'-(*R*)-myristyl)-FMN (myrFMN); R= ribitol phosphate

### *Flavin reductase (LuxG)*

Based on the fact that reduced flavin is required for the luciferase reaction, there must be an enzyme, which supplies the luciferase with reduced FMN. There is one gene in the *lux*-operon, which encodes such a reductase, LuxG. Due to cloning and expression problems, less information about LuxG is available. This homodimeric protein contains no tight bound flavin cofactor<sup>36</sup>.

Chaiyen and co-workers, could demonstrate that a knockout of this gene results in a less luminescent strain, indicating that LuxG provides most of the reduced FMN required for light emission<sup>37</sup>.

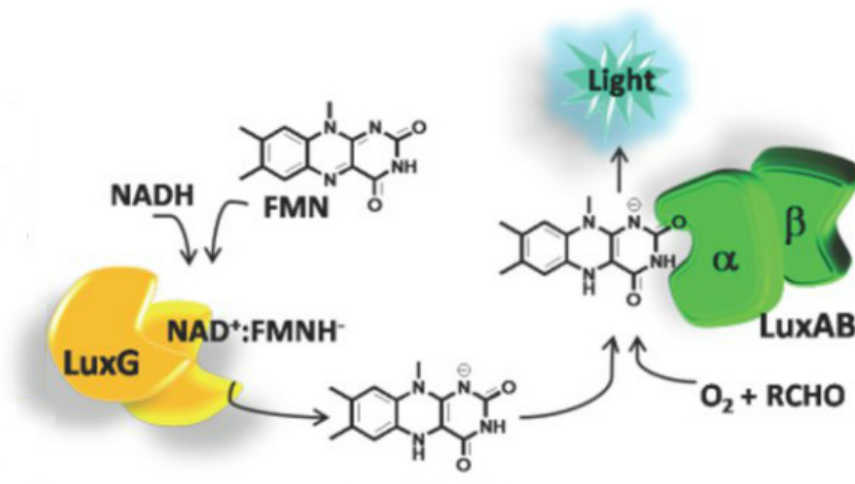


**Figure 13:** Reaction catalysed by LuxG and linkage to the luciferase reaction<sup>38</sup>.

Regarding mechanism and transfer of the reduced flavin to the luciferase no consistent view is present in the scientific community.

Tu and co-workers have demonstrated that the reductase from *Vibrio harveyi* follows a ping-pong mechanism. The mechanism changed to a sequential mechanism when they coupled LuxG with the luciferase of *Vibrio harveyi*. They suggest that flavin transfer occurs via protein-protein interaction. To support their hypothesis they have shown that the  $K_m$  values for FMN and NADPH were changed in the presence of luciferase<sup>39</sup>.

In contrast to this, Chaiyen and co-workers suggest free diffusion as the method of choice. In their studies with LuxG from *Photobacterium leiognathi* TH1, they have found a sequential-ordered mechanism. To support their hypothesis of free diffusion, they demonstrated that no protein-protein interaction from LuxG and the luciferase is occurring. Furthermore, LuxG could be combined with other acceptors for the reduced flavin, which does not alter the kinetic parameters of the reductase<sup>38</sup>. Further evidence for the free diffusion model is that bacterial luciferase accepts reduced flavin from reductases, that do not share structural similarities to LuxG<sup>17, 40</sup>.

## The luciferase (LuxAB)

Bacterial luciferases are one of the best studied two component monooxygenase systems. They catalyse the conversion of a long chain aldehyde into the corresponding fatty acid (Figure 14). Beside the aldehyde they need oxygen and reduced FMN as a substrate, the reduced flavin is provided from LuxG or other FMN reductases. Unique about this reaction is the emission of blue-green light<sup>25</sup>.

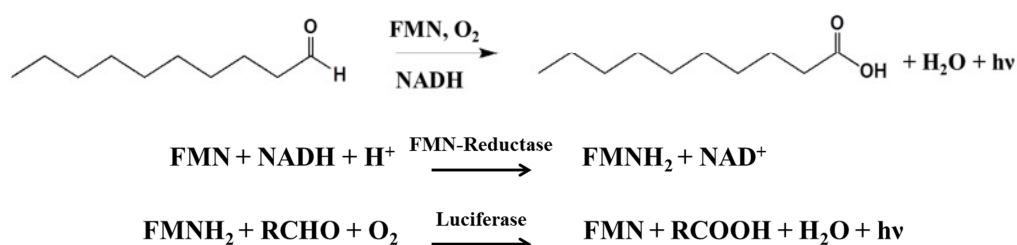


**Figure 14:** Reaction scheme of the bacterial luciferase, showing the conversion of the aldehyde, thereby one molecule of reduced FMN gets consumed, resulting in the formation of the corresponding carboxylic acid, oxidised FMN, water and light ( $\lambda \sim 490 \text{ nm}$ )<sup>25</sup>.

### *Structural features of the luciferase*

Bacterial luciferases have no evolutionary relationship to non-bacterial luciferases. They consist of two subunits encoded by the genes *luxA* and *luxB*, the  $\alpha$  and  $\beta$  subunit have an average molecular mass of 40 and 35 kDa, respectively<sup>41</sup>. Presently, the crystal structural of the luciferase from *Vibrio harveyi* (Figure 15) is available<sup>41-43</sup>.

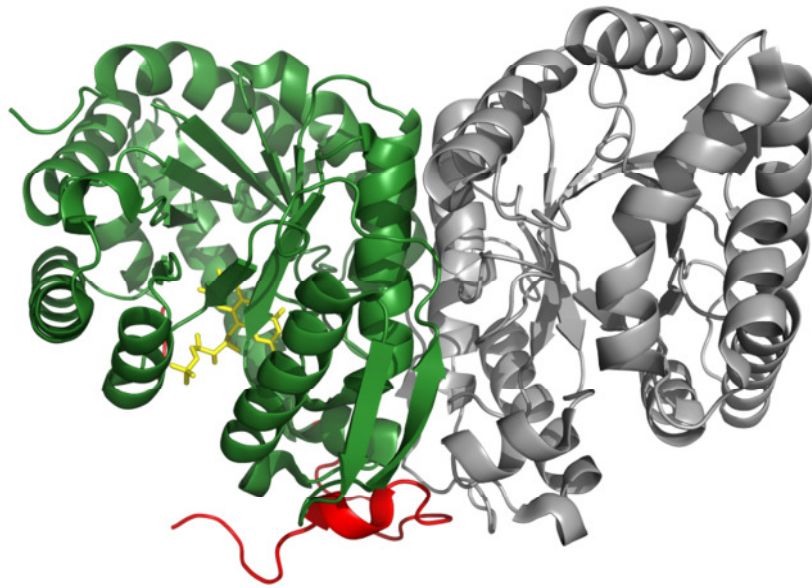


**Figure 15:** Crystal structure of the luciferase from *Vibrio harveyi* (PDB ID: 3FGC),  $\alpha$  and  $\beta$  subunits are shown in green and grey respectively. The bound FMN is shown as yellow stick representation; furthermore the mobile loop is indicated in red<sup>42</sup>.

Sequence alignments of both subunits show a high sequence similarity of  $\sim 30\%$ <sup>44</sup>. Based on this finding it is assumed that the genes have arisen by gene duplication<sup>30</sup>. LuxA contains 31 amino acids which are not present in the  $\beta$  subunit. The luciferase has only one active site which is located exclusively on the  $\alpha$  subunit, with the function of the  $\beta$  subunit being less clear. Nevertheless the presence of LuxB is important, because only as heterodimeric protein a high quantum yield is observed<sup>44</sup>.

Within the  $\alpha$  subunit a protease sensitive region is observed, this loop is missing in the crystal structures. Protease treatment results in a decreased light activity<sup>45</sup>, the total deletion of the loop does not change the luciferase reaction, but results in a dramatically decreased bioluminescence yield<sup>46</sup>. It was shown that the stability of the mobile loop is enhanced in the presence of substrates (reduced FMN and aldehyde), furthermore it is assumed that movement of the loop has a protecting function for the highly reactive intermediates<sup>46, 47</sup>. This loop was the starting point of many mutagenesis studies to demonstrate which residues might be essential for catalysis<sup>46-48</sup>.

All members of the bacterial luciferase family have less similarity regarding the amino acid sequence, however their 3-dimensional structure is similar. Both subunits have  $\alpha/\beta$

structure, which form a TIM-barrel fold and as usual for this class of enzymes the active site is at the C-terminal end of the  $\beta$ -barrel<sup>17</sup>.

### *The active site of the luciferase*

In the first available structures of the luciferase from *Vibrio harveyi*, the flavin cofactor and the aldehyde were not present<sup>41, 43</sup>. More recently a crystal structure with FMN bound in the putative active site (Figure 16) was solved<sup>42</sup>.

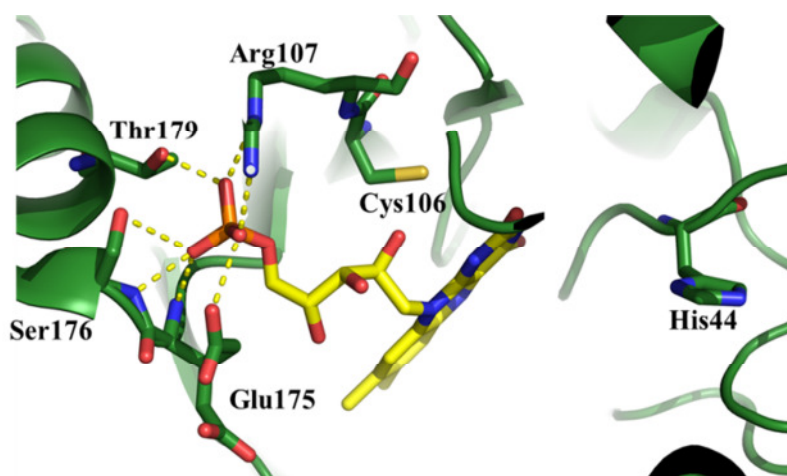


**Figure 16:** Active site of the luciferase from *Vibrio harveyi* (PDB ID: 3FGC). FMN is shown in yellow; residues important for binding of the phosphate group of FMN (Arg107, Glu175, Ser176 and Thr179) are shown, including possible interactions (yellow dashed lines). Furthermore residues important for catalysis (Cys106 and His44) are shown<sup>42</sup>.

Substrate binding takes place in a deep pocket, the flavin is bound by interactions with hydrophobic and polar residues. Interactions between Arg107, Glu175, Ser176 and Thr179 with the phosphate group could be observed<sup>42, 49</sup>. The importance of Arg107 was already known before, because replacement of arginine by other amino acids resulted in decreased bioluminescence<sup>50</sup>.

Furthermore, Cys106 is of interest because this residue is in hydrogen bonding distance to the flavin. This and the fact that other amino acid exchanges in this position lead to a

decrease in bioluminescence gave rise to the assumption that Cys106 might be important for the stabilisation of the C(4a)-hydroperoxyflavin<sup>51-53</sup>.

Sequence alignments demonstrated that there is a conserved histidine residue present in the active site of the luciferase. In former publications it was demonstrated that an exchange of His44 to alanine, results in a dramatic decrease in bioluminescence. Activity could be restored by the addition of imidazole or simple amines<sup>54, 55</sup>.

### *Reaction mechanism of the bacterial luciferase*

Although the substrates and the products of the luciferase reaction are known, there are still several proposed reaction mechanism. The common feature of them is the formation of the FMN-4a-peroxyhemiacetal as a key intermediate. This species is formed by nucleophilic attack of the C(4a)-peroxyflavin onto the aldehyde (Figure 17)<sup>56</sup>.

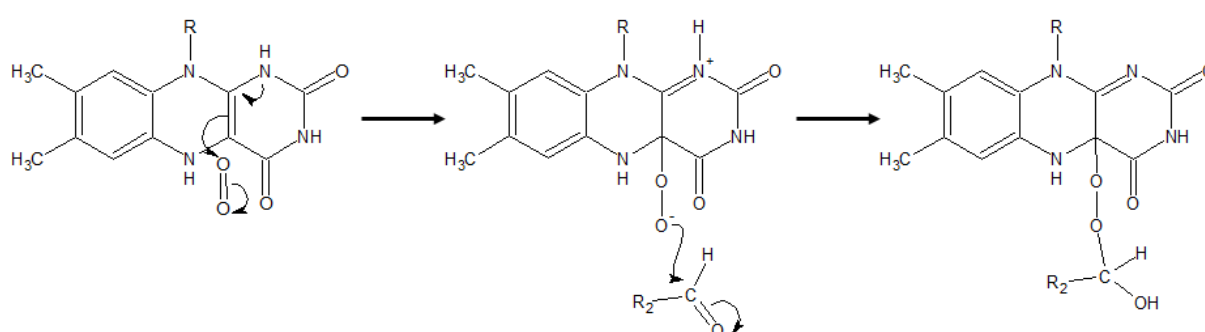


**Figure 17:** Formation of the FMN-4a-peroxyhemiacetal, arrows indicate electron migrations and consequent bond formation<sup>56</sup>. R= ribitol phosphate; R<sub>2</sub> aliphatic chain of the aldehyde

Although C(4a)-peroxyflavin is responsible for the formation of FMN-4a-peroxyhemiacetal, it was possible to isolate C(4a)-hydroperoxyflavin bound to the luciferase of *Vibrio harveyi*, prior to the reaction with the aldehyde<sup>57</sup>.

The two most prominent mechanisms for the conversion of the FMN-4a-peroxyhemiacetal to the final product are described below.

### *Luciferase mechanism according to the CIEEL mechanism*

The chemically initiated electron exchange luminescence (CIEEL)<sup>58</sup> mechanism was adapted to the luciferase reaction by Eckstein et al<sup>59</sup>. The reaction according to the CIEEL mechanism is shown in Figure 18.

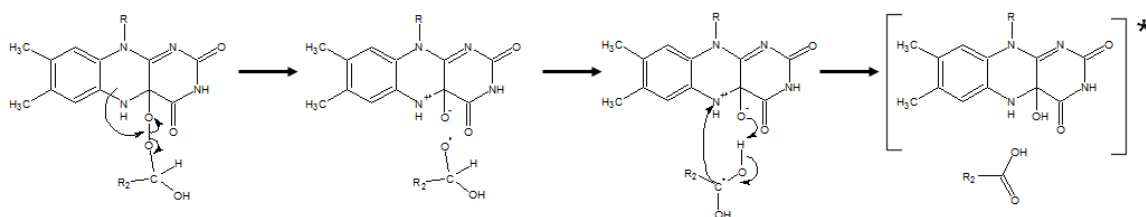


**Figure 18:** Luciferase mechanism according to the CIEEL mechanism: Intermediates and electron rearrangements are shown, finally resulting in the formation on an excited state (indicated by a star) and the carboxylic acid<sup>59</sup>. R= ribitol phosphate; R<sub>2</sub> = aliphatic chain of the aldehyde

In a first step a one electron rearrangement results in the cleavage of the oxygen-oxygen bond and the formation of a radical intermediate. The back-transfer of one electron to the 4a-hydroxyflavin radical cation leads to the formation of the excited state flavin<sup>59, 60</sup>.

### *Luciferase mechanism involving a dioxirane intermediate*

This mechanism proposed by Raushel and Baldwin<sup>61</sup> (Figure 19) starts with the attack of the carbonyl oxygen on the peroxide, thereby the oxygen-oxygen bond is broken and the dioxirane is formed. Subsequently one electron is transferred to the dioxirane, resulting in the formation of a radical ion pair. Rearrangement of the dioxirane radical anion leads to the formation of a carboxyl radical, which then donates one electron to the flavin, resulting in an excited state flavin and the carboxylic acid<sup>17, 61, 62</sup>.

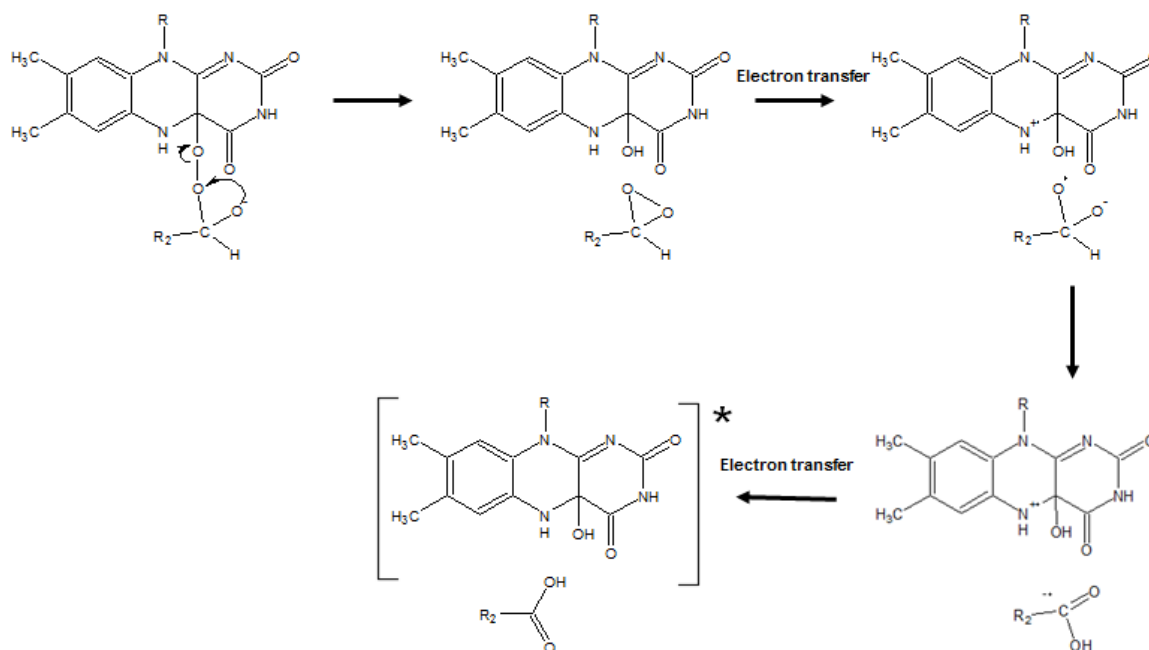


**Figure 19:** Luciferase reaction with a dioxirane intermediate: Intermediates and electron rearrangements are shown, finally resulting in the formation of an excited state (indicated by a star) and the carboxylic acid<sup>17, 61, 62</sup>. R = ribitol phosphate; R<sub>2</sub> = aliphatic chain of the aldehyde

The excited state emerges by cleaving of the carboxylic acid. After light emission flavin 4a-hydroxide, was isolated. It is assumed that this molecule represents the ground state of the light emitting species. Elimination of water from the flavin 4a-hydroxide, is the last step of the luciferase reaction and yields oxidised FMN, thereby completing the reaction-cycle for FMN<sup>57, 63, 64</sup>.

---

## References

1. Warburg, O. & Christian, W. Ein zweites sauerstoffübertragendes Ferment und sein Absorptionsspektrum. *Naturwissenschaften* **20**, 688 (1932).
2. Macheroux, P., Kappes, B. & Ealick, S. E. Flavogenomics - A genomic and structural view of flavin-dependent proteins. *FEBS Journal* **278**, 2625-2634 (2011).
3. Joosten, V. & van Berkel, W. J. Flavoenzymes. *Curr. Opin. Chem. Biol.* **11**, 195-202 (2007).
4. Hefti, M. H., Vervoort, J. & Van Berkel, W. J. H. Dehalogenation and reconstitution of flavoproteins: Tackling fold and function. *European Journal of Biochemistry* **270**, 4227-4242 (2003).
5. Bacher, A., Eberhardt, S., Fischer, M., Kis, K. & Richter, G. Biosynthesis of vitamin B2 (riboflavin). *Annual Review of Nutrition* **20**, 153-167 (2000).
6. Fischer, M. & Bacher, A. Biosynthesis of vitamin B2: Structure and mechanism of riboflavin synthase. *Arch. Biochem. Biophys.* **474**, 252-265 (2008).
7. Massey, V. Activation of molecular oxygen by flavins and flavoproteins. *J. Biol. Chem.* **269**, 22459-22462 (1994).
8. Huijbers, M. M. E., Montersino, S., Westphal, A. H., Tischler, D. & Van Berkel, W. J. H. Flavin dependent monooxygenases. *Arch. Biochem. Biophys.* **544**, 2-17 (2014).
9. van Berkel, W. J. H., Kamerbeek, N. M. & Fraaije, M. W. Flavoprotein monooxygenases, a diverse class of oxidative biocatalysts. *J. Biotechnol.* **124**, 670-689 (2006).
10. Ghisla, S. & MASSEY, V. Mechanisms of flavoprotein-catalyzed reactions. *European Journal of Biochemistry* **181**, 1-17 (1989).
11. Entsch, B. & Van Berkel, W. J. H. Structure and mechanism of para-hydroxybenzoate hydroxylase. *FASEB Journal* **9**, 476-483 (1995).
12. Entsch, B. & Van Berkel, W. J. H. Structure and mechanism of para-hydroxybenzoate hydroxylase. *FASEB Journal* **9**, 476-483 (1995).
13. Palfey, B. A. & McDonald, C. A. Control of catalysis in flavin-dependent monooxygenases. *Arch. Biochem. Biophys.* **493**, 26-36 (2010).
14. Schreuder, H. A. *et al.* Crystal structures of wild-type p-hydroxybenzoate hydroxylase complexed with 4-aminobenzoate, 2,4-dihydroxybenzoate, and 2-hydroxy-4-aminobenzoate and of the Tyr222Ala mutant complexed with 2-hydroxy-4-aminobenzoate. Evidence for a proton channel and a new binding mode of the flavin ring. *Biochemistry* **33**, 10161-10170 (1994).
15. Gatti, D. L. *et al.* The mobile flavin of 4-OH benzoate hydroxylase. *Science* **266**, 110-114 (1994).
16. Van Berkel, W. J. H., Eppink, M. H. M. & Schreuder, H. A. Crystal structure of p-hydroxybenzoate hydroxylase reconstituted with the modified FAD present in alcohol oxidase from methylotrophic yeasts: Evidence for an arabinoflavin. *Protein Science* **3**, 2245-2253 (1994).
17. Ellis, H. R. The FMN-dependent two-component monooxygenase systems. *Arch. Biochem. Biophys.* **497**, 1-12 (2010).

- 
18. Schühle, K., Jahn, M., Ghisla, S. & Fuchs, G. Two similar gene clusters coding for enzymes of a new type of aerobic 2-aminobenzoate (Anthranilate) metabolism in the bacterium *Azoarcus evansii*. *J. Bacteriol.* **183**, 5268-5278 (2001).
  19. Braun, K. & Gibson, D. T. Anaerobic degradation of 2-aminobenzoate (anthranilic acid) by denitrifying bacteria. *Appl. Environ. Microbiol.* **48**, 102-107 (1984).
  20. Buder, R., Ziegler, K., Fuchs, G., Langkau, B. & Ghisla, S. 2-Aminobenzoyl-CoA monooxygenase/reductase, a novel type of flavoenzyme. Studies on the stoichiometry and the course of the reaction. *European Journal of Biochemistry* **185**, 637-643 (1989).
  21. Langkau, B. & Ghisla, S. Kinetic and mechanistic studies on the reactions of 2-aminobenzoyl-CoA monooxygenase/reductase. *European Journal of Biochemistry* **230**, 686-697 (1995).
  22. Hartmann, S. *et al.* NIH shift in flavin-dependent monooxygenation: Mechanistic studies with 2-aminobenzoyl-CoA monooxygenase/reductase. *Proc. Natl. Acad. Sci. U. S. A.* **96**, 7831-7836 (1999).
  23. Torres, R. A. & Bruice, T. C. Theoretical investigation of the [1,2]-sigmatropic hydrogen migration in the mechanism of oxidation of 2-aminobenzoyl-CoA by 2-aminobenzoyl-CoA monooxygenase/reductase. *Proc. Natl. Acad. Sci. U. S. A.* **96**, 14748-14752 (1999).
  24. Langkau, B., Vock, P., Massey, V., Fuchs, G. & Ghisla, S. 2-Aminobenzoyl-CoA monooxygenase/reductase - Evidence for two distinct loci catalyzing substrate monooxygenation and hydrogenation. *European Journal of Biochemistry* **230**, 676-685 (1995).
  25. Meighen, E. A. Molecular biology of bacterial bioluminescence. *Microbiol. Rev.* **55**, 123-142 (1991).
  26. Dunlap, P. V. in *Encyclopedia of Microbiology (Third Edition)* (ed Schaechter, M.) 45-61 (Academic Press, Oxford, 2009).
  27. Meighen, E. A. Bacterial bioluminescence: Organization, regulation, and application of the lux genes. *FASEB Journal* **7**, 1016-1022 (1993).
  28. Cao, J. -. & Meighen, E. A. Purification and structural identification of an autoinducer for the luminescence system of *Vibrio harveyi*. *J. Biol. Chem.* **264**, 21670-21676 (1989).
  29. Eberhard, A. *et al.* Structural identification of autoinducer of *Photobacterium fischeri* luciferase. *Biochemistry* **20**, 2444-2449 (1981).
  30. Urbanczyk, H., Ast, J. C. & Dunlap, P. V. Phylogeny, genomics, and symbiosis of *Photobacterium*. *FEMS Microbiol. Rev.* **35**, 324-342 (2011).
  31. Raibekas, A. A. Green flavoprotein from *P. leiognathi*: purification, characterization and identification as the product of the lux G(N) gene. *J. Biolumin. Chemilumin.* **6**, 169-176 (1991).
  32. Moore, S. A. & James, M. N. G. Structural refinement of the non-fluorescent flavoprotein from *Photobacterium leiognathi* at 1.60 Å resolution. *J. Mol. Biol.* **249**, 195-214 (1995).
  33. Moore, S. A., James, M. N. G., O'Kane, D. J. & Lee, J. Crystallization of *Photobacterium leiognathi* non-fluorescent flavoprotein, an unusual flavoprotein with limited sequence identity to bacterial luciferase. *J. Mol. Biol.* **224**, 523-526 (1992).
  34. Moore, S. A. & James, M. N. G. Common structural features of the luxF protein and the subunits of bacterial luciferase: Evidence for a (Ba)<sub>8</sub> fold in luciferase. *Protein Science* **3**, 1914-1926 (1994).
  35. Moore, S. A., James, M. N. G., O'Kane, D. J. & Lee, J. Crystal structure of a flavoprotein related to the subunits of bacterial luciferase. *EMBO J.* **12**, 1767-1774 (1993).
-

- 
36. Nijvipakul, S., Ballou, D. P. & Chaiyen, P. Reduction kinetics of a flavin oxidoreductase LuxG from photobacterium leiognathi (TH1): Half-sites reactivity. *Biochemistry* **49**, 9241-9248 (2010).
37. Nijvipakul, S. *et al.* LuxG is a functioning flavin reductase for bacterial luminescence. *J. Bacteriol.* **190**, 1531-1538 (2008).
38. Tinikul, R. *et al.* The transfer of reduced flavin mononucleotide from luxg oxidoreductase to luciferase occurs via free diffusion. *Biochemistry* **52**, 6834-6843 (2013).
39. Jeffers, C. E. & Tu, S. -. Differential transfers of reduced flavin cofactor and product by bacterial flavin reductase to luciferase. *Biochemistry* **40**, 1749-1754 (2001).
40. Campbell, Z. T. & Baldwin, T. O. Fre is the major flavin reductase supporting bioluminescence from *Vibrio harveyi* luciferase in *Escherichia coli*. *J. Biol. Chem.* **284**, 8322-8328 (2009).
41. Fisher, A. J. Three-dimensional structure of bacterial luciferase from *vibrio harveyi* at 2.4 Å resolution 1,2. *Biochemistry*® **34**, 6581-6586 (1995).
42. Campbell, Z. T., Weichsel, A., Montfort, W. R. & Baldwin, T. O. Crystal structure of the bacterial luciferase/flavin complex provides insight into the function of the β subunit. *Biochemistry* **48**, 6085-6094 (2009).
43. Fisher, A. J., Thompson, T. B., Thoden, J. B., Baldwin, T. O. & Rayment, I. The 1.5-Å resolution crystal structure of bacterial luciferase in low salt conditions. *J. Biol. Chem.* **271**, 21956-21968 (1996).
44. Baldwin, T. O. *et al.* Structure of bacterial luciferase. *Curr. Opin. Struct. Biol.* **5**, 798-809 (1995).
45. Baldwin, T. O., Hastings, J. W. & Riley, P. L. Proteolytic inactivation of the luciferase from the luminous marine bacterium *Beneckeia harveyi*. *J. Biol. Chem.* **253**, 5551-5554 (1978).
46. Sparks, J. M. & Baldwin, T. O. Functional implications of the unstructured loop in the (β/a)<sub>8</sub> barrel structure of the bacterial luciferase a subunit. *Biochemistry* **40**, 15436-15443 (2001).
47. Campbell, Z. T. & Baldwin, T. O. Two lysine residues in the bacterial luciferase mobile loop stabilize reaction intermediates. *J. Biol. Chem.* **284**, 32827-32834 (2009).
48. Campbell, Z. T., Baldwin, T. O. & Miyashita, O. Analysis of the bacterial luciferase mobile loop by replica-exchange molecular dynamics. *Biophys. J.* **99**, 4012-4019 (2010).
49. Lin, L. Y. *et al.* Modeling of the bacterial luciferase-flavin mononucleotide complex combining flexible docking with structure-activity data. *Protein Science* **10**, 1563-1571 (2001).
50. Moore, C., Lei, B. & Tu, S. Relationship between the Conserved α Subunit Arginine 107 and Effects of Phosphate on the Activity and Stability of *Vibrio harveyi* Luciferase. *Arch. Biochem. Biophys.* **370**, 45-50 (1999).
51. Abu-Soud, H. M., Clark, A. C., Francisco, W. A., Baldwin, T. O. & Raushel, F. M. Kinetic destabilization of the hydroperoxy flavin intermediate by site-directed modification of the reactive thiol in bacterial luciferase. *J. Biol. Chem.* **268**, 7699-7706 (1993).
52. Baldwin, T. O., Chen, L. H., Chlumsky, L. J., Devine, J. H. & Ziegler, M. M. Site-directed mutagenesis of bacterial luciferase: analysis of the 'essential' thiol. *J. Biolumin. Chemilumin.* **4**, 40-48 (1989).
53. Nicoli, M. Z., Meighen, E. A. & Woodland Hastings, J. Bacterial luciferase. Chemistry of the reactive sulfhydryl. *J. Biol. Chem.* **249**, 2385-2392 (1974).

54. Xin, X., Xi, L. & Tu, S. -. Functional consequences of site-directed mutation of conserved histidyl residues of the bacterial luciferase a subunit. *Biochemistry* **30**, 11255-11262 (1991).
55. Huang, S. & Tu, S. -. Identification and characterization of a catalytic base in bacterial luciferase by chemical rescue of a dark mutant. *Biochemistry* **36**, 14609-14615 (1997).
56. Eberhard, A. & Hastings, J. W. A postulated mechanism for the bioluminescent oxidation of reduced flavin mononucleotide. *Biochem. Biophys. Res. Commun.* **47**, 348-353 (1972).
57. Macheroux, P., Ghisla, S. & Hastings, J. W. Spectral detection of an intermediate preceding the excited state in the bacterial luciferase reaction. *Biochemistry* **32**, 14183-14186 (1993).
58. Schuster, G. B. Chemiluminescence of organic peroxides. Conversion of ground-state reactants to excited-state products by the chemically initiated electron-exchange luminescence mechanism. *Acc. Chem. Res.* **12**, 366-373 (1979).
59. Eckstein, J. W., Hastings, J. W. & Ghisla, S. Mechanism of bacterial bioluminescence: 4a,5-dihydroflavin analogs as models for luciferase hydroperoxide intermediates and the effect of substituents at the 8-position of flavin on luciferase kinetics. *Biochemistry* **32**, 404-411 (1993).
60. Mager, H. I. X., Sazou, D., Liu, Y. H., Tu, S. -. & Kadish, K. M. Reversible one-electron generation of 4a,5-substituted flavin radical cations: Models for a postulated key intermediate in bacterial bioluminescence. *J. Am. Chem. Soc.* **110**, 3759-3762 (1988).
61. Rauschel, F. M. & Baldwin, T. O. Proposed mechanism for the bacterial bioluminescence reaction involving a dioxirane intermediate. *Biochem. Biophys. Res. Commun.* **164**, 1137-1142 (1989).
62. Francisco, W. A. *et al.* Deuterium kinetic isotope effects and the mechanism of the bacterial luciferase reaction. *Biochemistry* **37**, 2596-2606 (1998).
63. Kurfurst, M., Ghisla, S. & Hastings, J. W. Characterization and postulated structure of the primary emitter in the bacterial luciferase reaction. *Proc. Natl. Acad. Sci. U. S. A.* **81**, 2990-2994 (1984).
64. Kurfuerst, M., Macheroux, P., Ghisla, S. & Hastings, J. W. Isolation and characterization of the transient, luciferase-bound flavin-4a-hydroxide in the bacterial luciferase reaction. *Biochimica et Biophysica Acta - General Subjects* **924**, 104-110 (1987).

---

# **CHAPTER 2**

## **2.1 Bioluminescence / The bacterial luciferase**

---

# A luciferous surprise: a new natural aldehyde substrate in bacterial bioluminescence

Thomas Bergner,<sup>1</sup> Chaitanya R. Tabib,<sup>1</sup> Jakov Ivkovic,<sup>2</sup> Rolf Breinbauer,<sup>2</sup> and Peter Macheroux<sup>1\*†</sup>

<sup>1</sup>Graz University of Technology, Institute of Biochemistry, Graz, Austria

<sup>2</sup>Graz University of Technology, Institute of Organic Chemistry, Graz, Austria

Running title: *a new substrate for bacterial luciferase*

To whom correspondence should be addressed:

Prof. Dr. Peter Macheroux, Graz University of Technology, Institute of Biochemistry, Petersgasse 12/II, A-8010 Graz, Austria, Tel.: +43-316-873 6450; Fax: +43-316-873 6952; Email: peter.macheroux@tugraz.at

## Abstract

Bacterial bioluminescence results from the oxidation of a long-chain fatty aldehyde, such as myristic aldehyde, to the corresponding long-chain fatty acid. This bioluminescent reaction is catalyzed by luciferase, an enzyme employing flavin mononucleotide (FMN) as a redox cofactor to drive the monooxygenation of the aldehyde substrate to the acid product. The free energy released during the oxidation of the aldehyde gives rise to an excited state FMN-4a-hydroxide, *i.e.* the luciferin in bacterial bioluminescence. Bacterial luciferase is a heterodimeric protein encoded by *luxA* and *luxB* in the so-called *lux*-operon of bioluminescent bacteria. In addition, the *lux*-operon contains three genes, *luxC*, *luxD* and *luxE*, encoding enzymes for the generation of the aldehyde substrate. Finally, a nicotinamide nucleotide dependent enzyme that produces reduced FMN for bacterial luciferase is encoded by *luxG*. In some Photobacteria, however, an additional gene, *luxF* was discovered. Sequence similarity to *luxB* suggests that *luxF* has arisen by gene duplication. X-ray crystallographic analysis revealed the presence of four flavin derivatives, *i.e.* 6-(3'-(*R*)-myristyl)-FMN (myrFMN), which are non covalently bound to LuxF. The discovery of this unique and unusually modified flavin raised the question of its generation and function in bacterial bioluminescence. According to a current hypothesis, myrFMN is accidentally produced in the luciferase-catalyzed light reaction and LuxF serves as a scavenger to prevent inhibition of the luciferase. To test this hypothesis, we have employed several methods from structural biology, biochemical characterization of recombinant proteins to chemical synthesis of alternative substrates. This has led to several new insights into bacterial bioluminescence and the discovery of a hitherto unknown substrate for bacterial luciferase.

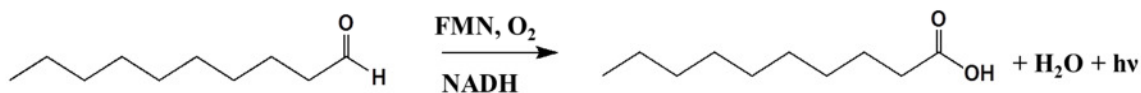
## Introduction

Bioluminescence is a long known phenomena, fascinating and mysterious at the same time. Luminescent bacteria can either be found free living in the ocean or in symbiosis as inhabitants of light organs from various species of fish<sup>1</sup>. Presently, 19 gram negative

species could be known, belonging either to the family *Vibrionaceae*, *Shewanellaceae* or *Enterobacteriaceae*. The most prominent genera belong to the *Vibrionaceae*, viz. *Vibrio*, *Photobacterium* and *Aliivibrio*<sup>2</sup>.

In all bioluminescent bacteria the genes encoding the enzymes responsible for light emission are located in the so-called *lux*-operon. Typically, the organisation of the genes is *luxCDAB(F)E*, which could be extended by genes responsible for riboflavin biosynthesis. The genes *luxA* and *luxB* encode the heterodimeric luciferase, the key enzyme in light emission. Currently, only the structure of the luciferase from *Vibrio harveyi* is known<sup>3-5</sup>. There is a high structural similarity between the  $\alpha$  and  $\beta$  subunit, which leads to the assumption that the luciferase is a product of a gene duplication<sup>6</sup>. The protein has a single active site located on the  $\alpha$  subunit, nevertheless the  $\beta$  subunit is required to observe a high quantum yield<sup>7</sup>.

In the active site, monooxygenation of the aldehyde to the acid takes place. Besides the aldehyde, reduced FMN, provided by an external FMN reductase and molecular oxygen serve as substrates<sup>8</sup>. The reaction catalysed by the luciferase is shown in Scheme 1.



**Scheme 1:** Reaction catalysed by the bacterial luciferase

Previously mentioned substrates play furthermore a role in stabilisation of the mobile loop, a part of the  $\alpha$  subunit, which is sensitive to proteolysis<sup>9</sup>. Movement of this flexible part of the protein seems to be involved in protecting the highly reactive intermediates from side reactions with the solvent<sup>5</sup>.

Although there are different proposed mechanisms, like the chemically initiated electron exchange luminescence (CIEEL)<sup>10, 11</sup> or a mechanism proposed by Raushel and Baldwin<sup>12</sup> including a dioxirane intermediate. The light emitting intermediate was not isolated till now, nevertheless it was possible to isolate FMN 4a-hydroxide, directly after light emission, which leads to the assumption that the excited form of this intermediate acting as

a luciferin. Elimination of water from the FMN 4a-hydroxide completes the cycle and provides oxidised FMN for the reductase<sup>13-15</sup>.

As mentioned before, the luciferase requires aldehyde as substrate, this aldehyde is produced by a multienzyme complex composed of LuxC, LuxD and LuxE; a reductase, a transferase and a synthetase, respectively. It is assumed that this “aldehyde synthesis machinery” interacts with the fatty synthase complex to produce tetradecanal. Evidence for tetradecanal as natural substrate is the high bioluminescence yield observed with this aldehyde compared to other aldehydes (C8-C12)<sup>8</sup>. Furthermore reduced FMN is required for activity. Within the *lux*-operon one FMN reductase could be identified. Recently, successful expression and characterisation of LuxG from *Photobacterium leiognathi* TH1 has indicated the importance of this gene. A knockout of this homodimeric protein results in reduced bioluminescence, leading to the assumption that LuxG is the main FMN reductase involved in light emission<sup>16, 17</sup>. Reduced flavin is sensitive regarding re-oxidation, therefore Jeffers and Tu<sup>18</sup> suggest, a transfer including protein-protein interaction. In recent studies a sequential-ordered mechanism with subsequent free diffusion of the reduced flavin to the luciferase could be shown for LuxG from *Photobacterium leiognathi* TH1<sup>19</sup>. Evidence for free diffusion have been found before, because reductases from other organisms could be coupled with luciferases<sup>20, 21</sup>.

In some species of the genera *Photobacterium* an additional gene could be found inserted between *luxB* and *luxE*<sup>6</sup>. This gene and the corresponding protein are known as LuxF, a protein with a high similarity to the  $\beta$  subunit of luciferase indicating that *luxF* is a product of gene duplication of *luxB*. The homodimeric protein shows a  $\alpha/\beta$  barrel fold, and contains two molecules of 6-(3'-(*R*)-myristyl)-FMN (myrFMN), a unusual derivative of FMN. MyrFMN has a covalent attachment of a fatty acid to C6 of the isoalloxazine ring, due to the stereoselectivity of the linkage and the fact that both FMN and fatty acid are products of the luciferase reaction, it was hypothesized that myrFMN is generated as by-product of the luciferase<sup>22-25</sup>. The inhibiting effect of myrFMN on the luciferase from *Vibrio harveyi* was demonstrated by Tu and coworkers<sup>26</sup>.

To investigate the role of the luciferase in the formation of myrFMN, we used an established isolation procedure<sup>27</sup> and found a correlation between myrFMN content and

light emission. But how can a linkage like the observed C-C bond formation occur in the luciferase reaction (Scheme 1).

Studies of bivalent linked proteins have demonstrated the reactivity of position 6 of the isoalloxazine ring. The formation of a covalent linkage to this position is achieved by a nucleophilic attack of a Cys-residue<sup>28</sup>. Whereas such a mechanism could not explain the formation of myrFMN, an electrophilic attack of reduced flavin onto an “activated” substrate could be the mechanism behind myrFMN formation. A possible method to activate the aldehyde is the introduction of a double bond between position 2 and 3. Trans-2,3-unsaturated aldehydes were tested as potential substrates and used in different *in-vitro* assays. Furthermore *in-vivo* approaches are used to solve the mystery about myrFMN.

## **Experimental procedures**

### ***Materials***

Glucose dehydrogenase and aldehydes with even number chain lengths from C8 to C12 were from Sigma (Vienna, Austria), C14 was from Chemos GmbH (Regenstauf, Germany). NADPH, glucose and buffer components were from Roth (Graz, Austria).

### ***Instrumentation***

UV/Vis absorption spectra were recorded with a Specord 205/210 spectrophotometer (Analytic Jena, Jena, Germany). Light emission was measured with a Cento LB 960 Luminometer (Berthold Technologies, Vienna, Austria)

### ***Photobacterial strains***

The following *Photobacterium leiognathi* strains were selected for our study: ATCC 25521, ATCC 25587, ATCC 27561, S1, TH1 and svers.1.1. The first two strains were reported to lack *luxF* (*luxF*<sup>-</sup>) whereas ATCC 27561, S1, TH1 and svers.1.1 possess *luxF* in the *lux*-operon (*luxF*<sup>+</sup>). Cultivation was performed in 2 l shaking flasks, containing 500 ml of SWC media. Strains were cultivated at 25 °C, for optimal aeration the flasks were

shaken with 130 rpm. Growth was followed by absorption measurement at 660 nm, to exclude the detection of artefacts due to bioluminescence. Furthermore the light emission was measured at the same time points.

### ***Bacterial strains, expression plasmids and protein purification***

Expression and purification of the bacterial luciferase from *Photobacterium leiognathi* S1 was done according to previous reports<sup>27</sup>. YcnD was used for reduction of FMN. The enzyme was expression and purification as described before<sup>29</sup>.

### ***Single turnover assays***

Assays were performed in a black 96 well plate, the final volume per well was 250  $\mu$ l. Subsequently the reaction was started by the addition of the NADPH solution, which was performed automatically. Final concentrations in the samples are as followed: 250 nM luciferase, 375 nM YcnD, 375 nM FMN and 1  $\mu$ M NADPH, with the exception of NADPH all components were dissolved in 100 mM potassium-phosphate-buffer pH 7, which was saturated with aldehyde. Measurements were started 5 sec before NADPH addition and recorded for 180 sec.

### ***Multiple turnover assays***

Multiple turnover assays were performed under aerobic and anaerobic conditions in 25-50 ml scale. NADPH regeneration was done by glucose-dehydrogenase. The final enzyme concentrations in the assays were 50  $\mu$ M luciferase, 75  $\mu$ M YcnD and 25 U glucose-dehydrogenase. Furthermore 100  $\mu$ M of FMN, 250  $\mu$ M NADPH and 250 mM glucose were present in the reaction mixture. For optimal aeration the sample was shaken with 300 rpm, the total incubation time was up to 72 hours, during this time light emission was observed when oxygen was present.

### ***Isolation and detection of myrFMN***

Multiple turnover reactions were stopped by the addition of 3 g of guanidine hydrochloride, using concentrated HCl to adjust the pH = 2. MyrFMN was extracted with 5 ml of butanol:ethylacetate (1:1 v/v) solution, further steps and detection of myrFMN were done as described before, with minor adaptations regarding the used volumes<sup>27</sup>.

### ***Inhibition assays with myrFMN***

Inhibition assays were performed similar to the single turnover assays. All concentrations and measured parameters were as described before; the only difference was the presence of myrFMN. The concentration of this luciferase inhibitor was varied from 0 up to 10  $\mu$ M.

## **Results**

### ***Cultivation and characterization of Photobacteria strains with luxF<sup>+</sup> and luxF<sup>-</sup> background***

A defined amount, normally between 15-25 g were analysed regarding the myrFMN content. The strain TH1, which had the highest total light yield (Figure 1; Panel A), was also the strain with the highest myrFMN content (Figure 1; Panel B), this strain was taken as 100% and all other strains were correlated to this value.

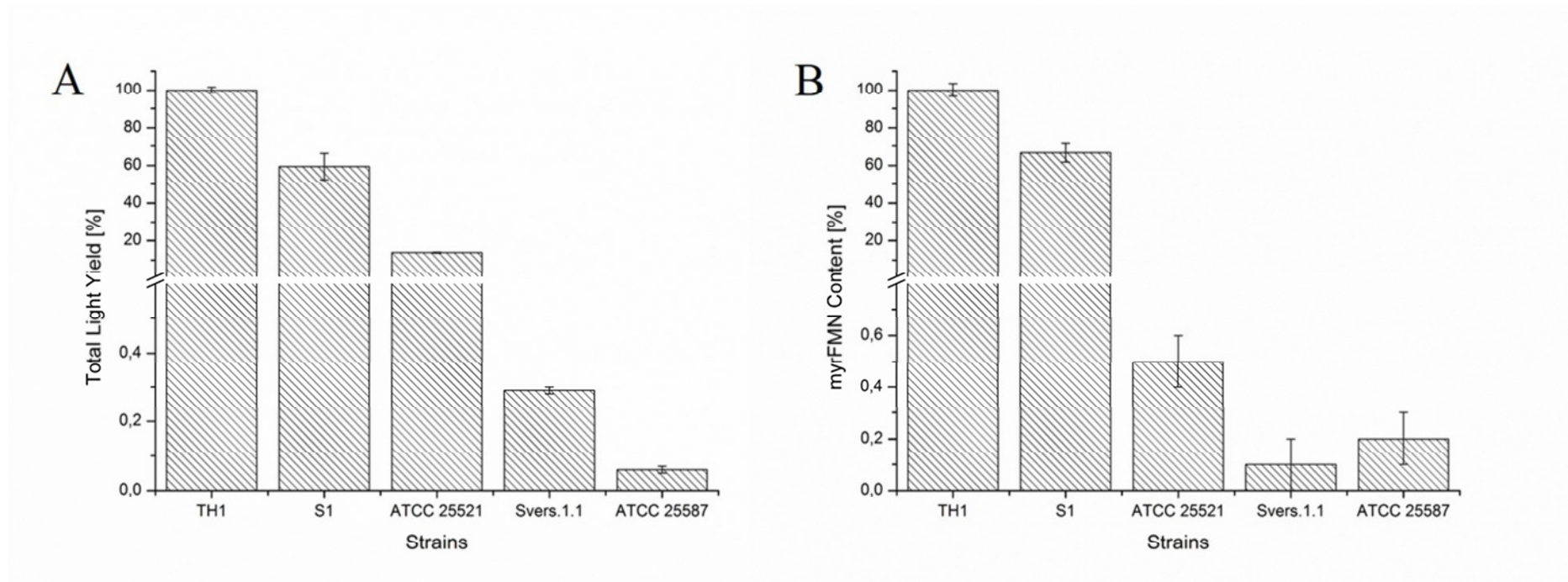


**Figure 1:** Comparison of different Photobacteria strains: Strains were grown under the same conditions and analysed regarding the total light yield (Panel A) and the corresponding myrFMN content. The strains TH1, S1 and svers.1.1 are *luxF*<sup>+</sup>; the two strains ATCC 25521 and ATCC 25587 are *luxF*<sup>-</sup>. TH1 shows the highest total light yield and the highest myrFMN content and was therefore set to 100%. Analyses were carried out at least in triplicate.

**Single and multiple turnover experiments with saturated aldehydes**

If myrFMN is a side product of the luciferase it should be possible to generate myrFMN *in-vitro*. To find the best conditions for such an assay, commercial available aldehydes with different even number chain lengths were tested regarding luciferase activity. In a single turnover experiment the total light yield for aldehydes from C8 up to C14 was measured. The corresponding result of this assay is shown in Figure 2.

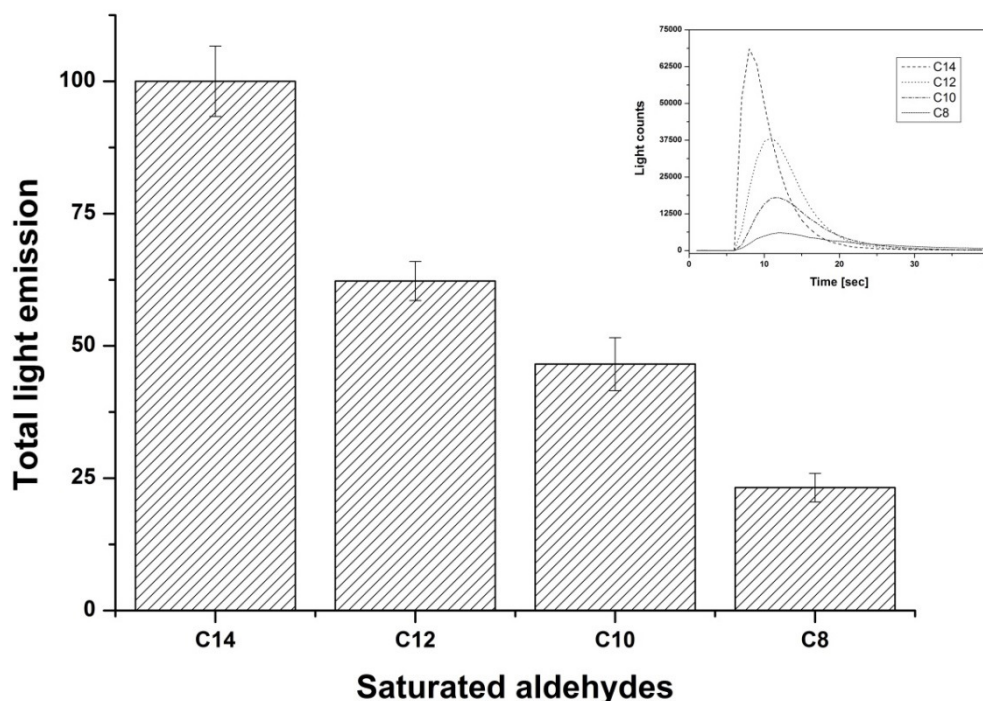


**Figure 2:** Bioluminescence yield observed for different saturated aldehydes. As reported before C14 shows the highest total light yield, with decreasing chain length, the total light emission was reduced. A reduction of the chain length from C14 to C8 resulted in a 75% decrease in the total bioluminescence yield. The observed light emissions as function of time are shown in the insert. Different aldehydes did not only show divergent total light yields, chain length also affected the kinetic behaviour of the luciferase.

As described before, the maximum activity was found for tetradecenal<sup>8</sup>. With decreasing chain length of the aldehyde, the measured activity went down. Since the volume used for bioluminescence measurement was limited by the slot volume of the 96-well plate and the number of possible counts was not high enough to find any myrFMN using the established HPLC detection protocol, an upscale of the reaction was required. Therefore a multiple turnover assay was investigated. Extraction and subsequent analysis did not result in the detection of myrFMN.

***Single and multiple turnover experiments with unsaturated aldehydes***

Analysis of the luciferase reaction (see Scheme 1), regarding the possible formation of a covalent linkage between fatty acid and the isoalloxazine ring revealed that the aldehyde must somehow be activated to force this reaction. In fatty acid biosynthesis such activation could be found during synthesis, an intermediate with a double bond between C2 and C3 is formed and in a subsequent step reduced. If this reduction step is missing, unsaturated fatty acids would be provided to the LuxCDE complex resulting in the formation of unsaturated aldehydes.

Thus, trans-2.3-unsaturated aldehydes with different chain lengths were tested as possible substrates for the bacterial luciferase. The luciferase from *Photobacterium leiognathi* S1 could use these unsaturated aldehydes as substrates. Single turnover assays revealed a decreased total light yield compared to the saturated aldehydes, see Figure 3.

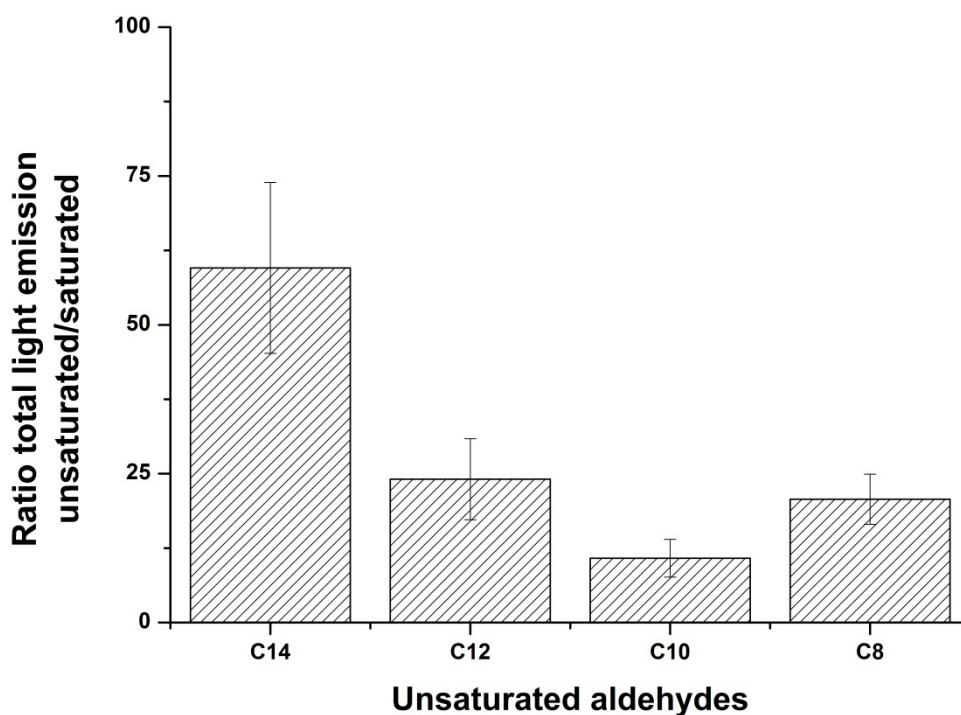


**Figure 3:** Ratios of the total light yields from unsaturated and saturated aldehydes. Since the total light yield observed with the saturated aldehydes was always higher, it was set to 100% and the value of the corresponding unsaturated aldehyde was correlated to this value. The observed ratio varied depending on the chain length.

Ratios varied between 10 and 60%, depending on chain length. The best ratio was observed for trans-2-tetradecenal, the substrate of choice for further experiments.

To set further insight into the generation of the mystery of myrFMN, multiple turnover assays were performed, to evaluate the importance of oxygen these assays were performed under aerobic and anaerobic conditions. A defined peak, with an elution volume of 18.2 ml (elution volume myrFMN main peak ~ 19.3) was present in aerobic samples (See Figure 4). The UV/Vis absorption spectrum was identical to previous reported spectra of myrFMN, with absorption maxima at 386 and 441 nm (Insert Figure 4), respectively.

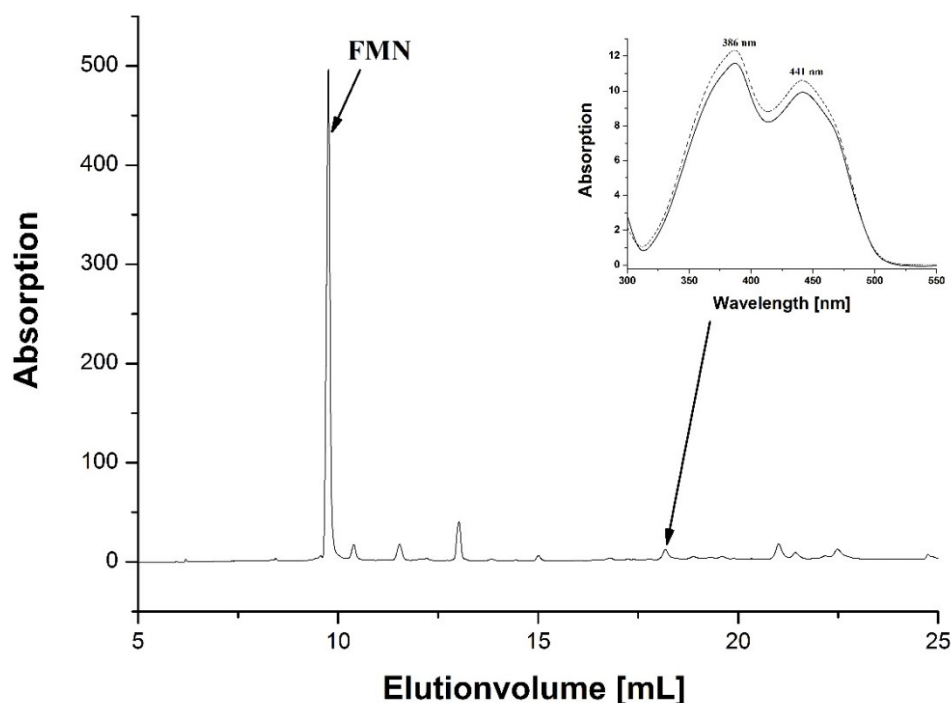


**Figure 4:** HPLC profiles from multiple turnover assays: HPLC elution profiles indicate the presence of several peaks, a peak with a retention time of 18.2 ml shows the characteristic spectrum for myrFMN with peak maxima at 386 and 441 nm. Absorption spectra of the sample (solid line) and myrFMN (dashed line) are shown in the insert.

Under strictly anaerobic conditions no peaks with according elution volume and the correct spectra were observed.

***Inhibition kinetics of the luciferase from *Photobacterium leiognathi* S1***

Tu and co-workers have demonstrated the inhibiting effect of myrFMN on the luciferase from *Vibrio harveyi* in 2001<sup>26</sup>. In a previous publication we used isothermal titration calorimetry (ITC) to evaluate the binding of myrFMN to the luciferase. Binding studies revealed that oxidized myrFMN binds to the luciferase weakly, with a  $K_d = 4.0 \mu\text{M}$ <sup>27</sup>. To study the effect of myrFMN on the bioluminescence yield, an inhibition assay was performed. The myrFMN content was varied from 0 up to 10  $\mu\text{M}$ , which is a 40 fold excess over the luciferase. With increasing myrFMN concentration the total light yield went down, a hyperbolic fit results in a  $K_i = 400 \text{ nM}$  (see Figure 5).

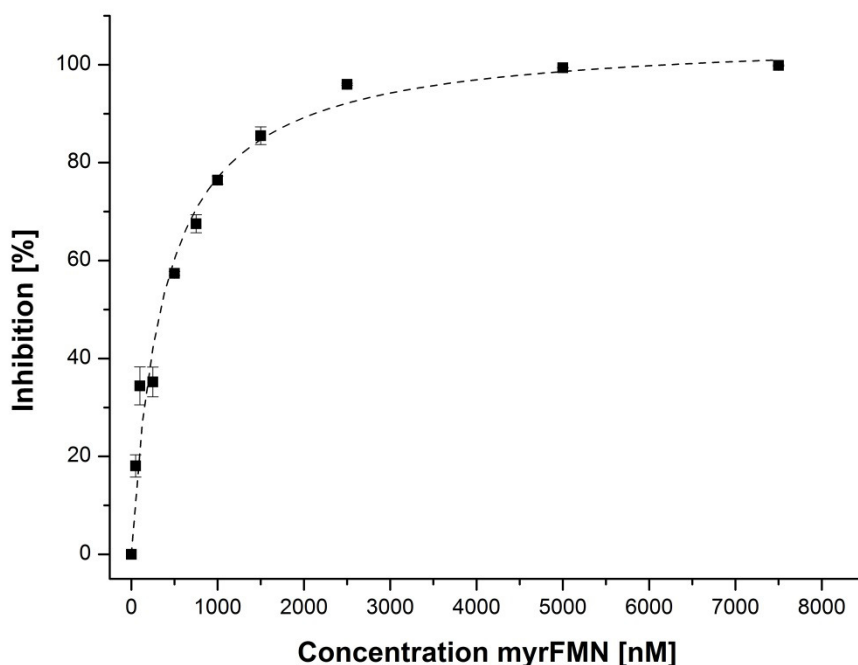


**Figure 5:** Inhibiting effect of myrFMN luciferase activity: myrFMN concentration was varied and the total light yield was determined. With increasing myrFMN concentration the observed activity decreased, a hyperbolic fit of the measured data, indicated a  $K_i$  of 400 nM.

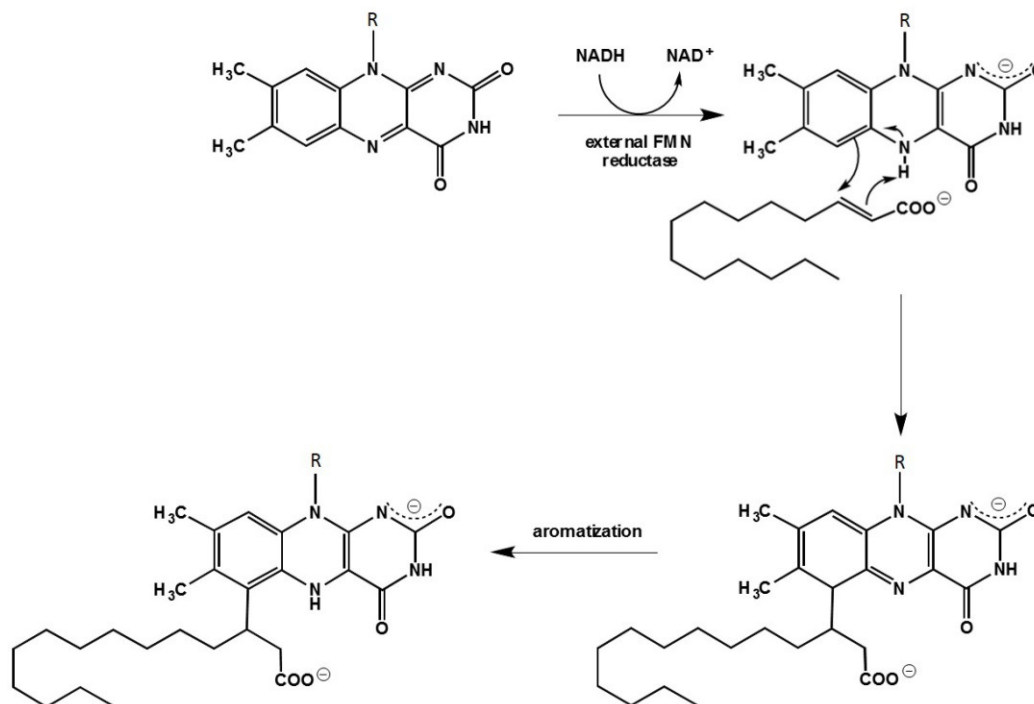
## Discussion

In a previous publication<sup>27</sup>, we have demonstrated that myrFMN production is not restricted to strains with *luxF*<sup>+</sup> background. To elucidate the role of the luciferase in the production of myrFMN, we analyzed strains regarding a potential correlation between light emission and myrFMN content. As indicated in Figure 1 such a correlation could be observed, especially the strains TH1 and S1 (both are *luxF*<sup>+</sup>) confirm this assumption. This finding supports the previous publications<sup>22-25</sup> where they have proposed that myrFMN might be a side product of the luciferase reaction, whereas they conclude this by the fact that both compounds (oxidised FMN and fatty acid) are products of the luciferase reaction, the experimental evidence was still missing.

Minor variations were observed for the other tested strains, these deviations could be explained by the fact that such low myrFMN contents were only slightly over the detection limit of the applied detection method (for further information regarding the applied detection method see Reference<sup>27</sup>). In the case of ATCC 25521 it must be taken into account that this strain is *luxF*<sup>-</sup>, the lack of LuxF would lead to an accumulation of myrFMN in the cell, resulting in a lower light emission. To overcome this problem, *luxF*<sup>-</sup> strains must somehow have found a way to reduce the formation of myrFMN to prevent the luciferase from inhibition as demonstrated in the inhibition assay.

To demonstrate the formation of myrFMN in an *in-vitro* approach, the recombinantly expressed luciferase was coupled with an external FMN reductase (YcnD). Single turnover experiments performed with different aldehydes (Figure 2) demonstrated the preference for tetradecanal, the proposed natural substrate of luciferase<sup>8</sup>. A reduction of the chain length did not only decrease the total light yield, furthermore a different kinetic behaviour, regarding the bioluminescence decay was observed (see Insert Figure 2). Nevertheless neither in single nor in multiple turnover assays any myrFMN could be detected, a possible explanation therefore might be the unreactive carboxylic acid produced during the luciferase reaction. To overcome this problem and facilitate the formation of the covalent linkage, an activated substrate might be beneficial. One possible method to activate the substrate might be the introduction of a double bond between C2 and C3. The presence of the double bond would allow the formation of myrFMN under low oxygen conditions in a mechanism similar to a Michael addition and subsequent rearomatisation, by

tautomerization. The proposed mechanism for the formation of myrFMN is shown in Scheme 2.



**Scheme 2:** Proposed mechanism for the formation of myrFMN

These aldehydes could emerge when the  $\alpha,\beta$ -trans-tetradecanoyl-ACP complex, transfers the fatty acid to the transferase (LuxD) of the “aldehyde synthesis machinery”. This would lead to an acceleration of the aldehyde synthesis and saves NADPH.

Chemically synthesized unsaturated aldehydes were accepted as substrates, with reduced total bioluminescence yield (Figure 3) compared to the saturated aldehydes. The usage of such aldehydes in multiple turn over assays, resulted in one peak, which showed the same UV/VIS absorption spectrum as myrFMN, with absorption maxima at 386 and 441 nm, respectively (Figure 4). The peaks differ in the elution volume, nevertheless also in myrFMN samples of bacterial origin the observed peak with the elution volume of 18.2 ml is present. A possible explanation for this variance might be modifications of the produced myrFMN. Such modifications might be degradation of the flavin, like de-phosphorylation or modifications of the side chains.

The inhibition assay revealed  $K_i$  of 400 nM (Figure 5), which is 10 fold decreased compared to the  $K_d = 4.0 \mu\text{M}$  observed by ITC<sup>27</sup>. Nevertheless it could be compared with the results from Tu and coworkers<sup>26</sup>, where they demonstrated that the luciferase from

*Vibrio harveyi* binds oxidized myrFMN with a  $K_i$  of 160 nM. It could be excluded that the measured  $K_i$  is the product of luciferase and YcnD inhibition, because kinetic parameters of YcnD were not changed in the presence of different myrFMN concentrations (data not shown). Nevertheless, it is possible, that reduced FMN provided by YcnD, could be used either as a substrate for the luciferase reaction or transfers two electrons two myrFMN. Reduced myrFMN could bind then to the luciferase, resulting in a low  $K_i$  compared to the measured  $K_d$ .

## Conclusion

A correlation of myrFMN content and emitted light was found, this finding supports the hypothesis that myrFMN is a side product of the luciferase reaction. During the search for optimal conditions for *in-vitro* myrFMN production, a new substrate for bacterial luciferase was found. Using trans-2-tetradecenal as substrate, the *in-vitro* production of myrFMN could be demonstrated. HPLC analysis of the reaction mixture indicated the presence of a peak with slightly different elution time compared to the main myrFMN peak, observed after isolation. Nevertheless the peak showed the characteristic maxima in the UV/VIS absorption spectrum. A closer look into HPLC elution profiles of isolated myrFMN fractions revealed the presence of the observed peak found in *in-vitro* experiments.

## Outlook

To verify the mechanism behind production of myrFMN further experiments will be performed. The peak observed in *in-vitro* assays will be purified, concentrated and analysed by HPLC/MS.

Furthermore two different *in-vivo* strategies will be used to demonstrate the luciferase involvement in myrFMN production. Therefore different knockouts (*luxAB* or *luxF*) will be done and the arising phenotype will be characterised regarding myrFMN content. If myrFMN is a side product of the luciferase reaction, a knockout of the luciferase should result in the formation in a non-luminescent mutant, which does not contain any myrFMN.

The knockout of *luxF* should lead to an increased intracellular myrFMN content, which inhibits the luciferase and results in a less bioluminescent phenotype.

Beside this, the simultaneous recombinant expression of luciferase and “aldehyde synthesis machinery” (*luxCDE*) in *E.coli*, should demonstrate the involvement of these proteins in myrFMN production.

## References

1. Meighen, E. A. Molecular biology of bacterial bioluminescence. *Microbiol. Rev.* **55**, 123-142 (1991).
2. Dunlap, P. V. in *Encyclopedia of Microbiology (Third Edition)* (ed Schaechter, M.) 45-61 (Academic Press, Oxford, 2009).
3. Fisher, A. J. Three-dimensional structure of bacterial luciferase from vibrio harveyi at 2.4 Å resolution 1,2. *Biochemistry* **34**, 6581-6586 (1995).
4. Fisher, A. J., Thompson, T. B., Thoden, J. B., Baldwin, T. O. & Rayment, I. The 1.5-Å resolution crystal structure of bacterial luciferase in low salt conditions. *J. Biol. Chem.* **271**, 21956-21968 (1996).
5. Campbell, Z. T., Weichsel, A., Montfort, W. R. & Baldwin, T. O. Crystal structure of the bacterial luciferase/flavin complex provides insight into the function of the  $\beta$  subunit. *Biochemistry* **48**, 6085-6094 (2009).
6. Urbanczyk, H., Ast, J. C. & Dunlap, P. V. Phylogeny, genomics, and symbiosis of Photobacterium. *FEMS Microbiol. Rev.* **35**, 324-342 (2011).
7. Baldwin, T. O. *et al.* Structure of bacterial luciferase. *Curr. Opin. Struct. Biol.* **5**, 798-809 (1995).
8. Meighen, E. A. Bacterial bioluminescence: Organization, regulation, and application of the lux genes. *FASEB Journal* **7**, 1016-1022 (1993).
9. Baldwin, T. O., Hastings, J. W. & Riley, P. L. Proteolytic inactivation of the luciferase from the luminous marine bacterium Beneckeia harveyi. *J. Biol. Chem.* **253**, 5551-5554 (1978).
10. Schuster, G. B. Chemiluminescence of organic peroxides. Conversion of ground-state reactants to excited-state products by the chemically initiated electron-exchange luminescence mechanism. *Acc. Chem. Res.* **12**, 366-373 (1979).
11. Eckstein, J. W., Hastings, J. W. & Ghisla, S. Mechanism of bacterial bioluminescence: 4a,5-dihydroflavin analogs as models for luciferase hydroperoxide intermediates and the effect of substituents at the 8-position of flavin on luciferase kinetics. *Biochemistry* **32**, 404-411 (1993).
12. Raushel, F. M. & Baldwin, T. O. Proposed mechanism for the bacterial bioluminescence reaction involving a dioxirane intermediate. *Biochem. Biophys. Res. Commun.* **164**, 1137-1142 (1989).
13. Macheroux, P., Ghisla, S. & Hastings, J. W. Spectral detection of an intermediate preceding the excited state in the bacterial luciferase reaction. *Biochemistry* **32**, 14183-14186 (1993).

14. Kurfurst, M., Ghisla, S. & Hastings, J. W. Characterization and postulated structure of the primary emitter in the bacterial luciferase reaction. *Proc. Natl. Acad. Sci. U. S. A.* **81**, 2990-2994 (1984).
15. Kurfuerst, M., Macheroux, P., Ghisla, S. & Hastings, J. W. Isolation and characterization of the transient, luciferase-bound flavin-4a-hydroxide in the bacterial luciferase reaction. *Biochimica et Biophysica Acta - General Subjects* **924**, 104-110 (1987).
16. Nijvipakul, S. *et al.* LuxG is a functioning flavin reductase for bacterial luminescence. *J. Bacteriol.* **190**, 1531-1538 (2008).
17. Nijvipakul, S., Ballou, D. P. & Chaiyen, P. Reduction kinetics of a flavin oxidoreductase LuxG from photobacterium leiognathi (TH1): Half-sites reactivity. *Biochemistry* **49**, 9241-9248 (2010).
18. Jeffers, C. E. & Tu, S. -. Differential transfers of reduced flavin cofactor and product by bacterial flavin reductase to luciferase. *Biochemistry* **40**, 1749-1754 (2001).
19. Tinikul, R. *et al.* The transfer of reduced flavin mononucleotide from luxg oxidoreductase to luciferase occurs via free diffusion. *Biochemistry* **52**, 6834-6843 (2013).
20. Campbell, Z. T. & Baldwin, T. O. Fre is the major flavin reductase supporting bioluminescence from *Vibrio harveyi* luciferase in *Escherichia coli*. *J. Biol. Chem.* **284**, 8322-8328 (2009).
21. Ellis, H. R. The FMN-dependent two-component monooxygenase systems. *Arch. Biochem. Biophys.* **497**, 1-12 (2010).
22. Moore, S. A., James, M. N. G., O'Kane, D. J. & Lee, J. Crystallization of *Photobacterium leiognathi* non-fluorescent flavoprotein, an unusual flavoprotein with limited sequence identity to bacterial luciferase. *J. Mol. Biol.* **224**, 523-526 (1992).
23. Moore, S. A. & James, M. N. G. Common structural features of the luxF protein and the subunits of bacterial luciferase: Evidence for a (Ba)<sub>8</sub> fold in luciferase. *Protein Science* **3**, 1914-1926 (1994).
24. Moore, S. A. & James, M. N. G. Structural refinement of the non-fluorescent flavoprotein from *Photobacterium leiognathi* at 1.60 Å resolution. *J. Mol. Biol.* **249**, 195-214 (1995).
25. Moore, S. A., James, M. N. G., O'Kane, D. J. & Lee, J. Crystal structure of a flavoprotein related to the subunits of bacterial luciferase. *EMBO J.* **12**, 1767-1774 (1993).
26. Wei, C. -, Lei, B. & Tu, S. -. Characterization of the binding of *Photobacterium phosphoreum* P-flavin by *Vibrio harveyi* luciferase. *Arch. Biochem. Biophys.* **396**, 199-206 (2001).
27. Bergner, T. *et al.* Distribution of 6-(3'-(R)-myristyl)-FMN among bioluminescent marine bacteria and its binding properties to luciferase and LuxF. *unpublished data*.
28. Heuts, D. P. H. M., Scrutton, N. S., McIntire, W. S. & Fraaije, M. W. What's in a covalent bond?: On the role and formation of covalently bound flavin cofactors. *FEBS Journal* **276**, 3405-3427 (2009).
29. Morokutti, A. *et al.* Structure and function of YcnD from *Bacillus subtilis*, a flavin-containing oxidoreductase. *Biochemistry* **44**, 13724-13733 (2005).

---

# **CHAPTER 2.2**

## **2.2 Bioluminescence / The mystery of myrFMN**

---

## Distribution of 6-(3'-(*R*)-myristyl)-FMN among bioluminescent marine bacteria and its binding properties to luciferase and LuxF

Thomas Bergner,<sup>1</sup> Andreas Winkler,<sup>1</sup> Chaitanya R. Tabib,<sup>1</sup> Steve Stipsits,<sup>1</sup> Heidemarie Kayer,<sup>1</sup> John Lee,<sup>2</sup> J. Paul Malthouse,<sup>3</sup> Stephen Mayhew,<sup>3</sup> Franz Müller,<sup>4</sup> Karl Gruber,<sup>5</sup> and Peter Macheroux<sup>1\*†</sup>

<sup>1</sup>Graz University of Technology, Institute of Biochemistry, Graz, Austria

<sup>2</sup>University of Georgia, Department of Biochemistry and Molecular Biology, Athens, GA 30602, U.S.A.

<sup>3</sup>Conway Institute, University College Dublin, Dublin, Ireland

<sup>4</sup>Wylstrasse 13, CH-6052 Hergiswil (formerly Novartis AG, Basel), Switzerland

<sup>5</sup>University of Graz, Institute of Molecular Biosciences, Graz, Austria

Running title: *occurrence and binding properties of myrFMN*

To whom correspondence should be addressed:

Prof. Dr. Peter Macheroux, Graz University of Technology, Institute of Biochemistry, Petersgasse 12/II, A-8010 Graz, Austria, Tel.: +43-316-873 6450; Fax: +43-316-873 6952; Email: peter.macheroux@tugraz.at

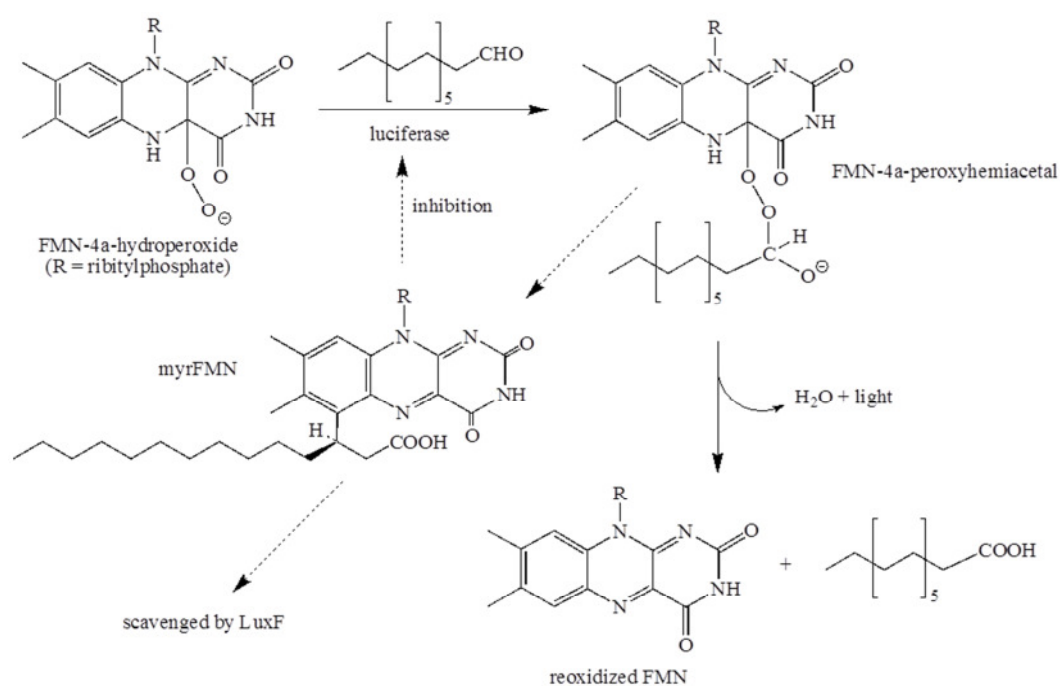
## Abstract

The *lux*-operon of bioluminescent bacteria contains the genes coding for the enzymes required for light emission. Some species of Photobacteria feature an additional gene, *luxF*, which shows similarity to *luxA* and foremost *luxB*, the genes encoding the heterodimeric luciferase. Isolated dimeric LuxF was shown to bind four molecules of an unusually derivatized flavin, *i.e.* 6-(3'-(*R*)-myristyl)-FMN (myrFMN). In the present study we have isolated myrFMN from *Photobacterium leiognathi* S1 to investigate binding to recombinant luciferase and LuxF employing UV/Vis absorption spectroscopy and isothermal microcalorimetry. We found that LuxF tightly binds myrFMN with a dissociation constant of  $80 \pm 20$  nM demonstrating that the purified apo-form of LuxF is fully competent in myrFMN binding. Structure determination by X-ray crystallography confirmed that apo-LuxF possesses four pre-organized binding sites, which are further optimized by adjusting the orientation of amino acid side chains. In contrast to LuxF, binding of myrFMN to luciferase is much weaker ( $K_d = 4.0 \pm 0.4$   $\mu$ M) enabling LuxF to prevent inhibition of the enzyme by scavenging myrFMN. In addition, we have exploited the affinity of apo-LuxF for myrFMN to show that it occurs in all Photobacteria tested irrespective of the presence of *luxF*. Moreover, we have found trace amounts of myrFMN in bioluminescent *Vibrio* and *Aliivibrio* strains thus demonstrating that it is more widely occurring in bioluminescent bacteria than previously assumed.

## Introduction

Bacterial bioluminescence results from the oxidation of a long-chain fatty aldehyde, such as myristic aldehyde, to the corresponding long-chain fatty acid (*e.g.* myristic acid<sup>1, 2</sup>). The bioluminescent reaction is catalyzed by luciferase, an enzyme employing FMN as a redox cofactor to drive the monooxygenation of the aldehyde substrate to the acid product. The free energy released during the oxidation of the aldehyde gives rise to an excited state FMN-4a-hydroxide serving as the luciferin in bacterial bioluminescence<sup>3</sup>. Bacterial luciferase is a heterodimeric protein encoded by *luxA* and *luxB* in the so-called *lux*-operon of bioluminescent bacteria. In addition, the *lux*-operon contains three genes, *luxC*, *luxD* and *luxE*, encoding enzymes for the generation of the aldehyde substrate. Finally, a nicotinamide nucleotide dependent enzyme that produces reduced FMN for bacterial luciferase is encoded by *luxG*<sup>4, 5</sup>. Generally, these genes occur in the order CDABEG in

most bioluminescent bacteria with the exception of some species in the genera *Photobacterium*, such as *P. leiognathi* and *P. phosphoreum*<sup>6</sup>. These bacteria have an additional gene termed *luxF* inserted into the *lux* operon between *luxB* and *luxE*<sup>7-9</sup>. Sequence similarity to *luxB* suggests that *luxF* has arisen by gene duplication, however, its role in bacterial bioluminescence is obscure especially because only free-living but not symbiotic photobacteria appear to exhibit the *luxF* insertion in their *lux*-operon<sup>7</sup>. To shed more light on the role of *luxF*, James and colleagues have solved the structure of the protein isolated from *P. leiognathi*<sup>10, 11</sup>. Interestingly, X-ray crystallographic analysis revealed the presence of four flavin derivatives in the homodimeric protein. The flavins occupy two types of symmetry related binding sites, two at the interface and two at the N-termini. In all four flavins the C-6 carbon of the isoalloxazine ring system is linked to C-3 of myristic acid, *i.e.* 6-(3'-(*R*)-myristyl)-FMN is non-covalently bound to LuxF<sup>12</sup>. Because of its lower fluorescence efficiency (ca. 10-13% compared to FMN<sup>13</sup>) the protein was also referred to as non-fluorescent protein (NFP). The discovery of the myristylated flavin derivative (myrFMN) raised the question of its origin, especially since an unusual carbon-carbon bond is formed in a stereospecific fashion<sup>14</sup>. Since luciferase uses FMN as a co-substrate and myristic acid is the product of the light-producing reaction, it was speculated that myrFMN might be generated as a by-product in this reaction<sup>11, 15</sup>. A summary of the reactions catalyzed by bacterial luciferase and the proposed role of LuxF is shown in Scheme 1.



**Scheme 1:** Reactions catalysed by the luciferase and the role of LuxF

According to this model, LuxF scavenges myrFMN and thus prevents inhibition of luciferase by the side product. In fact, Tu and coworkers could demonstrate that myrFMN inhibits luciferase from *Vibrio harveyi*<sup>16</sup>. Its role as a “molecular sponge” of myrFMN is also supported by the large amounts of LuxF produced by *P. phosphoreum* and *P. leiognathi*. However, production of myrFMN in the luciferase reaction has never been demonstrated and remains to be shown. To better understand the binding of myrFMN to LuxF and luciferase, we have developed a heterologous expression system for *luxF* and *luxAB* in *Escherichia coli*. Here we present a study of the interaction of isolated myrFMN with recombinant LuxF and luciferase (LuxAB). Furthermore, we have employed recombinant LuxF to investigate the relationship of myrFMN production and the presence of *luxF* in the lux operon in various bioluminescent bacteria.

## Experimental procedures

### *Photobacterial strains*

The following *Photobacterium leiognathi* strains were selected for our study: ATCC 25521, ATCC 25587, ATCC 27561, S1, TH1 and svers.1.1. The first two strains were reported to lack *luxF* (*luxF*<sup>-</sup>) whereas ATCC 27561, S1 and svers.1.1 possess *luxF* in the *lux* operon (*luxF*<sup>+</sup>). The presence of *luxF* in TH1 was not reported prior to our study.

### *Instrumentation*

UV/Vis absorption spectra were recorded with a Specord 205/210 spectrophotometer (Analytic Jena, Jena, Germany). Difference absorption spectra were recorded using tandem cuvettes. Isothermal calorimetry titrations were performed with a VP-ITC system (MicroCal, Northampton, MA, USA). <sup>31</sup>P-NMR spectra at 11.75 T were recorded with a Bruker Avance DRX 500 standard-bore spectrometer operating at 202.45631 MHz for <sup>31</sup>P nuclei. 10 mm-diameter sample tubes were used. The spectral conditions for the samples at 11.75 T were: 8192 time-domain data points; spectral width 40 ppm; acquisition time 1.0 s; 3 s relaxation delay time; 90° pulse angle; 256 transients were recorded per spectrum. Spectra were transformed using an exponential weighting factor of 5 Hz. <sup>31</sup>P chemical shifts were referenced to external 85% phosphoric acid (= 0.00 ppm).

***Construction of the expression plasmid for LuxF, LuxAB and LuxB***

Based on the reported amino acid sequence of LuxF<sup>17, 18</sup> a synthetic gene was designed and optimized for expression in *E. coli*. Furthermore a synthetic gene for LuxAB was designed corresponding to the DNA-sequence obtained from S1, with a C-terminal octa-histidine tag, which could be removed by TEV-protease and optimized for expression in *E. coli* (DNA 2.0, CA, USA). The synthetic DNA was integrated into the vector pET-21a(+) using the restriction sites *NdeI* and *XhoI*, allowing the use of the C-terminal hexa-histidine tag of the vector if required for facilitated protein purification by Ni-NTA affinity chromatography. *E. coli* BL21 (DE3) was used for heterologous expression.

Site directed mutagenesis was used to insert an *NdeI* restriction site at the 5-prime end of the *luxB* gene. Further cloning steps were done according the steps described for *luxF* and *luxAB*.

***Expression and purification of the recombinant His<sub>6</sub>-tagged proteins***

*E. coli* BL21 (DE3) cells harboring the expression plasmids were grown at 37 °C in LB broth containing ampicillin (100 µg/ml) as selection marker. The cells were induced with 0.5 mM IPTG at OD<sub>600</sub> = 0.6. After induction the cells were further grown for 4 h at 37 °C (LuxF) or 16 h at 20 °C (LuxAB and LuxB), respectively. Cells were harvested by centrifugation (7,000 g, 10 min, at 4 °C) and the wet cell pellet was stored at -20 °C for further use.

Recombinant protein was purified by resuspension of wet cell paste in lysis buffer pH 8 (50 mM NaH<sub>2</sub>PO<sub>4</sub>·H<sub>2</sub>O, 300 mM NaCl and 10 mM imidazole) and lysed by sonication. To remove cell debris the resulting suspension was centrifuged at 30,000 g for 45 min at 4 °C, followed by an additional filtration step. The cleared solution was then loaded onto a pre-equilibrated 5 ml HisTrap FF column (GE Healthcare), washed with about 10 column volumes of wash buffer (50 mM NaH<sub>2</sub>PO<sub>4</sub>, 300 mM NaCl and 20 mM imidazole) and finally eluted with elution buffer (50 mM NaH<sub>2</sub>PO<sub>4</sub>·H<sub>2</sub>O, 300 mM NaCl and 150 mM imidazole). Protein containing fractions were pooled. In the case of LuxF, the protein was dialyzed against 20 mM Tris buffer containing 100 mM NaCl, pH 8. For LuxAB and LuxB a 45 mM Tris-buffer containing 20 mM L-malic acid and 40 mM MES, pH 8 was used for dialysis. After concentration the proteins were further purified using a Superdex-200 gel

filtration column equilibrated with dialysis buffer. The purified protein was further concentrated and stored at  $-20\text{ }^{\circ}\text{C}$ . The concentration were determined spectrophotometrically at 280 nm using a molar extinction coefficient employing ProtParam at the ExPASy site following the method of Gill and von Hippel<sup>19</sup>. The extinction coefficient for LuxF is  $26,025\text{ M}^{-1}\text{ cm}^{-1}$ , the protein amount isolated from 1 l culture was about 40 mg. LuxAB and LuxB have extinction coefficients of  $83,825\text{ M}^{-1}\text{ cm}^{-1}$  and  $36,580\text{ M}^{-1}\text{ cm}^{-1}$ , respectively. The amount of protein isolated from 1l was 35 mg for LuxAB and 45 mg for LuxB.

### ***Crystallisation and X-ray structure determination***

For crystallization trials purified, recombinant LuxF was used at a concentration of 16 mg/ml. Drops of 1  $\mu\text{l}$  were set up using the microbatch method employing an Oryx 7 crystallisation robot (Douglas Instruments Ltd.). After mixing equal volumes of protein and precipitant solution (0.15 M malic acid, 20% w/v polyethylene glycol 3,350, pH 7.0) tetragonal LuxF crystals grew to full size within 1-2 weeks at 289 K. Crystals were harvested directly from their mother liquor and flash-frozen in liquid nitrogen.

Data from diffraction quality crystals were collected at beamline X06DA (PX-III) of the Swiss Light Source (Paul Scherrer Institute, Villigen, Switzerland). The dataset was integrated and scaled using the XDS suite<sup>20</sup>. Initial phases were obtained by molecular replacement using Phaser<sup>21</sup> with the holo-LuxF structure (pdb-code: 1NFP<sup>12</sup>) as search model. The initial model was further refined against reflection data in alternating cycles of real-space refinement against  $\sigma\text{A}$ -weighted 2FO-FC and FO-FC electron density maps and least squares optimisation (including five TLS groups<sup>21</sup>) using the programs Coot<sup>22</sup> and PHENIX<sup>23</sup>, respectively. Rfree values were computed from 5% randomly chosen reflections, which were not used throughout the refinement<sup>24</sup>.

No electron density was observed for the 8 C-terminal residues originating from the cloning strategy with a hexa-His tag and its two amino acid linker. In addition, weak electron density was observed for one loop region and amino acids 56-59 was therefore omitted from the final model. Coordinates and structure factors were deposited in the Protein Data Bank (PDB) under accession number 4J2P.

***Isolation and purification of LuxF from P. leiognathi S1***

The isolation and purification of LuxF from *P. leiognathi* was described only briefly previously<sup>25</sup>. In the present study, one kg (wet weight) of frozen cell paste was suspended in 500 ml 100 mM Tris/HCl, pH 7.5, containing 1 mM dithiothreitol (DDT) and NaN<sub>3</sub> (in the following called “buffer”). The cells were desintegrated at 4 °C using a French press. The resulting suspension was centrifuged at 27,000 g for one hour at 4 °C. The supernatant was treated with 80% ammonium sulfate (AS) and centrifuged. The precipitate was dissolved in and dialyzed against 4 l of buffer, with two changes in 24 hours, centrifuged 10 min at 39,000 g and 4 °C to remove insoluble material. The clear supernatant was loaded onto a Sepharose Q (11 x 2 cm) column equilibrated with buffer, then washed with buffer, followed by washing with 400 ml buffer containing 0.2 M NaCl and then buffer containing 0.5 M NaCl. Fractions showing absorption at 450 nm were collected and pooled. The pooled fractions were dialyzed against 4 l of buffer, with one change in 24 hours. The lemon yellow dialysate was loaded again onto a Sepharose Q column, washed with 200 ml buffer, followed by 400 ml buffer containing 0.05 M NaCl, 200 ml buffer containing 0.1 M NaCl, 200 ml buffer containing 0.15 M NaCl and 400 ml buffer containing 0.2 M NaCl. Finally, a gradient of 0.2 M – 0.4 M NaCl in buffer (300 ml) was used to elute a brightly yellow protein. The fractions exhibiting a ratio of  $A_{280}/A_{442}$  between 7 and 10 were pooled, concentrated to about 20 ml in an ultrafiltration device (Amicon, 10 kDa filter), and applied to a Sephadex G75 column (90 x 2.5 cm diameter), equilibrated with buffer. Fractions showing a ratio of  $A_{280}/A_{442}$  smaller than four were collected and combined. The yield of LuxF was about 200 mg and exhibited a single band on SDS-PAGE.

***Isolation of 6-(3'-(R)-myristyl)-FMN (myrFMN) from Photobacterium leiognathi S1 using recombinant expressed LuxF***

For isolation of myrFMN, frozen cell paste (~250 g) was allowed to thaw before the cells were suspended in 250 ml of a 0.1 M potassium phosphate buffer, pH 7. To improve cell lysis, the cell suspension was incubated with lysozyme for 30 min before sonication. The lysate was further centrifuged at 30,000 g for 45 min at 4 °C to remove cell debris and the supernatant was filtrated through a Whatman filter (No.1). The supernatant contained free myrFMN as well as protein-bound myrFMN (mostly LuxF).

To retrieve free myrFMN, the supernatant was incubated for 30 min with recombinant histidine-tagged apo-LuxF, which binds four molecules of myrFMN per dimer. LuxF was then collected by Ni-NTA affinity chromatography and purified as described above. The eluent fractions were yellow in color, suggesting the presence of myrFMN, pooled and stored at 4 °C for further use.

For the isolation of myrFMN from LuxF, the flow-through was treated with 4 M guanidinium hydrochloride and adjusted to pH 2 with concentrated HCl to release myrFMN. It was then extracted from the aqueous solution by adding 50-100 ml of n-butanol:ethylacetate (1:1 v/v) solution. The organic phase was separated by centrifugation (4,000 g for 10 min at 4 °C) and removed from the aqueous phase. This procedure was repeated until no yellow color was seen in the precipitate at the phase interface. The organic solvent was then removed in a vacuum evaporator at 50 °C under reduced pressure. The residual powder was dissolved in potassium phosphate buffer.

Free myrFMN captured by recombinant apo-LuxF was released from the protein and extracted as described in the previous section. Desalting of isolated myrFMN was achieved dissolving the yellow powder in 100 mM potassium phosphate buffer pH 7 and loading onto a C18-sepak column, washed with 20 ml of water. The yellow organic eluent was further dried by evaporation and the yellow powder was stored at -20 °C. The purity of myrFMN was evaluated by HPLC.

### ***Detection of luxF in Photobacteria***

In order to analyze the presence of *luxF* in the *lux*-operon colony PCR was conducted using the following primers: 5'-GGAATTCCATATGACAAAATGGAATTATGGCGTCTTCTTCCTTAATTTTACC-3' (forward) and 5'-CCGCTCGAGGTTAAGGTTGTGTTCTTTTCTATAATTAATAACGCG-3' (reverse). An alignment of the known *luxF* sequences is shown in supplementary Figure S1.

***Detection of myrFMN by HPLC***

HPLC analysis was performed with a Dionex UltiMate 3000 HPLC using an Atlantis® dC18 5 $\mu$ M (4.6 x 250 mm) column. Separation was achieved using a linear gradient of 0.1% TFA in water and 0.1% TFA in acetonitrile (20 min, 25 °C) from 0% to 95% at a flow rate of 1 ml/min. Peak detection was at 280, 370 and 450 nm, respectively. Under these conditions FAD, FMN and riboflavin elute at around 10 ml whereas myrFMN elutes at 19 ml.

**Results*****Expression and purification of recombinant LuxF***

Heterologously expressed LuxF was purified using a C-terminal hexa-histidine tag by means of Ni-NTA affinity chromatography (supplementary Figure S2). From 1 liter of bacterial culture 35 mg of purified protein was obtained. The concentrated protein (ca. 20 mg/ml) was colorless with no absorption in the visible range (350-800 nm). This result was not unexpected as the myristylated flavin derivative (myrFMN) is thought to be a side product of the luciferase reaction and the expression host lacks the enzymes responsible for light production (see introduction). Obviously LuxF has a low affinity to other naturally occurring flavin molecules, such as riboflavin, FMN and FAD and hence is isolated as an apoprotein.

***Binding of FMN and myrFMN to apo-LuxF***

To evaluate the binding capacity of isolated apo-LuxF we performed difference titration experiments with FMN and myrFMN isolated from *P. leiognathi* S1 (for isolation of myrFMN see Experimental Procedures). Initially, we observed the absorption changes in the spectrum of FMN and myrFMN, respectively, as a function of LuxF concentration (Figure 1, panel A and B). The concentration dependence yielded a  $K_d$  of ~50  $\mu$ M for the binding of FMN to apo-LuxF (Figure 1, panel A). In contrast to FMN, myrFMN bound much more tightly to apo-LuxF as indicated by the sharp titration end point (Figure 1B, insert).

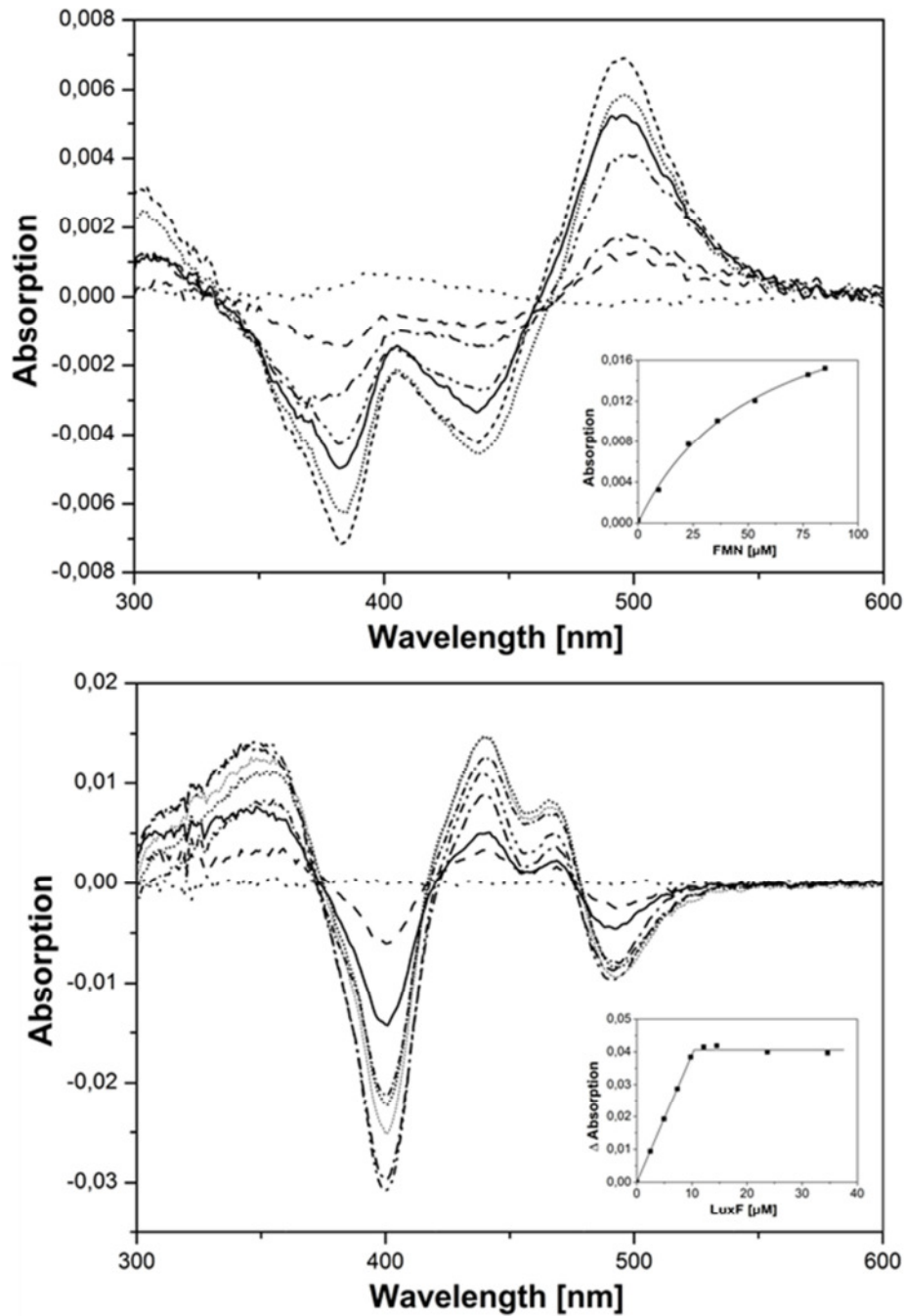


**Figure 1:** Titration of apo-LuxF with FMN (panel A) and myrFMN (panel B) monitored by UV/Vis differential absorption spectroscopy.

Panel A, 50  $\mu\text{M}$  apo-LuxF was titrated with 2.5 mM FMN in tandem cuvettes at 25  $^{\circ}\text{C}$  and absorption spectra were recorded after each addition from 300 to 600 nm. The data points in the insert were fitted to a hyperbolic equation yielding a  $K_d$  of 50  $\mu\text{M}$ .

Panel B, 20  $\mu\text{M}$  myrFMN were titrated with 450  $\mu\text{M}$  apo-LuxF at 25  $^{\circ}\text{C}$  and absorption spectra were recorded after each addition from 300 to 600 nm. Based on the sharp titration endpoint a stoichiometry of four molecules of myrFMN per LuxF-homodimer can be calculate.

Therefore we used isothermal microcalorimetry to determine the dissociation constant for the binding of myrFMN to apo-LuxF. A single binding isotherm was obtained for the titrations with FMN (data not shown) and myrFMN (Figure 2, panel A) indicating that the two binding sites are thermodynamically indistinguishable. Hence, isotherms were fitted to a single binding site model yielding dissociation constants of  $\sim 25 \mu\text{M}$  and  $80 \pm 20 \text{ nM}$  for FMN and myrFMN, respectively.

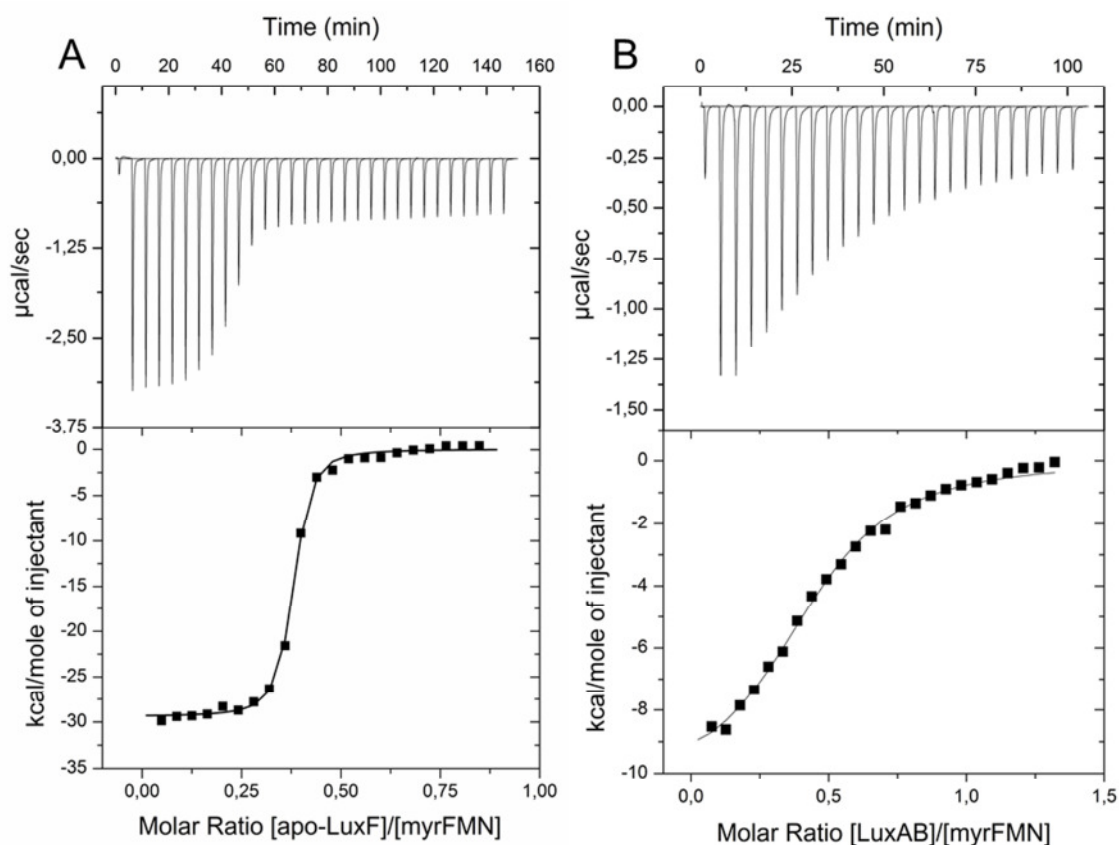


**Figure 2:** Determination of dissociation constants by isothermal titration calorimetry.

Panel A: The measurement shows the titration of 40-45  $\mu\text{M}$  myrFMN with recombinant apo-LuxF (300  $\mu\text{M}$  in 20 mM Tris-buffer, containing 100 mM NaCl, pH 8 at 25  $^{\circ}\text{C}$ ).

Panel B: The measurement shows the titration of  $\sim 45 \mu\text{M}$  myrFMN with recombinant luciferase (450  $\mu\text{M}$  in 45 mM Tris-buffer containing 20 mM L-Malic acid and 40 mM, pH 8 at 25 $^{\circ}\text{C}$ )

***Binding of myrFMN to photobacterial luciferase***

In parallel microcalorimetry experiments, myrFMN was titrated with recombinant luciferase (LuxAB from *P. leiognathi* S1) (Figure 2, panel B). This yielded a dissociation constant of  $4.0 \pm 0.4 \mu\text{M}$  (three independent ITC measurements). Thus binding of myrFMN to luciferase is 50-fold weaker than to apo-LuxF. In a similar experiment recombinant  $\beta$ -homodimer of *P. leiognathi* luciferase was titrated with myrFMN. No binding was observed in this case indicating that the  $\beta$ -homodimer does not bind myrFMN.

***Crystal structure of apo-LuxF***

The high affinity of LuxF to myrFMN suggested that the recombinant protein adopts a native structure, which is fully competent to scavenge the derivatised flavin. To get more insight into the apo-structure of LuxF and the changes occurring upon myrFMN binding we analyzed our colorless LuxF crystals by X-ray crystallography. Data sets diffracting to 1.85 Å resolution were collected using synchrotron radiation at the Swiss-Light-Source (SLS) in Villigen, Switzerland and the structure was solved by molecular replacement. The tetragonal crystal form (space group I422) contained one protein chain in the asymmetric unit which forms a dimer with a symmetry equivalent molecule according to a PISA (Proteins, Interfaces, Structures and Assemblies) analysis<sup>26</sup>. As shown in Figure 3, the overall structure of recombinant LuxF is very similar to the one determined earlier for the holo-protein. The dimeric structures could be aligned with an RMSD of ca. 0.42 Å using the protein structure alignment tool in PyMol. The largest differences were found in loop regions located at the interface of the homodimer (Figure 4). Two myrFMN binding sites in the homodimer are located near these loops and are reorganized upon ligand binding. A comparison of this region (Figure 3, panels A and B) shows substantial movement of some amino acid side chains that engage with hydroxyl groups of the ribitylphosphate side chain attached to N(10) of the isoalloxazine ring.

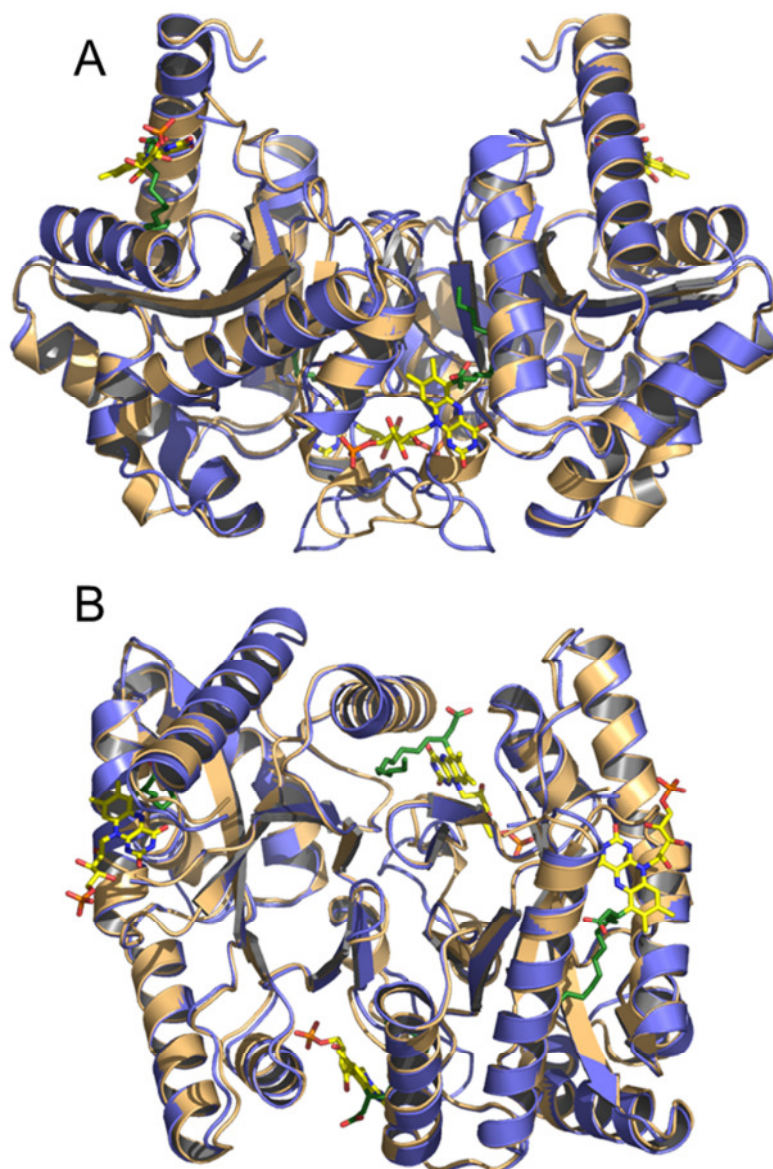


**Figure 3:** Structure alignment of recombinant apo-LuxF with native LuxF. Both structures are shown as cartoon models. The native LuxF (1NFP) is shown in blue and apo-LuxF in light brown. The myristylated flavin derivative (myrFMN) is shown as a stick model with the FMN moiety in yellow and the myristyl chain in green. (A) The homodimer features two sets of equivalent myrFMN binding sites: two at the interface (lower central part) and two at the N-termini (upper left and right). (B) View into the LuxF barrel (90° rotated with respect to structure shown in panel A).

These amino acids form hydrogen bonds to C2'(OH) (Lys84), C3'(OH) (Tyr14), C4'(OH) (Thr81) and a salt bridge to the phosphate group (Lys61). In contrast to these pronounced changes near the ribitylphosphate side chain, the isoalloxazine ring system, as well as the C6-myristyl side chain, are embedded in a pre-organized binding pocket with rather small spatial adjustments of amino acid side chains (see Figure 4, panels A and B).

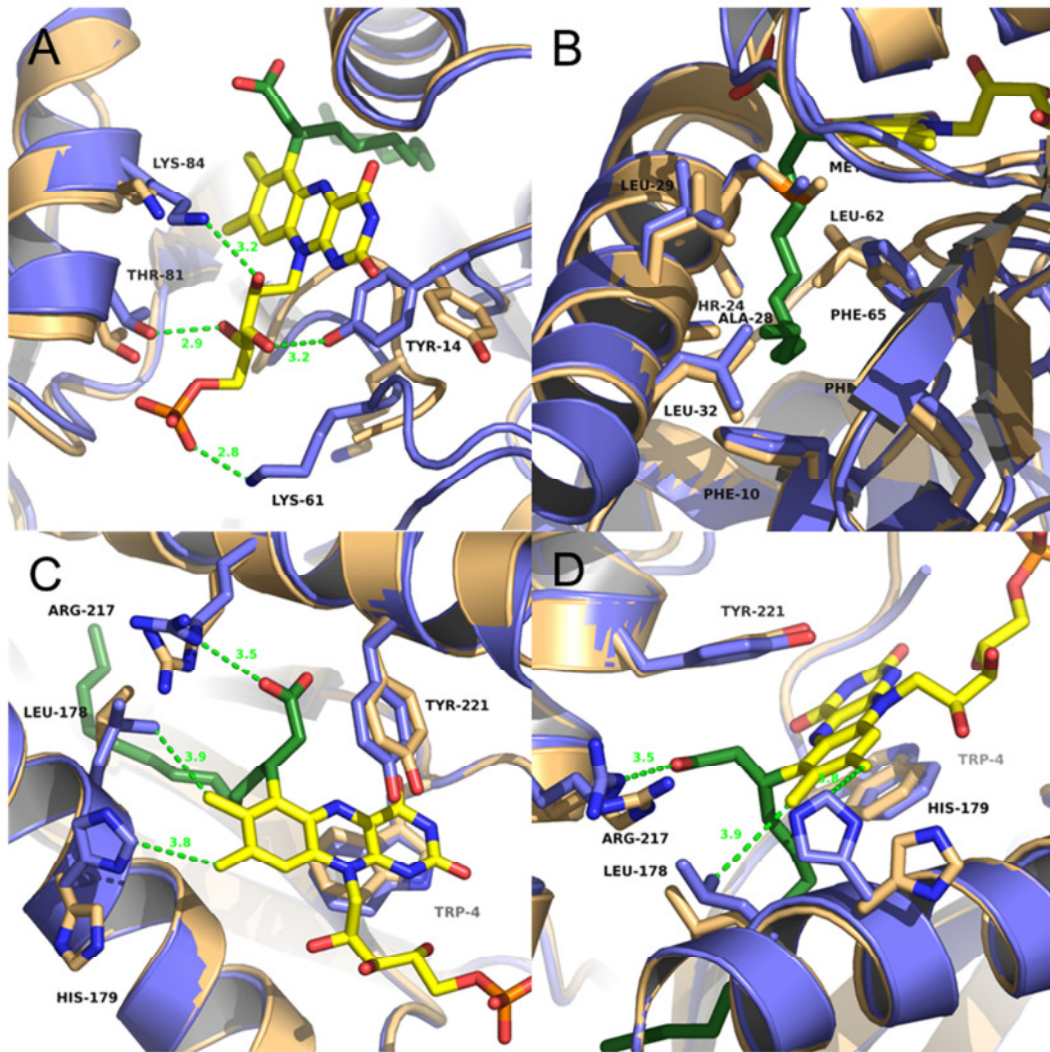


**Figure 4:** Detailed view of the binding sites of myrFMN. (A) Interaction between amino acids and the ribitylphosphate side chain. Amino acids are shown as stick models using the same color-coding as in Figure 3. Hydrogen bond interactions are formed between the hydroxyl group of Thr81 and the C4'-OH (2.9 Å), the hydroxyl group of Tyr14 and the C3'-OH (3.2 Å) and the amino group of Lys84 (3.2 Å) and the C2'-OH of the ribityl side chain. In addition a salt bridge between the amino group of Lys61 and the phosphate group is established (2.8 Å). (B) Rendition of the hydrophobic channel accommodating the myristyl chain. (C) Side-chain interaction between Arg217 and the carboxyl group of the myristic acid moiety (3.5 Å, top left) and Leu178 and His179 to the benzene ring moiety of the isoalloxazine ring (3.9 Å and 3.8 Å, respectively, central left). Note the similar position of Tyr221 and Trp4 in the apo- and holo-structures. (D) Edge-on view of the isoalloxazine ring showing the different orientations of Leu178 and His179.

In addition to the two binding sites at the dimer interface, two myrFMN binding sites are found near the N-terminus (Figure 4, panels C and D). The N-terminal binding site is distinct from the interface binding site by having fewer interactions between amino acid side chains and the ribitylphosphate side chain (three versus nine<sup>11</sup>) or in other words, the

ribitylphosphate side chain appears much less involved in binding interactions to the protein in the N-terminal binding site. Closer inspection of the apo- and holo-protein structure at the N-terminal binding sites reveals that other amino acid side chains appear to play a role in accommodating the myrFMN: Most notably, the imidazole ring of His179 swings by ca. 90 degree to lock the isoalloxazine ring in an appropriate position (see Figure 4, panel D). In addition, Leu178 moves closer to the edge of the benzene moiety of the isoalloxazine ring (3.9 Å) and hence the side chains of these two amino acids apparently function as gates of the N-terminal myrFMN binding site. The carboxyl group of the myristyl residue forms a salt-bridge to the guanidinium group of Arg217. This residue is already in place in apo-LuxF and just moves slightly to interact with the carboxyl group. Similar to the interface binding site the hydrophobic channel that holds the remainder of the myristyl moiety is preformed and seems to undergo only slight adjustments upon binding of myrFMN (Figure 4D).

In summary, the two structurally different binding sites respond in different ways to accommodate myrFMN: the interface binding site has a pre-organized acyl- and isoalloxazine binding site and establishes contacts near the ribitylphosphate side chain, whereas the N-terminal binding site features a salt-bridge to the carboxyl group of the myristyl moiety and engages Leu178 and His179 as gates for the isoalloxazine ring with a comparably small number of contacts to the ribitylphosphate side chain.

Some more detailed information regarding flavin binding was obtained by  $^{31}\text{P}$ -NMR spectroscopy. At pH 7.27 there are two main peaks observed resonating at 4.1 ppm and 4.8 ppm and a smaller one at 4.7 ppm. Deconvolution of the spectrum revealed that the peak at 4.1 ppm accounts for 49% of the total intensity while the smaller peak at 4.8 ppm accounts for 35%. The origin of the small peak at 4.7 ppm (16 %) remains unassigned. The line width of the peak at 4.1 and 4.8 ppm is 22 Hz and 9 Hz, respectively (determined under proton decoupling conditions). The line widths strongly indicate that the two phosphate groups of the two flavins in the protein experience a different environment and/or mobility. Additions of incremental amounts of  $\text{Mn}^{2+}$  to the preparation revealed that the peak at 4.8 ppm broadens somewhat faster than the peak at 4.1 ppm. These data, in combination with the line widths, very strongly indicate that the peak at 4.8 ppm can be assigned to the phosphate group of the flavin located at the interface of the protein. Conversely the peak at 4.1 ppm is assigned to the flavin located close to the surface at the N-terminal binding site.

---

This interpretation is in full agreement with the X-ray data (see above). The accessibility of the two phosphate groups bound to the protein prompted us to undertake a pH-dependent study of the  $^{31}\text{P}$ - NMR spectra. For the high and low field peak a pKa value of 6.3 and 6.0, respectively, was determined (data not shown). The current  $^{31}\text{P}$ - NMR data of the protein show very unusual features as compared to those of flavoproteins of similar sizes, e.g. flavodoxins<sup>27</sup> as none show a pH-dependency or bulk solvent accessibility.

#### ***Screening several species of Photobacteria with apo-LuxF***

Since binding of myrFMN to recombinant apo-LuxF is very tight we used it to monitor its occurrence in several bioluminescent marine bacteria (see Experimental Procedures). This analysis was performed in two ways: Primarily, we incubated the supernatant of cell extracts with recombinant apo-LuxF to scavenge free myrFMN. Furthermore, we precipitated the proteins using 4 M guanidinium hydrochloride to release any protein-bound myrFMN (from LuxF and possibly luciferase) and then repeated the analysis. In each case, the histidine-tagged LuxF was isolated by affinity chromatography. Bound myrFMN was then released by acid precipitation from the purified recombinant LuxF and the supernatant subjected to HPLC analysis. As shown in Figure 5, myrFMN was clearly detectable in the untreated supernatant of crude extracts as well as in the acid-treated fraction. Furthermore our analysis showed that the majority of myrFMN was in the bound fraction, *i.e.* bound to either LuxF or luciferase.

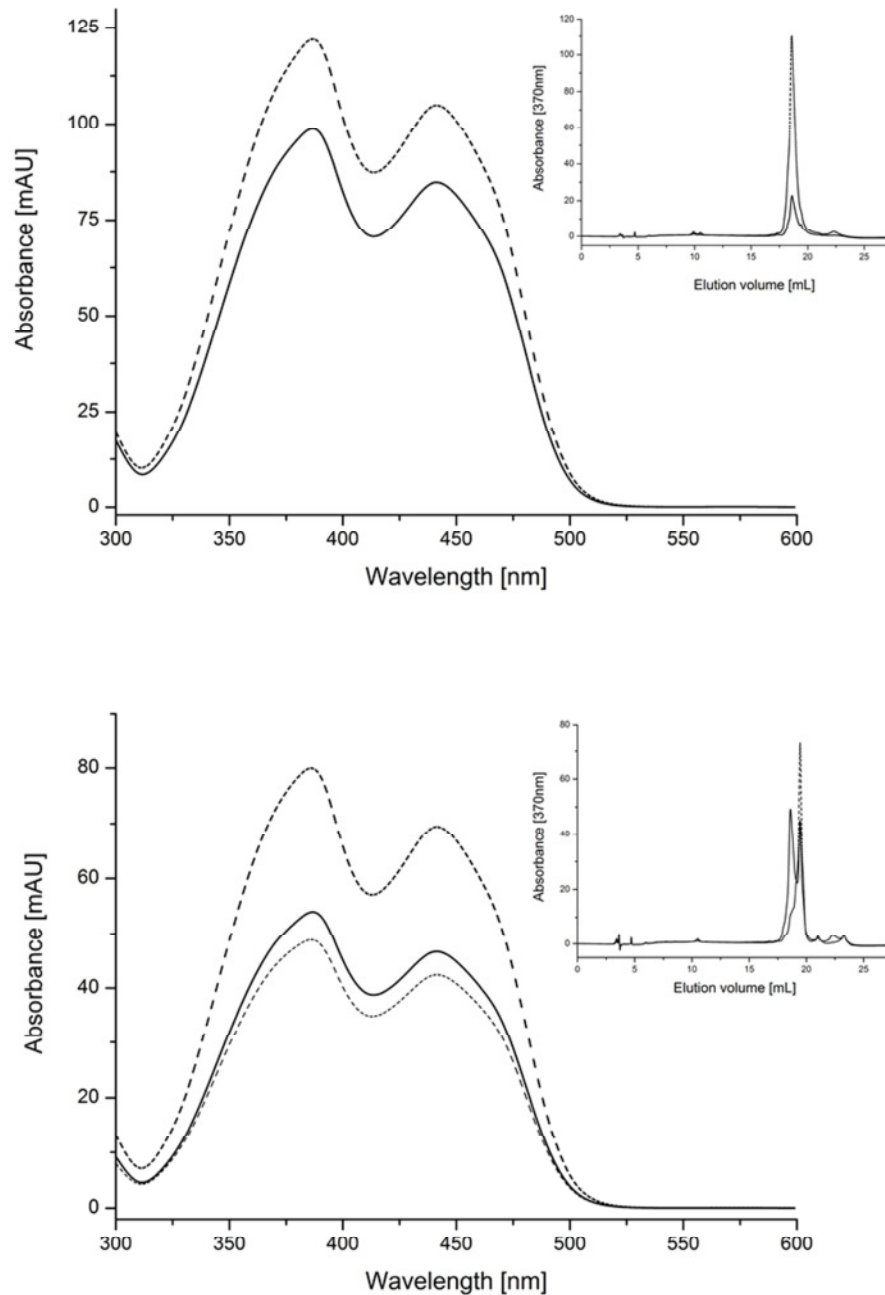


**Figure 5:** Identification of myrFMN scavenged by apo-LuxF from *P. leiognathi* S1 (top panel) and TH1 (bottom panel). Top, UV/Vis absorption spectrum of the flavin released from recombinant LuxF after incubation with cell lysate from *P. leiognathi* S1 before (solid line) and after acid precipitation (dashed line). Insert shows the chromatograms from HPLC analysis. A similar analysis using *P. leiognathi* TH1 is shown in the bottom panel: UV/Vis absorption spectrum of the flavin released from recombinant LuxF before (dashed-dotted line) and after acid-treatment of the crude cell lysate (solid line and dotted line, representing the phosphorylated and dephosphorylated form of myrFMN). myrFMN isolated from the bound fraction was further treated with phosphatase resulting in a shift from 18 ml to 19.5 ml elution volume. The insert shows the HPLC trace of myrFMN isolated from the bound fraction before (solid line featuring two peaks) and after phosphatase treatment (dashed line with a single peak at 19.5 ml elution volume).

The highest amount of myrFMN was found in *P. leiognathi* S1 and TH1. However, trace amounts were also detected in all other photobacterial strains analyzed in our study. Because the composition of the *lux*-operon was not clear for TH1 we performed colony PCR with *luxF* specific primers to check for the presence of *luxF* (see Experimental Procedures). As expected a PCR product with the calculated size of ~680 bp was obtained for *P. leiognathi* S1, ATCC 27561 and svers.1.1 but not for ATCC 25521 and ATCC 25587 (Figure 6A, insert). In addition, a PCR product was obtained for strain TH1 indicating the presence of *luxF*.

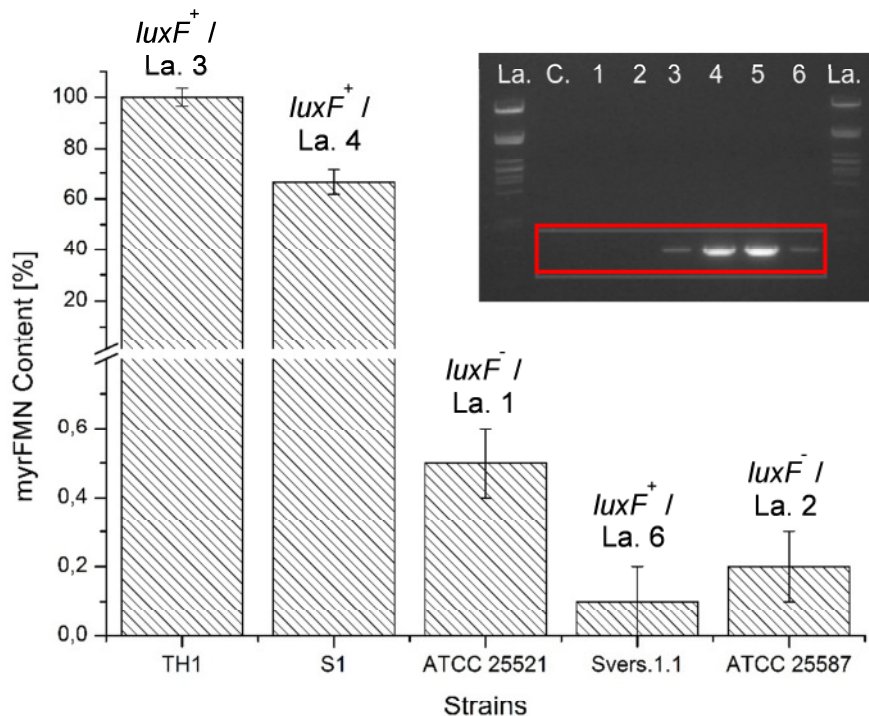


**Figure 6:** Generation of myrFMN in various species of *Photobacteria*. Total amount of myrFMN isolated from the cells grown in liquid culture. TH1 produced the highest amount of myrFMN and was set to 100%. The strains TH1, S1 and svers.1.1 are *luxF*<sup>+</sup> and the two strains ATCC 25521 and ATCC 25587 are *luxF*<sup>-</sup>. The analysis was carried out in triplicate. Insert shows the analysis of different *P. leiognathi* strains for the presence of *luxF* in the *lux*-operon. Shown are the results from colony PCR with common primers for *luxF* (see Experimental Procedures). Lanes were loaded with the following samples: La., λPstI ladder; C., sterile control (sample contains H<sub>2</sub>O instead of DNA); 1, ATCC 25521; 2 ATCC 25587; 3, TH1; 4, *P. leiognathi* S1; 5, ATCC 27561 and 6, svers.1.1.

To further substantiate the presence of *luxF* in TH1, the PCR product was sequenced and compared with known *luxF* sequences. As shown in supplementary Figure S1, the PCR product obtained for TH1 is highly similar to previously reported *luxF* sequences and thus confirms the presence of *luxF* in this strain.

Since the occurrence of myrFMN in all tested photobacterial strains appears to be independent from the presence of *luxF*, we wondered whether myrFMN is also produced in other bioluminescent genera, e.g. *Vibrio* and *Aliivibrio*. Using recombinant apo-LuxF as a scavenger, we were able to detect myrFMN in *Aliivibrio* and *Vibrio*. Albeit the amount found in these species were considerably lower amounting below 4% and around 2% for *Aliivibrio* and *Vibrio*, respectively, in comparison to *P. leiognathi* TH1. This result suggests that generation of myrFMN occurs ubiquitously in bioluminescent bacteria and is not confined to *Photobacteria*.

## Discussion

The generation of 6-(3'-(*R*)-myristyl)-FMN (myrFMN) in some species of *Photobacteria* is a largely unexplored phenomenon in bacterial bioluminescence. According to a current hypothesis, myrFMN is produced in a side-reaction of luciferase and LuxF functions as a scavenger to prevent its inhibition (Scheme 1)<sup>11</sup>. Although this appears to be a plausible explanation, solid experimental evidence is limited to a study of the affinity and inhibitory effect of myrFMN on luciferase from *Vibrio harveyi*<sup>16</sup>. However, the relationship between the occurrence of *luxF* and the generation of myrFMN remained to be analyzed. Therefore, we set out to study the binding properties of apo-LuxF because despite the availability of a three-dimensional structure of holo-LuxF<sup>10-12</sup> nothing was known about the ligand binding specificity and affinity of the protein. Similarly, binding of myrFMN to photobacterial luciferase was not investigated in any detail yet. Furthermore, we were interested whether the generation of myrFMN is linked to the presence of *luxF* in the *lux*-operon. To address these questions we established the recombinant production of LuxF and luciferase by expressing *luxF* and *luxAB* from *P. leiognathi* S1, respectively, in *E. coli* host cells. To assess the binding specificity and affinity of LuxF, we performed difference absorption titrations with FMN and myrFMN isolated from *P. leiognathi* S1 (see Experimental Procedures). These experiments showed that both flavins bind to recombinant apo-LuxF albeit with different affinities (Figure 1). In the case of myrFMN the sharp titration

endpoint suggested binding in the low micromolar range and therefore accurate determination of the dissociation constant was achieved by ITC (Figure 2). These measurements yielded dissociation constants of 25  $\mu\text{M}$  and 80 nM for FMN and myrFMN, respectively, indicating that the myristic acid moiety substantially contributes to the binding energy. Interestingly, the two distinct binding sites appear to be fairly similar in their affinity to myrFMN and FMN since the binding isotherm could be fitted to a single site-binding model despite the differences seen in  $^{31}\text{P}$ -NMR spectroscopy. Similarly, the spectral changes observed in difference absorption spectroscopy proceeded with a single set of isosbestic points again indicating that the two sites provide similar environments with similar binding affinities.

Crystals obtained with recombinant LuxF were colorless and this led to the conclusion that LuxF was isolated in an unliganded form, *i.e.* as an apo-protein. This was not unexpected since *E. coli* lacks the genes *luxAB* encoding luciferase, which is held responsible for the generation of myrFMN. On the other hand, this initial observation also indicated that other naturally occurring flavin derivatives, such as riboflavin, FMN and FAD, do not bind (tightly) to LuxF. This was confirmed for FMN (as the most likely candidate to bind to apo-LuxF), which exhibits a dissociation constant in the range of 25-50  $\mu\text{M}$  and is thus 300-600 fold higher than for myrFMN.

Structural analysis by X-ray crystallography confirmed that the four binding sites in the LuxF dimer were not occupied. The overall topology of apo-LuxF is nearly identical to the previously reported (holo-) LuxF structure (RMSD of 0.42 Å, see Figure 3). Differences are seen mainly in the interface binding pocket where loops are reorganized to enable contacts between amino acid side chains and the N(10)-ribitylphosphate chain of myrFMN, *e.g.* formation of contacts to Tyr14 and Lys61 (Figure 4). On the other hand, the changes observed in the other binding site near the N-terminus involve reorientation of amino acid side chains to form additional contacts (*e.g.* Arg217 and the carboxyl group of the myristic acid) or to bind the dimethylbenzene moiety of the isoalloxazine moiety (*e.g.* His179). Hence, LuxF provides two preorganized binding pockets, which are further optimized in the course of myrFMN binding.

Having demonstrated that recombinant apo-LuxF tightly binds myrFMN we exploited this property to analyze different bioluminescent species for their myrFMN content. This revealed that myrFMN occurs in all strains regardless of the presence of *luxF* in the *lux*-operon. This finding rules out that LuxF is the source of myrFMN as speculated earlier<sup>28</sup>.

In the strongest producers of myrFMN, TH1 and S1, we found that a substantial fraction of myrFMN occurred free in the cell indicating that its production outruns the biosynthesis of the scavenger protein LuxF. Moreover, we could also detect myrFMN in all of the *Vibrio* (*Vibrio harveyi*, etc.) and *Aliivibrio* strains, albeit to a much lower extent. This finding further supports our conclusion that the generation of myrFMN is independent of the presence of *luxF* and also demonstrates that myrFMN generation is by no means confined to *Photobacteria*. This suggests that the postulated luciferase side reaction is a ubiquitously occurring phenomenon in bacterial bioluminescence.

## References

1. Hastings, J. W., Spudich, J. & Malnic, G. The influence of aldehyde chain length upon the relative quantum yield. *The Journal of biological chemistry* **238**, 3100-3105 (1963).
2. Ulitzur, S. & Hastings, J. W. Evidence for tetradecanal as the natural aldehyde in bacterial bioluminescence. *Proc. Natl. Acad. Sci. U. S. A.* **76**, 265-267 (1979).
3. Kurfurst, M., Ghisla, S. & Hastings, J. W. Characterization and postulated structure of the primary emitter in the bacterial luciferase reaction. *Proc. Natl. Acad. Sci. U. S. A.* **81**, 2990-2994 (1984).
4. Li, X., Chow, D. -. & Tu, S. -. Thermodynamic analysis of the binding of oxidized and reduced FMN cofactor to *Vibrio harveyi* NADPH-FMN oxidoreductase FRP apoenzyme. *Biochemistry* **45**, 14781-14787 (2006).
5. Nijvipakul, S. *et al.* LuxG is a functioning flavin reductase for bacterial luminescence. *J. Bacteriol.* **190**, 1531-1538 (2008).
6. Meighen, E. A. Bacterial bioluminescence: Organization, regulation, and application of the lux genes. *FASEB Journal* **7**, 1016-1022 (1993).
7. Lee, C. Y., Szittner, R. B. & Meighen, E. A. The lux genes of the luminous bacterial symbiont, *Photobacterium leiognathi*, of the ponyfish. Nucleotide sequence, difference in gene organization, and high expression in mutant *Escherichia coli*. *European Journal of Biochemistry* **201**, 161-167 (1991).
8. Soly, R. R., Mancini, J. A., Ferri, S. R., Boylan, M. & Meighen, E. A. A new lux gene in bioluminescent bacteria codes for a protein homologous to the bacterial luciferase subunits. *Biochem. Biophys. Res. Commun.* **155**, 351-358 (1988).
9. Mancini, J. A., Boylan, M., Soly, R. R., Graham, A. F. & Meighen, E. A. Cloning and expression of the *Photobacterium phosphoreum* luminescence system demonstrates a unique lux gene organization. *J. Biol. Chem.* **263**, 14308-14314 (1988).
10. Moore, S. A. & James, M. N. G. Common structural features of the luxF protein and the subunits of bacterial luciferase: Evidence for a (Ba)<sub>8</sub> fold in luciferase. *Protein Science* **3**, 1914-1926 (1994).
11. Moore, S. A., James, M. N. G., O'Kane, D. J. & Lee, J. Crystal structure of a flavoprotein related to the subunits of bacterial luciferase. *EMBO J.* **12**, 1767-1774 (1993).

12. Moore, S. A. & James, M. N. G. Structural refinement of the non-fluorescent flavoprotein from *Photobacterium leiognathi* at 1.60 Å resolution. *J. Mol. Biol.* **249**, 195-214 (1995).
13. Raibekas, A. A. Green flavoprotein from *P. leiognathi*: purification, characterization and identification as the product of the lux G(N) gene. *J. Biolumin. Chemilumin.* **6**, 169-176 (1991).
14. Kasai, S. Preparation of P-flavin-bound and P-flavin-free luciferase and P-flavin-bound β-subunit of luciferase from *Photobacterium phosphoreum*. *J. Biochem.* **115**, 670-674 (1994).
15. Hastings, J. W., Potrikus, C. J., Gupta, S. C., Kurfürst, M. & Makemson, J. C. Biochemistry and physiology of bioluminescent bacteria. *Adv. Microb. Physiol.* **26**, 235-291 (1985).
16. Wei, C. -, Lei, B. & Tu, S. -. Characterization of the binding of *Photobacterium phosphoreum* P-flavin by *Vibrio harveyi* luciferase. *Arch. Biochem. Biophys.* **396**, 199-206 (2001).
17. Illarionov, B. A. *et al.* Isolation of bioluminescent functions from *Photobacterium leiognathi*: analysis of luxA, luxB, luxG and neighboring genes. *Gene* **86**, 89-94 (1990).
18. Illarionov, B. A., Protopopova, M. V., Karginov, V. A., Mertvetsov, N. P. & Gitelson, J. I. Nucleotide sequence of part of *Photobacterium leiognathi* lux region. *Nucleic Acids Res.* **16**, 9855 (1988).
19. Gill, S. C. & Von Hippel, P. H. Erratum: Calculation of protein extinction coefficients from amino acid sequence data (Analytical Biochemistry (1989) 182 (319-326)). *Anal. Biochem.* **189**, 283 (1990).
20. Kabsch, W. XDS. *Acta Crystallographica Section D: Biological Crystallography* **66**, 125-132 (2010).
21. McCoy, A. J. *et al.* Phaser crystallographic software. *Journal of Applied Crystallography* **40**, 658-674 (2007).
22. Emsley, P., Lohkamp, B., Scott, W. G. & Cowtan, K. Features and development of Coot. *Acta Crystallographica Section D: Biological Crystallography* **66**, 486-501 (2010).
23. Adams, P. D. *et al.* PHENIX: A comprehensive Python-based system for macromolecular structure solution. *Acta Crystallographica Section D: Biological Crystallography* **66**, 213-221 (2010).
24. Kleywegt, G. J. & Brünger, A. T. Checking your imagination: Applications of the free R value. *Structure* **4**, 897-904 (1996).
25. O'Kane, D., Vervoort, J., Müller, F. & Lee, J. Purification and characterization of an unusual 'non-fluorescent' flavoprotein from *Photobacterium leiognathi*. *Flavins and flavoproteins* (Edmondson, D. E. M., D. B. ed.), Walter de Gruyter, Berlin, New York., 641-645 (1987).
26. Krissinel, E. & Henrick, K. Inference of Macromolecular Assemblies from Crystalline State. *J. Mol. Biol.* **372**, 774-797 (2007).
27. Müller, F. Nuclear magnetic resonance studies on flavoproteins. *Chemistry and biochemistry of flavoproteins* (Müller, F. ed.), CRC Press, Boca Raton, Ann Arbor, London., 557-595 (1992).
28. O'Kane, D. J. & Prasher, D. C. Evolutionary origins of bacterial bioluminescence. *Mol. Microbiol.* **6**, 443-449 (1992).

## Acknowledgements

We like to thank Profs. Chaiyen, Mahidol University, and Paul Dunlap, University of Michigan, for the generous gift of *Photobacterium leiognathi* TH1 and ATCC25521, ATCC25587, ATCC27561 and svers.1.1, respectively. We also appreciate the help of Jakov Ivkovic for his support with the HPLC-MS analysis of isolated myrFMN samples.

†This work was supported by the Austrian “Fonds zur Förderung der wissenschaftlichen Forschung” (FWF) through grant P24189-B17 and the PhD program “Molecular Enzymology” (W901).

## Supplementary Figures

```

ATCC27561      ATGACAAAATGGAATTATGGCGTCTTCTTCCTTAATTTTACCATGTAGGACAGCAAGAG 60
TH1           ATGACAAAATGGAATTATGGCGTCTTCTTCCTTAATTTTACCATGTAGGACAGCAAGAG 60
svers.1.1     ATGACAAAATGGAATTATGGTGTCTTCTTCCTTAACCTTTACCATATAGGACAACAAGAG 60
S1 (optimized) ATGACAAAATGGAACACTACGGTGTCTTTTTCTTGAACCTTCTACCACGTTGGTCAACAGGAG 60
fw_primer     ATGACAAAATGGAATTATGGCGTCTTCTTCCTTAATTTTACC
              *****.***** ** ** ***** ** * ** ** ***** .*:**:**.**.***

ATCC27561      CCATCATTAACCATGAGCAATGCGTTAGAAACATTACGTATTATAGATGAAGATACATCT 120
TH1           CCATCATTAACCATGAGCAATGCGTTAGAAACATTACGTATTATGGATGAAGATACCTCC 120
svers.1.1     CCATCATTAACCATGAACAATGCGTTAGAAACATTGCGCATTATGGATGAAGACACATCT 120
S1 (optimized) CCATCCCTGACCATGAGCAACGCCCTGGAAACCTTGCGTATTATCGACGAGGACACGAGC 120
              *****. *.*****.*** ** *.*****.**.** ***** ** *.** ** * ;

ATCC27561      ATCTATGATGTTGTTGCATTTAGCGAACACCACATAGATAAAAAGCTACAATGATGAAACG 180
TH1           ATCTATGATGTTGTTGCATTTAGCGAACACCACATAGATAAAAAGCTACAATGATGAAACG 180
svers.1.1     ATCTATGATGTTGTACATTTAGCGAGCACCACATAGATAAAAAGTTACAATGATGAAACG 180
S1 (optimized) ATCTACGACGTTGTGGCTTTCAGCGAACATCATATTGATAAGAGCTACAATGACGAAACC 180
              ***** ** ***** .*:** *****.** ** **:*****.** ***** *****

ATCC27561      AAATTAGCGCCATTTGTTAGCCTTGGCAAACAAATTCATGTTTTAGCCACCAGCCCTGAA 240
TH1           AAATTAGCGCCATTTGTTAGCCTTGGCAAACAAATTCATGTTTTAGCCACCAGCCCTGAA 240
svers.1.1     AAATTAGCGCCATTTGTTAGCCTTGGCAATCATGTTTATCTTTTAGCCACCAGCACAGAA 240
S1 (optimized) AAGTTGGCGCCGTTCTGTTCTCTGGGTAAGCAGATCCACATCTGGCTACGAGCCGAGAA 240
              **.**.*****.**.** **: ** ** ** ** * * * ** **.*** ** ** *:***

ATCC27561      ACGGTTGTAAAAGCGGCTAAATATGGGATGCCACTACTGTTTAAATGGGATGATAGTCAA 300
TH1           ACGGTTGTAAAAGCGGCTAAATATGGGATGCCACTACTGTTTAAATGGGATGATAGTCAA 300
svers.1.1     ACCGTTGTAAAAGCGGCTAAATATGGGATGCCATTGCTTTTTAAGTGGGATGATAGTCAA 300
S1 (optimized) ACCGTCGTCAAGCGCGCAAATACGGTATGCCGCTGCTGTTCAAGTGGGACGATTCCCAA 300
              ** ** *.** **.***** ***** ** *****. *.** ** **.***** **: **

```

```

ATCC27561      CAAAAGCGTATAGAATTATTAACCATTACCAAGCAGCTGCGGCTAAATTTAATGTCGAT 360
TH1            CAAAAGCGTATCGAATTATTAACCATTACCAAGCAGCTGCGGCTAAATTTAATGTCGAT 360
svers.1.1     CAAAACGTATCGATTTTATTAACCATTACCAAGCTGCTGCGGCTAAATTTAATGTCGAT 360
S1 (optimized) CAGAAGCGTATTGAACTGCTGAACCACTATCAGGCGGCGGCGCAAAGTTCAATGTCGAT 360
               **..***** **: * . * .***** ** **..* ** *****:*** ** *****

ATCC27561      ATTGCAGGTGTTTCGTCATCGATTAATGTTATTTGCAATGTTAATGACAACCCAACGCAA 420
TH1            ATTACAGGAGTTCGTCATCGATTAATGTTATTTGCAATGTTAATGACAACCCAACGCAA 420
svers.1.1     ATTACCGATGTTTCGTCATCGATTAATGGTATTTATCAATGTGAATGAAAACCCAACACAA 420
S1 (optimized) ATCGCTGGCGTGCGCCACCGCTGATGCTGTTTCGTCACAGTTAATGATAATCCAACCCAG 420
               ** . * * . ** * * * * * . * . * * * . * * * * * * * * * * * * * * * * .

ATCC27561      GCCAAAGCTGAGCTTAGCATTACTTAGAAGATTACCTCTCTTACACCCAAGCAGAAACA 480
TH1            GCCAAAGCTGAGCTTAGCATTACTTAGAAGATTACCTCTCTTACACCCAAGCAGAGACA 480
svers.1.1     GCCAAAGCTGAGCTCAGTATTACTTAGAAGATTACCTCTCTTACACCCAAGCAGAGGCA 480
S1 (optimized) GCGAAGGCGGAATTGAGCATTACTTGAGGATTATCTGAGCTACACCCAAGCGGAGACG 480
               ** **..* * . * ** ***** *..***** ** : *****..*..*

ATCC27561      TCCATTGATGAAATCATCAATAGCAATGCTGCAGGCAACTTCGATACGTTGTTACATCAC 540
TH1            TCCATTGATGAAATCATCAATAGTAATACTGCAGGCAACTTCGATACGTTGTTACATCAC 540
svers.1.1     TCTATTGATGAAATCATTAAACAGTAATGCTGCAGGTAACCTTCAATACGTTGTTACCCAC 540
S1 (optimized) TCCATTGACGAAATCATTAAATAGCAATGCAGCAGGCAACTTTGATACCTGCCTGCACCAT 540
               ** ***** ***** ** ** * * .:***** ***** .***** ** * .. **

ATCC27561      GTTGCTGAAATGGCTCAAGGTTTAAATAATAAAGTCGATTTCTTATTTTGCTTTGAATCG 600
TH1            GTTACTGAAATGGCTCAAGGTTTAAATAATAAAGTCGATTTCTTATTTTGCTTTGAATCG 600
svers.1.1     ATTGAGGAAATGGCTCAAGGTTTAAATAATAAAGTTGATTTTTTATTTGTTTGAATCG 600
S1 (optimized) GTGGCGGAGATGGCCAGGTTTGAACAACAAGTCGACTTCTGTTTTGCTTTGAGTCC 600
               . * .. **..***** **..***** ** ** **..* ** * * * .***** *****..**

ATCC27561      ATGAAAGATCAAGAGAATAAAAAATCACTAATGATTAACCTTTGATAAACGCGTTATTAAT 660
TH1            ATGAAGGATCAAGAGAATAAAAAATCACTAATGATTAACCTTTGATAAACGCGTTATTAAT 660
svers.1.1     ATAAAGCTTCAAGACAATAAAAAATCACTAATGATTAATATTGATAAAATAGTTGTTAAT 660
S1 (optimized) ATGAAGGATCAAGAGAACA AAAAGTCTCTGATGATTAATTTGACAACGCGTGATCAAT 660
rv_primer                                           CGCGTTATTAAT
               **..* . :***** ** *****:***.***** :* ** * * . * * *

ATCC27561      TATAGAAAAGAACACAACCTTAACATA 687
TH1            TATAGAAAAGAACACAACCTTAACATA 687
svers.1.1     TATAGAAAAGACACCAACTTAATAA 687
S1 (optimized) TACCGTAAAGAGCACAACCTGAACATA 687
rv_primer     TATAGAAAAGAACACAACCTTAACATA
               ** .*:***...***. . * **..**

```

**Figure S1:** Alignment of different Strains with *luxF*<sup>+</sup> background, DNA sequences and universal primers used for amplification are shown

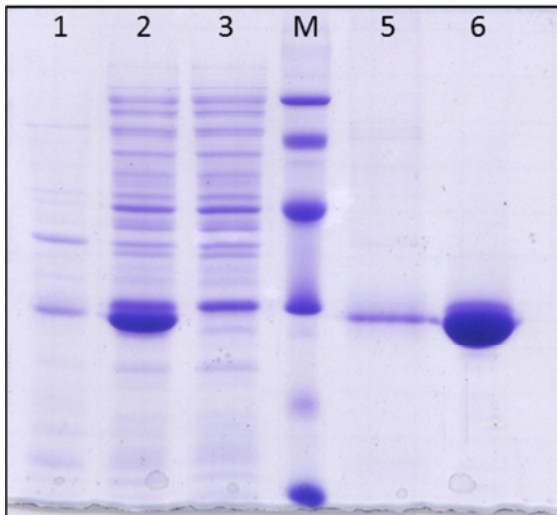


**Figure S2:** Purification profile of LuxF; Lane description: 1: Pellet, 2: Supernatant, 3: Flow through, 4: Pre-stained Protein ladder (M), 5: Ni-NTA purified fraction, 6: Gel Filtration purified fraction.

---

# CHAPTER 3

## **3 Antranoyl-CoA monooxygenase/reductase**

---

## Anthranoyl-CoA monooxygenase/reductase from *Azoarcus evansii* possesses two distinct active sites

Thomas Bergner<sup>1</sup>, Tea Pavkov-Keller<sup>2</sup>, Katharina Lukas<sup>1</sup>, Jakob Kowaliuk<sup>1</sup>, Markus Plank<sup>1</sup>, Kathrin Runggatscher<sup>1</sup>, Benjamin Zucol<sup>1</sup>, Karl Gruber<sup>2</sup> and Peter Macheroux<sup>1\*</sup>

<sup>1</sup>Institute of Biochemistry, Graz University of Technology, A-8010 Graz, Austria

<sup>2</sup>Institute of Chemistry, University of Graz, A-8010 Graz, Austria

<sup>3</sup>Institute of Molecular Biosciences, University of Graz, A-8010 Graz, Austria

\*Running title: *anthranoyl-CoA monooxygenase / reductase*

To whom correspondence should be addressed:

Prof. Dr. Peter Macheroux, Graz University of Technology, Institute of Biochemistry, Petersgasse 12, A-8010 Graz, Austria; Tel.:+43-316-8736450; Fax: +43-316-8736952; Email: peter.macheroux@tugraz.at

## Abstract

In *Azoarcus evansii* an unusual pathway for the degradation of aromatic compounds was investigated. The pathway contains eight enzymes, which are clustered in form of an operon. During evolution the operon was duplicated and integrated into the genome of the organism. In an initial step the substrate (anthranilic acid) is activated by linkage to coenzyme A. The formed CoA-thioester is further processed by the enzyme anthranoyl-CoA monooxygenase/reductase (ACMR), which can catalyse two different reactions. After an initial monooxygenation the resulting intermediate is reduced to a non-aromatic product. Further steps of the pathway are not known yet, but it is assumed that the product is degraded in a way similar to  $\beta$ -oxidation. ACMR is a 87 kDa fusion protein containing one molecule of FAD and one molecule of FMN in the monooxygenase and reductase subunit, respectively. Both substrate binding pockets can be occupied at the same time. Furthermore we could demonstrate that the binding constants were not affected in the presence of the other ligand.

## Introduction

Anthranilic acid is an important intermediate in the synthesis and degradation of many *N*-heterocyclic compounds such as tryptophan. As a consequence of its wide occurrence, anthranilic acid is a common substrate for many microorganisms, which are able to cleave aromatic rings. *Azoarcus evansii* has developed an unusual way for the degradation of such compounds, where typical intermediates like catechol or gentisate were not observed. In contrast to the other known pathways the degradation is linked to the activation of the substrate by the initial formation of a CoA-thioester. The first two enzymes involved in the degradation of anthranilic acid to a nonaromatic product are aminobenzoate-CoA ligase and anthranoyl-CoA monooxygenase/reductase (ACMR). ACMR is a bifunctional flavoenzyme which catalyzes both monooxygenation and hydrogenation of anthranoyl-CoA requiring two NADH and one O<sub>2</sub> molecule<sup>1,2</sup>.

All proteins of the degradation pathway found in *Azoarcus evansii* are encoded by an operon, containing eight genes, besides the before mentioned proteins, three enzymes involved in  $\beta$ -oxidation were identified. During evolution the operon was duplicated and integrated into the genome. When *Azoarcus evansii* is grown under aerobic conditions both operons are

expressed simultaneously resulting in the formation of three different active isoforms of ACMR<sup>2</sup>.

The first reaction catalysed by the homodimeric ACMR is a nucleophilic attack of the C(4a)-hydroperoxyflavin, formed in the active site of the monooxygenase domain, thereby one molecule of oxygen is transferred to position 5 of the activated substrate. Subsequently the intermediate is transferred to the reductase domain, where a hydride transfer leads to the formation of the nonaromatic cyclohexene product. The overall reaction strongly depends on the present NADH concentration. Under NADH limitation no reduction of the formed intermediate occurs, instead of this re-aromatisation is observed<sup>3</sup>.

The N-terminal monooxygenase domain of the protein (amino acid 1-362) shows a high similarity to salicylate hydroxylase of *Bacillus subtilis*. Amino acid 403-773 encoding the C-terminal reductase domain shows high similarity to OYE from *Saccharomyces cerevisiae*<sup>2</sup>.

Binding studies revealed that anthranoyl-CoA can bind to the fully reduced or oxidized form of the enzyme. The binding affinity is quite high with a  $K_d$  of 1-2  $\mu$ M. Previous publications reported the presence of two FAD molecules<sup>1</sup>. In contrast to their finding we could demonstrate the presence of FAD and FMN, respectively. This could be explained with the homology model of the protein, which suggests that the reductase domain adopts a TIM barrel structure, a typical FMN binding fold<sup>4</sup>. The remaining FAD molecule could be assigned to the monooxygenase subunit where it is bound in a Rossman-fold. Furthermore the presence of two independent substrate binding pockets could be demonstrated using difference titration and isothermal titration calorimetry.

## Experimental Procedures

### ***Construction of the expression plasmid for ACMR, ACM and ACR***

Based on the reported DNA sequence found in operon II, a synthetic gene of the ACMR was designed and optimized for expression in *E. coli* (DNA 2.0, CA, USA). Furthermore it contains a C-terminal octa-histidine tag, which can be removed on genetic and protein level (TEV-protease cleaving-site). The synthetic DNA was integrated into the vector pET-21a(+) or pET-28a using the restriction sites *Nde*I and *Xho*I, allowing the use of the N-terminal hexa-

histidine tag of the vector (pET-28a) if required for facilitated protein purification by Ni-NTA affinity chromatography. *E. coli* BL21 (DE3) was used for heterologous expression.

For the expression of the monooxygenase (ACM) and the reductase domain (ACR) either site directed mutagenesis or common PCR with primer overhang was performed (sequences of the used primers are summarized in Supplementary Table T1) so that the construct contained a *Nde*I restriction site at the 5' and a *Xho*I site at the 3' end. Both subunits were expressed with and without the linker region.

*E. coli* BL21 (DE3) and *E. coli* Rosetta (DE3) were used for heterologous expression of ACM and ARC, respectively.

### ***Expression and purification of recombinant His-tagged proteins in E. coli***

*E. coli* cells harbouring the expression plasmids were grown at 37 °C in LB broth depending on the used expression plasmid either ampicillin (100 µg/ml) (for pET-21a) or kanamycin (50 µg/ml) (for pET-28a) were used for selection. The cells were induced with 0.5 mM IPTG at  $OD_{600} = 0.6$ . After induction the cells were further grown for 16 h at 20 °C. Cells were harvested by centrifugation (7,000 g, 10 min, at 4 °C) and the cell pellet was stored at -20 °C for further use.

For purification of the recombinant proteins, the cell paste was resuspended in lysis buffer pH 8 (50 mM  $NaH_2PO_4 \cdot H_2O$ , 300 mM NaCl and 10 mM imidazole) or pH 8.5 for ACR and lysed by sonication. To remove cell debris the resulting suspension was centrifuged at 30,000 g for 45 min at 4 °C, followed by an additional filtration step. The cleared solution was then loaded onto a pre-equilibrated 5 ml HisTrap FF column (GE Healthcare), washed with about 10 column volumes of wash buffer (50 mM  $NaH_2PO_4$ , 300 mM NaCl and 20 mM imidazole) and finally eluted with elution buffer (50 mM  $NaH_2PO_4 \cdot H_2O$ , 300 mM NaCl and 150 mM imidazole). Protein containing fractions were pooled and dialysed against 20 mM Tris buffer containing 100 mM NaCl, pH 8 or pH 8.5 for ACMR and ACM or ACR, respectively. After concentration the proteins were further purified using a Superdex-200 gel filtration column equilibrated with dialysis buffer. The purified protein was concentrated and stored at -20 °C. The concentrations were determined spectrophotometrically. Molar extinction coefficient were determined using the method described by Macheroux<sup>5</sup>, resulting in an extinction coefficient of 21,500  $M^{-1} cm^{-1}$  (459 nm) and 10,130  $M^{-1} cm^{-1}$  (450 nm) for ACMR and ACM, respectively. In the case of ACR the molar extinction coefficient at 280 nm was calculated

employing ProtParam at the ExPASy site following the method of Gill and von Hippel<sup>6</sup>. The extinction coefficient for ACR is  $57785 \text{ M}^{-1} \text{ cm}^{-1}$  (280nm). The amount of isolated protein obtained from 1 l culture was about 25 mg, 30 mg and 15 mg for ACMR, ACM and ACR, respectively.

### ***Determination of flavin composition of ACMR***

For cofactor determination concentrated protein samples were heated up to 95 °C, the precipitate was resuspended in water and denatured protein was removed by centrifugation (7,000 g, 5 min, at 4 °C). To remove the residual protein an additional separation step using an Amicon with a 10 kDa cut off was performed. The flow-through was concentrated at 50 °C under reduced pressure and subsequently loaded on the HPLC.

HPLC analysis was performed with a Dionex UltiMate 3000 HPLC using an Atlantis® dC18 5 $\mu$ M (4.6 x 250 mm) column. As liquid phase a 0.1% TFA solution and acetonitrile containing 0.1% TFA were used, within 20 min the concentration of the organic solvent was increased from 0% to 95% in a linear gradient (T = 25 °C; flow rate = 1 ml/min). The samples were analysed using a diode array detector, the detection wavelengths were set to 280, 370 and 450 nm, respectively.

### ***Transient Kinetics***

Reductive half-reactions were analyzed with a stopped-flow device (SF-61DX2, Hi-Tech) in an anaerobic atmosphere of approx. 0.8 ppm oxygen in a glove box from Belle technology. All samples were rendered oxygen-free by flushing with nitrogen and subsequent incubation in the glove box. The flavin cofactor was reduced using NADPH and changes in flavin absorbance were followed using a PM-61s photomultiplier or a KinetaScanT diode array detector (MG-6560).

### ***Homology modelling***

Structural models of both domains were generated using the Phyre2<sup>7</sup> and Swiss-Model<sup>8</sup> servers. The structures of the OYE from *Thermus scotoductus* (PDB-entry: 3HGJ) and of VioD hydroxylase from *Chromobacterium violaceum* (PDB-entry: 3C4A) were used as

templates for the respective monooxygenase and reductase domain of ACMR. Sequence identities were 34% (for the OYE domain) and 32% (for the hydroxylase domain).

### ***Circular dichroism (CD) analysis***

The CD spectra of purified ACMR were measured on a JASCO (Tokyo, Japan) J-715 spectropolarimeter. CD measurements were performed with protein concentrations of 1.7 mg/ml (10 mM PIPES/Na pH 7.2), 0.9 mg/ml (2 mM Tris/HCl pH 8.0) and 1.2 mg/ml (MilliQ) using a 0.02 cm water-jacket cylindrical cell, thermostatically controlled by an external computer-controlled water bath. The far-UV spectra were recorded at 20 °C as an average of 3 scans from 190 to 260 nm with a 0.5 nm step resolution and a scan speed of 50 nm/min. The correction of the final spectra was accomplished by subtracting the baseline spectra obtained with the corresponding buffer under identical conditions. The results are expressed as the mean residue ellipticity ( $\Theta$ ) at a given wavelength. Protein secondary structure contents were estimated from CD spectra using the CDSSTR method implemented in DICHROWEB<sup>9</sup>.

Thermal denaturation data were recorded in the temperature range from 20 °C to 95 °C by a step scan procedure with a heating rate of 1 °C/min. The thermal denaturation curves were fitted with sigmoidal functions and the 'melting' temperature ( $T_m$ ) was determined as the point of inflection using Origin v6.1 (OriginLab).

### ***ThermoFAD***

A ThermoFAD analysis was performed with an RT-PCR instrument (Bio-Rad). 1  $\mu$ l of ACMR at 30 mg/ml (in 10 mM Tris/HCl pH 8.0) was mixed with the buffer solution to a final volume of 25  $\mu$ L. Two buffer screens were used for the pH-dependent measurements: a) the NOVEL6 buffer system (L-malic acid, MES, Tris) in the pH range 4.0-9.0 containing NaCl (0-1000 mM); b) the JBS solubility screen (Jena Bioscience)<sup>10</sup> containing different buffer solutions at a concentration of 100 mM. A temperature gradient from 25 °C to 95 °C was applied and the fluorescence signal was measured every 0.5 min. Fluorescence measurements were performed using an excitation wavelength range between 470 and 500 nm and a SYBR Green fluorescence emission filter (523–543 nm). The unfolding temperature was determined

as the maximum of the derivative of the sigmoidal curve obtained by plotting the fluorescence intensity against the temperature.

### **SAXS**

Small angle x-ray scattering data were collected on the X33 EMBL beamline at the storage ring DORIS III (DESY, Hamburg, Germany)<sup>11</sup>. The data were recorded using a MAR345 two-dimensional imaging plate detector at a sample-detector distance of 2.7 m and a wavelength of  $\lambda = 0.15$  nm, covering the range of momentum transfer  $0.12 < s < 4.5$  nm<sup>-1</sup> ( $s = 4\pi \sin\theta/\lambda$ , where  $2\theta$  is the scattering angle). Data processing was performed using the program package PRIMUS<sup>12</sup>. The ACMR protein solution (in 10 mM Tris/HCl buffer pH 8.0) was measured at three different concentrations: 3.6, 6.7 and 14.8 mg/ml. Data obtained at the low and high concentration were cut accordingly and merged for subsequent data analysis. The forward scattering  $I(0)$ , the radius of gyration ( $R_g$ ) and the maximum diameter  $D_{max}$  were evaluated using the Guinier approximation<sup>13</sup> and the program GNOM<sup>14</sup>. A solution of bovine serum albumin (MM = 66 kDa) at 5 mg/ml in water was used as a reference.

The *ab initio* shape reconstruction was performed using the program GASBOR<sup>15</sup>. The results from at least ten separate GASBOR runs were averaged to determine common structural features using the programs SUPCOMB<sup>16</sup> and DAMAVER<sup>17</sup>.

## **Results**

### ***Expression of ACMR and its two domains***

The full-length gene of ACMR cloned into expression plasmid pET-21a(+) was successfully expressed in *E. coli* BL21 host cells. The recombinant protein was obtained in a soluble form and purified using the C-terminal octa-histidine tag by Ni-NTA affinity chromatography. From 1 l of bacterial culture we obtained about 25 mg of purified protein. The purified protein exhibited the characteristic UV/Vis absorption spectrum of a flavin-dependent protein with peaks at 380 and 459 nm. To assess the identity of the flavin cofactors, recombinant ACMR was denatured and the released flavins were analysed by HPLC. As shown in Figure 1, two peaks with similar intensity and UV/Vis absorption properties were obtained with retention times corresponding to FAD and FMN, respectively.

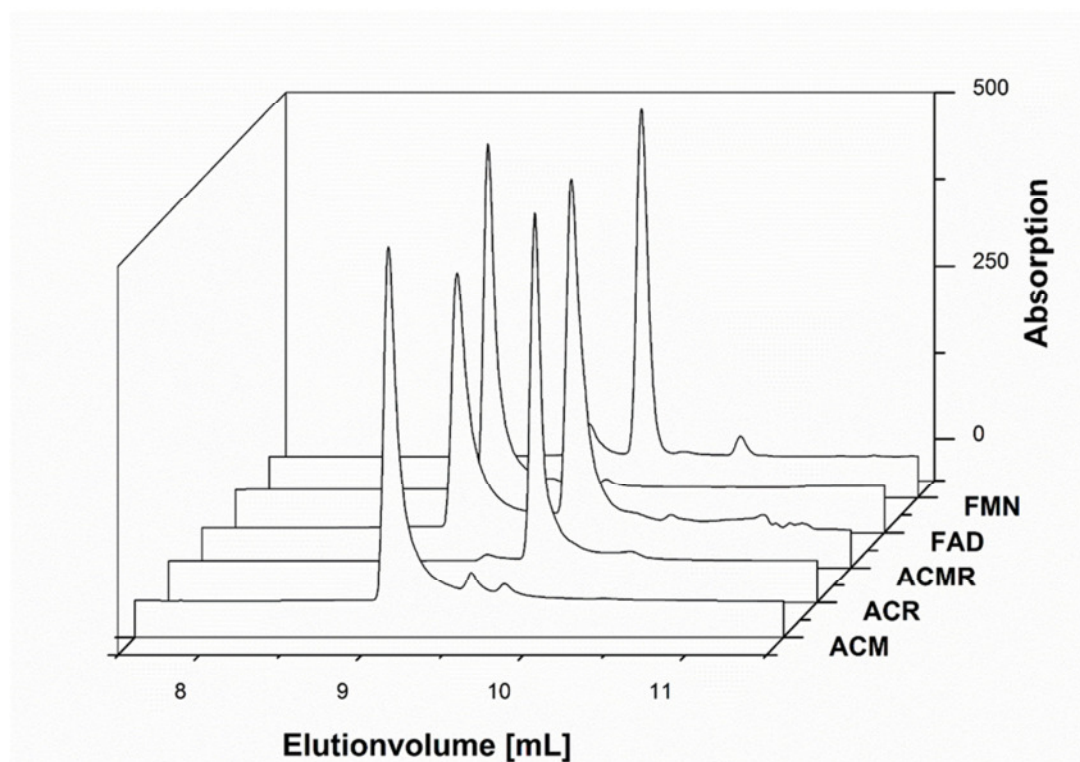
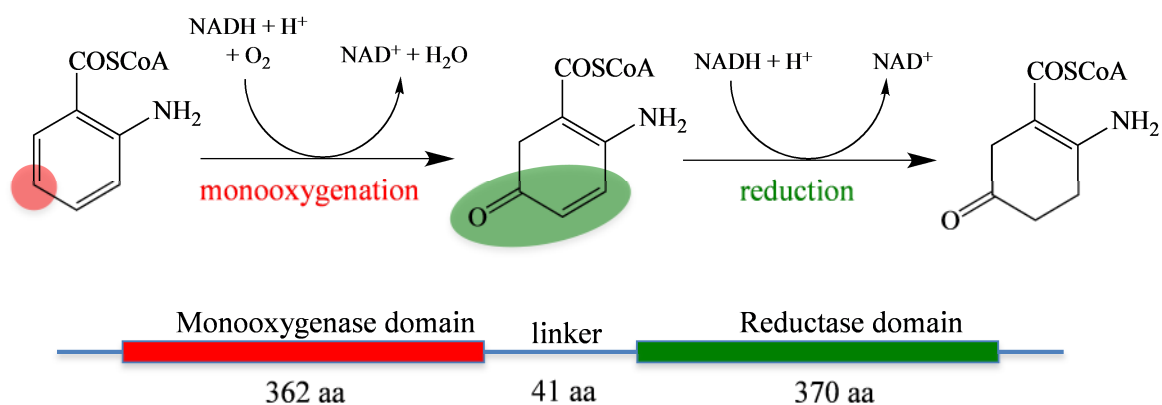


**Figure 1:** Isolation and analysis of flavin cofactors from ACMR and the separated subunits: HPLC-elution-profiles of isolated cofactors and references are shown, the presence of FMN and FAD in ACMR could be demonstrated. Furthermore it was possible to allocate FMN to the ACR and FAD to the ACM domain.

This was unexpected because earlier work proposed two FAD cofactors per protomer<sup>1, 18</sup>. Assuming 1:1 stoichiometry an average extinction coefficient of  $21,500 \text{ M}^{-1} \text{ cm}^{-1}$  was determined at the absorption maximum of 459 nm. To assign the FMN and FAD cofactor to the two proposed domains, we expressed the N-terminal part of ACMR comprising amino acids 1-364 (ACM) and the C-terminal part of ACMR comprising amino acids 406-773 (ACR) as individual proteins in *E. coli*. The monooxygenase domain was expressed as a stable and soluble yellow protein with absorption maxima at 374 and 450 nm. HPLC analysis of the flavin cofactor revealed the presence of FAD (Figure 1). The extinction coefficient at  $\lambda = 450 \text{ nm}$  was  $10,130 \text{ M}^{-1} \text{ cm}^{-1}$  (using  $\epsilon_{\text{FAD,free}} = 11,300 \text{ M}^{-1} \text{ cm}^{-1}$ ). On the other hand, the expression of the reductase domain (ACR) yielded an unstable and colourless protein. Efforts to stabilize the reductase domain by addition of FMN or the monooxygenase domain did not result in cofactor binding or improved stability. Furthermore, co-expression of the ACM and ACR domain was unsuccessful. Therefore we extended the N-terminus of the reductase domain to include 41 amino acids of the linker region (see Scheme 1).



**Scheme 1:** Subdomains of ACMR and catalysed reaction of the subunit

In this case the reductase domain led to the expression of an at least partially reconstituted protein. Isolation of the bound flavin and analysis by HPLC confirmed the presence of FMN (Figure 1). Precipitate formation made it impossible to determine the extinction coefficient of the reductase domain.

Assuming that the extinction coefficient determined for the FAD in the monooxygenase domain is not affected by the removal of the reductase domain, the extinction coefficient for FMN bound to ACM is  $11,370 \text{ M}^{-1} \text{ cm}^{-1}$  (using  $\epsilon_{\text{FMN,free}} = 12,500 \text{ M}^{-1} \text{ cm}^{-1}$ ). Hence both flavin chromophores experience a hypochromic effect upon binding to ACMR. Because recombinant ACR was unstable and lacked the flavin cofactor our biochemical characterisation focused on ACMR and the ACM domain.

### ***Binding studies with aminobenzoyl-CoA (AbCoA) and p-hydroxybenzaldehyde (pHB)***

In an earlier work, Langkau *et al.*<sup>1</sup> demonstrated tight binding of AbCoA ( $K_d \leq 1 \mu\text{M}$ ) to a “half-site” of ACMR isolated from *A. Evansii*. The dissociation constant for AbCoA to recombinant ACMR, was determined by two independent methods. First, we measured the perturbations of the UV/Vis absorption spectrum as a function of AbCoA concentration (Figure 2, left panel) and secondly, we determined the binding isotherm with a microcalorimetry (Figure 3, left panel). This yielded dissociation constants of  $8 \pm 1.5$  and  $5 \pm 2.0 \mu\text{M}$ , respectively.

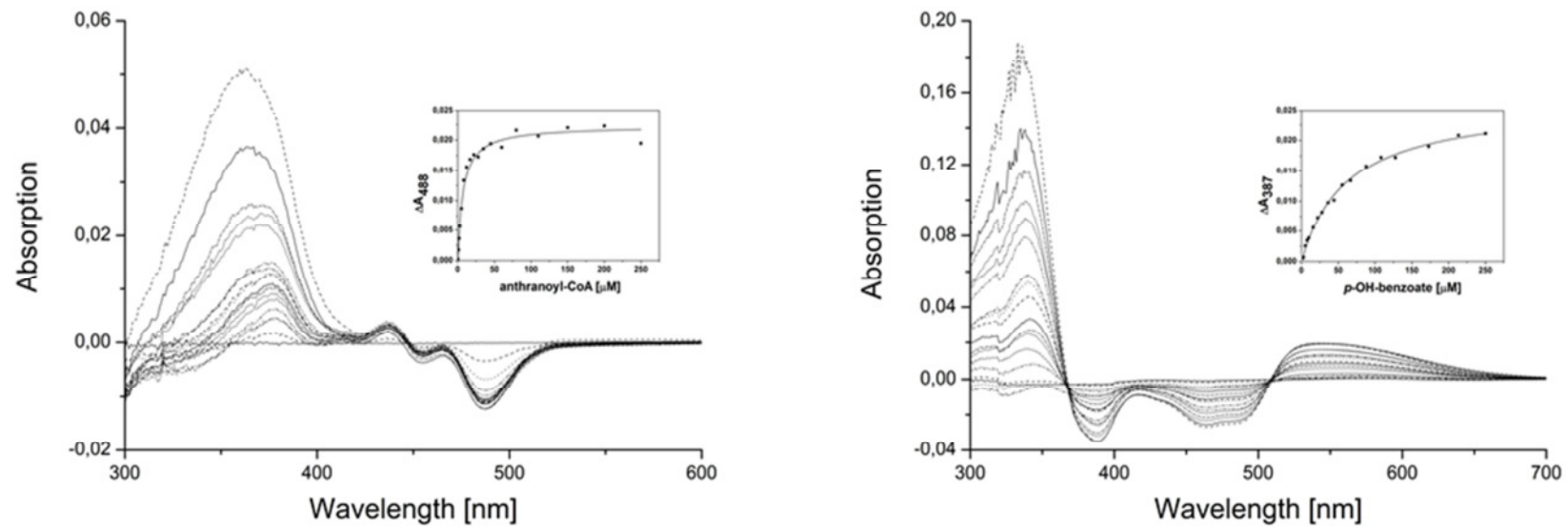


**Figure 2:** Titration of ACMR with AbCoA (left panel) and pHB (right panel) monitored by UV/Vis differential absorption spectroscopy:

Left panel: 25  $\mu\text{M}$  ACMR was titrated with a 1 mM AbCoA solution in tandem cuvettes at 25  $^{\circ}\text{C}$  and absorption spectra were recorded after each addition from 300 to 600 nm. The data points in the insert were fitted to a hyperbolic equation yielding a KD of 8  $\mu\text{M}$ .

Right panel: 20  $\mu\text{M}$  ACMR was titrated with a 1 mM solution of pHB at 25  $^{\circ}\text{C}$ , the absorption spectra was recorded from 300 to 600 nm. The fit shown in the insert was obtained from the data points and represents there hyperbolic fit. The observed KD is 57  $\mu\text{M}$ .

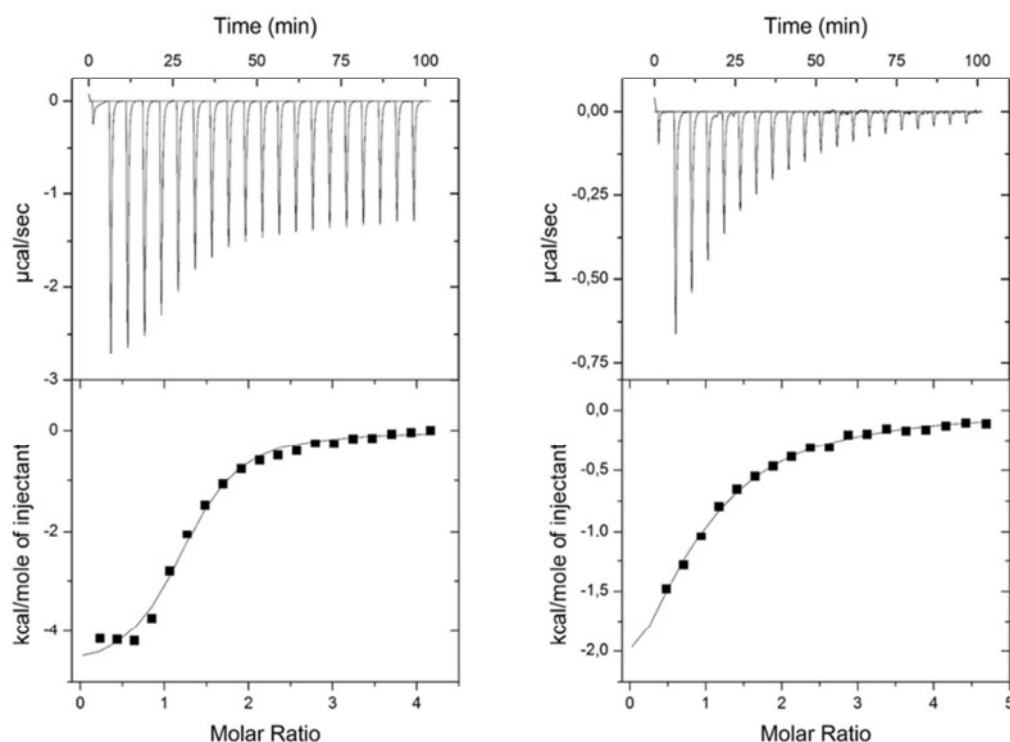


**Figure 3:** Determination of dissociation constants by isothermal titration calorimetry:

Left panel: 40  $\mu\text{M}$  ACMR was titrated with a 1 mM AbCoA solution. Protein and substrate was dissolved in 20 mM Tris-buffer, containing 100 mM NaCl pH 8

Right panel: 45  $\mu\text{M}$  ACMR was titrated with a 1 mM solution of pHB at 25  $^{\circ}\text{C}$

Because the reductase domain of ACMR exhibits high similarity to OYE (structures of the modelled domains are shown in Supplementary Figure S1) and the residues required for binding of *para*-substituted phenols appear to be conserved in ACMR, we employed a typical OYE model ligand, *p*-hydroxybenzaldehyde (pHB), as a probe for the active site of the reductase domain<sup>19</sup>. As shown in Figure 2 (right panel), pHB produces spectral perturbations typical for the charge-transfer interaction between the isoalloxazine ring of the bound FMN and the aromatic ring of the ligand. The observed absorption changes varied as a function of pHB concentration and were used to determine a dissociation constant of  $57 \pm 10 \mu\text{M}$ . Employing isothermal microcalorimetry as before the dissociation constant for pHB was determined to  $36 \pm 1.0 \mu\text{M}$  (Figure 3, right panel).

Next, we determined dissociation constants for AbCoA and pHB in the presence of a saturating concentration of pHB and AbCoA, respectively. As before, we employed UV/Vis

difference absorption spectroscopy and microcalorimetry. As shown in Table 1, this yielded dissociation constants similar to those observed in the absence of the other ligand, i.e. the presence of one ligand does not affect the binding of the other.

**Table 1:** Comparison of the binding constants, observed with difference titration and ITC: for saturation the samples were pre- incubated with about 100  $\mu$ M for AbCoA or 500  $\mu$ M for pHB, respectively. Afterwards the  $K_D$  was determined as already described in Experimental Procedures.

	AbCoA		pHB	
		Saturated with pHB		Saturated with AbCoA
<b>Difference titration</b>	8,0 $\pm$ 1,5	10,5 $\pm$ 2,0	57,5 $\pm$ 10,5	61,0 $\pm$ 7,0
<b>ITC</b>	5,0 $\pm$ 2,0	7,0 $\pm$ 1,0	36,0 $\pm$ 1,0	36,5 $\pm$ 2,0

This result clearly shows that AbCoA and pHB bind independently to different active sites of ACMR. Interestingly, titration experiments with AbCoA and the recombinant monooxygenase domain failed to demonstrate binding indicating that truncation of the linker region and the reductase domain abolished binding of the substrate.

### ***Kinetic parameters of ACMR***

The reduction of the two flavin cofactors present in the ACMR confirmed the reduction rate published by Langkau *et al.*<sup>1</sup>. This indicates that there is no difference between isolated and recombinantly expressed ACMR.

### ***Protein folding and thermal stability of ACMR***

Protein folding and thermal stability of ACMR were monitored by circular dichroism (CD) and ThermoFAD®<sup>20</sup>. At room temperature the CD spectrum shows a mixed  $\alpha/\beta$ -fold, as expected from the homology models (Supplementary Figure S1). The estimation of secondary structure content using CDSSTR indicates the presence of some unordered regions (up to 30%). When ACMR is dissolved in 2 mM Tris/HCl pH 8 or in MilliQ water, the unfolding starts around 40 °C and reaches its  $T_m$  at 48 °C. In PIPES buffer or in the presence of AbCoA the protein precipitates above 47 °C.

Protein stability in several buffers at different pH-values was monitored using the ThermoFAD method<sup>20</sup>. ACMR turned out to unfold at a pH lower than 5.5. Melting temperatures ( $T_m$ ) calculated from the curves measured at pH-values above 5.5 were comparable with the results obtained by CD measurements and showed that the melting temperature was not affected by the increasing pH. Furthermore, adding different compounds to the protein solution showed no significant influence on  $T_m$ . A slight increase of 2-3 °C was observed when AbCoA or the reductase inhibitor, pHB were added. The CD spectra were also not affected by the addition of these ligands, indicating no changes in the secondary structure content of ACMR.

### *Small-angle scattering studies of ACMR*

In order to investigate the structure of ACMR in solution, small angle X-ray scattering experiments (SAXS) were performed. The measured SAXS curves of ACMR solutions at three different concentrations (3.6, 7 and 14.8 mg/ml) are displayed in Figure 4A. For the measurement at the highest protein concentration, the superposition of the scaled scattering curves showed a decrease in intensity at very small q-values indicating interparticle repulsion (Figure 4A, inset). The estimated molecular mass (MM) of  $165 \pm 5$  kDa is compatible with ACMR forming a dimer in solution. The values of  $R_g$  ( $5.1 \pm 0.2$  nm) and  $D_{max}$  ( $17.6 \pm 0.8$  nm) also pointed at dimer formation. The  $p(r)$  function indicated the compact shape of the dimer with some unfolded regions (Figure 4B).

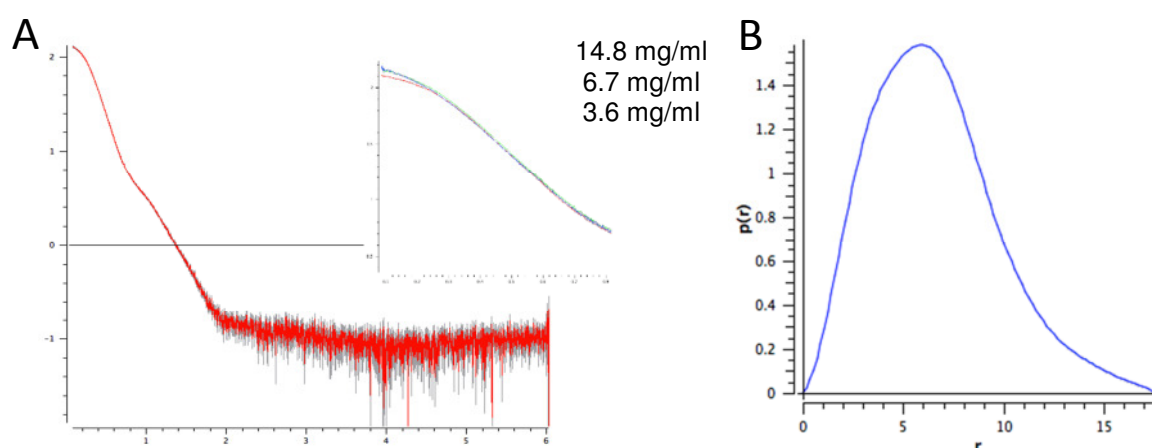


**Figure 4:** Structural features of the ACMR determined by small angle X-ray scattering experiments (SAXS).

Panel A: experimental X-ray scattering pattern of the ACMR, as inset the low angle scattering region at different protein concentrations is displayed.

Panel B: calculated distance distribution function  $p(r)$

## Discussion

Protein from recombinant expressed ACMR was obtained in a soluble form, showing an absorption spectra typical for flavin-dependent proteins. In contrast to previous publications<sup>1, 18</sup>, we could clearly demonstrate the presence of both FMN and FAD (see Figure 1). Furthermore it was possible to allocate the FMN molecule to the reductase subunit, while FAD is bound to the monooxygenase subdomain. This was not surprising, because ACM is a member of Group A flavin dependent monooxygenase. A typical structural feature of monooxygenases of this group is that the cofactor is bound in a Rossmann fold<sup>21</sup>, the most prominent FAD binding domain<sup>4</sup>. In contrast to this the reductase domain exhibits high similarity to OYE (Supplementary Figure S1). A common structural feature of all OYE is the presence of FMN as cofactor, which is bound in an  $\alpha/\beta$  barrel fold (TIM barrel)<sup>22</sup>.

Expression of the separated subdomains revealed decreased stability, furthermore the cofactor binding ability was affected. In the case of ACR the level of soluble protein and the cofactor content was low. The reduced FMN binding ability of ACR could not be overcome by adding the 42 amino acids of the linker or co-expression with ACM. This leads to the assumption that not just the linker region but also the protein in dimeric state is required for cofactor binding.

Binding studies demonstrated that both active sites could be occupied at the same time, either by the natural substrate AbCoA, which docks into the monooxygenase domain or pHB, a typical active site inhibitor for OYE. While AbCoA is bound tightly with a dissociation constant in the low  $\mu\text{M}$  range, pHB was bound more weakly (see Figure 2 and 3).

Nevertheless, the cofactor binding ability was lost completely when the subunits were separated. This finding supports the proposed reaction mechanism, where a chemical unstable intermediate was observed as product of the monooxygenase reaction<sup>3, 23, 24</sup>. For stabilization of such an intermediate the distance between the two active sites should be reduced to a minimum. This could be achieved by a single active sites, catalysing monooxygenation and subsequent reduction. In this case simultaneous binding of substrate and inhibitor might not be possible. An explanation which supports our finding is the presence of two independent binding pockets, however, there must be spatial interactions of both binding sites to explain the loss of co-factor and binding ability, when they are separated. Such interactions could be intramolecular or intermolecular, where the reductase subunit interacts with the monooxygenase subunit of the other protein chain from the dimer. To elucidate if intra- or

intermolecular interaction were responsible for our observations the crystal structure might be beneficial.

As indicated by the homology models (Supplementary Figure S1), a mixed  $\alpha/\beta$ -fold could be observed using CD measurements. The determination of the melting point revealed that the presence of AbCoA, pHB or both did not stabilise the enzyme significantly, the addition of these substances also did not result in any changes in the CD-spectra. ACMR gets unfolded at pH values lower than 5.5. If the pH was increased from this point no changes in the melting temperature could be observed.

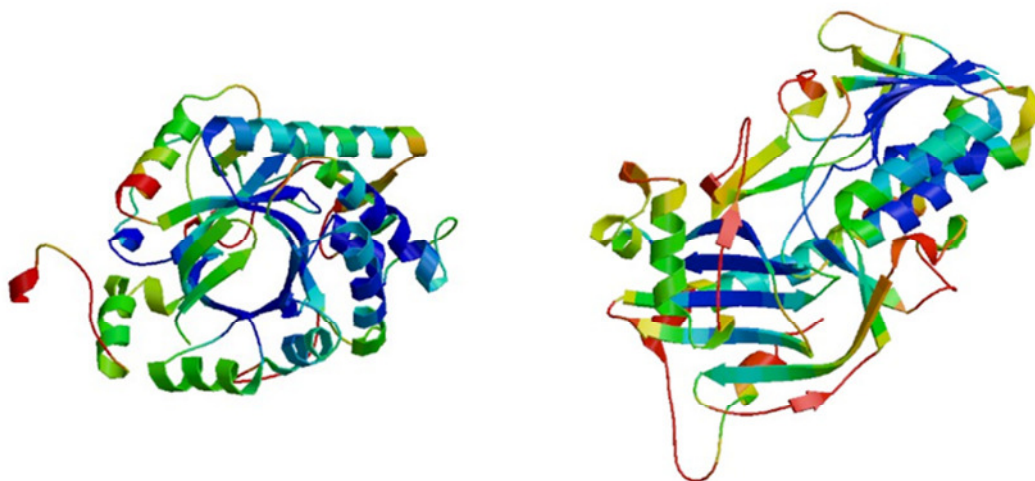
SAX measurements (Figure 4A) confirmed that ACMR exists as a dimer with a molecular mass of about 165 kDa. Furthermore the finding that ACMR has a compact shape with some unfolded regions was confirmed by the  $p(r)$ function.

## References

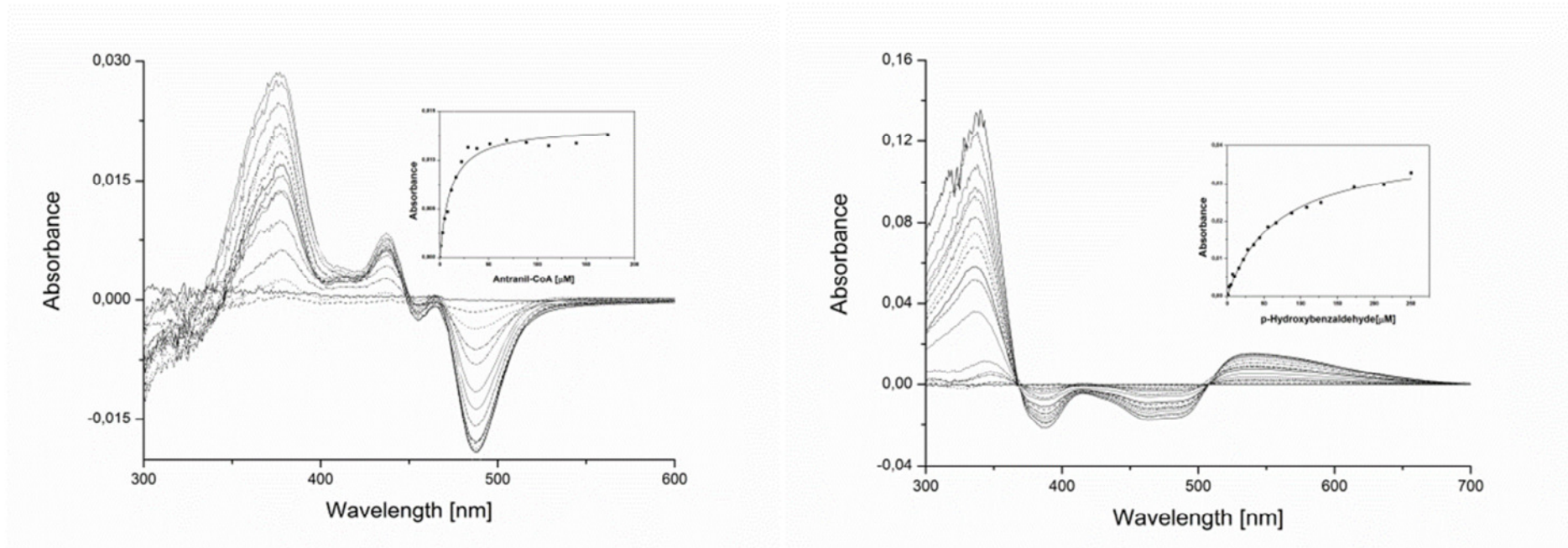
1. Langkau, B., Vock, P., Massey, V., Fuchs, G. & Ghisla, S. 2-Aminobenzoyl-CoA monooxygenase/reductase - Evidence for two distinct loci catalyzing substrate monooxygenation and hydrogenation. *European Journal of Biochemistry* **230**, 676-685 (1995).
2. Schühle, K., Jahn, M., Ghisla, S. & Fuchs, G. Two similar gene clusters coding for enzymes of a new type of aerobic 2-aminobenzoate (Anthranilate) metabolism in the bacterium *Azoarcus evansii*. *J. Bacteriol.* **183**, 5268-5278 (2001).
3. Hartmann, S. *et al.* NIH shift in flavin-dependent monooxygenation: Mechanistic studies with 2-aminobenzoyl-CoA monooxygenase/reductase. *Proc. Natl. Acad. Sci. U. S. A.* **96**, 7831-7836 (1999).
4. MacHeroux, P., Kappes, B. & Ealick, S. E. Flavogenomics - A genomic and structural view of flavin-dependent proteins. *FEBS Journal* **278**, 2625-2634 (2011).
5. Macheroux, P. UV-Visible Spectroscopy as a Tool to Study Flavoproteins. *Methods in Molecular Biology; Flavoprotein Protocols Volume 131*, 1-7 (1999).
6. Gill, S. C. & Von Hippel, P. H. Calculation of protein extinction coefficients from amino acid sequence data. *Anal. Biochem.* **182**, 319-326 (1989).
7. Kelley, L. A. & Sternberg, M. J. Protein structure prediction on the Web: a case study using the Phyre server. *Nature protocols* **4**, 363-371 (2009).
8. Arnold, K., Bordoli, L., Kopp, J. & Schwede, T. The SWISS-MODEL workspace: A web-based environment for protein structure homology modelling. *Bioinformatics* **22**, 195-201 (2006).
9. Whitmore, L. & Wallace, B. A. Protein secondary structure analyses from circular dichroism spectroscopy: Methods and reference databases. *Biopolymers* **89**, 392-400 (2008).

10. Jancarik, J., Pufan, R., Hong, C., Kim, S. -. & Kim, R. Optimum solubility (OS) screening: An efficient method to optimize buffer conditions for homogeneity and crystallization of proteins. *Acta Crystallographica Section D: Biological Crystallography* **60**, 1670-1673 (2004).
11. Boulin, C. J., Kempf, R., Gabriel, A. & Koch, M. H. J. Data acquisition systems for linear and area X-ray detectors using delay line readout. *Nuclear Instruments and Methods in Physics Research Section A: Accelerators, Spectrometers, Detectors and Associated Equipment* **269**, 312-320 (1988).
12. Konarev, P. V., Volkov, V. V., Sokolova, A. V., Koch, M. H. J. & Svergun, D. I. PRIMUS: A Windows PC-based system for small-angle scattering data analysis. *Journal of Applied Crystallography* **36**, 1277-1282 (2003).
13. Guinier, A. La diffraction des rayons X aux tres petits angles; application a l'etude de phenomenes ultramicroscopiques. *Annales de physique (Paris)* **12**, 161-237 (1939).
14. Svergun, D. I. Determination of the regularization parameter in indirect-transform methods using perceptual criteria. *Journal of Applied Crystallography* **25**, 495-503 (1992).
15. Svergun, D. I., Petoukhov, M. V. & Koch, M. H. J. Determination of domain structure of proteins from x-ray solution scattering. *Biophys. J.* **80**, 2946-2953 (2001).
16. Kozin, M. B. & Svergun, D. I. Automated matching of high- and low-resolution structural models. *Journal of Applied Crystallography* **34**, 33-41 (2001).
17. Volkov, V. V. & Svergun, D. I. Uniqueness of ab initio shape determination in small-angle scattering. *Journal of Applied Crystallography* **36**, 860-864 (2003).
18. Altenschmidt, U. & Fuchs, G. Novel aerobic 2-aminobenzoate metabolism. Purification and characterization of 2-aminobenzoate-CoA ligase, localisation of the gene on a 8-kbp plasmid, and cloning and sequencing of the gene from a denitrifying *Pseudomonas* sp. *European Journal of Biochemistry* **205**, 721-727 (1992).
19. Abramovitz, A. S. & Massey, V. Interaction of phenols with old yellow enzyme. Physical evidence for charge transfer complexes. *J. Biol. Chem.* **251**, 5327-5336 (1976).
20. Forneris, F., Orru, R., Bonivento, D., Chiarelli, L. R. & Mattevi, A. ThermoFAD, a ThermoFluor®-adapted flavin ad hoc detection system for protein folding and ligand binding. *FEBS Journal* **276**, 2833-2840 (2009).
21. Huijbers, M. M. E., Montersino, S., Westphal, A. H., Tischler, D. & Van Berkel, W. J. H. Flavin dependent monooxygenases. *Arch. Biochem. Biophys.* **544**, 2-17 (2014).
22. Fox, K. M. & Karplus, P. A. Old yellow enzyme at 2 Å resolution: Overall structure, ligand binding, and comparison with related flavoproteins. *Structure* **2**, 1089-1105 (1994).
23. Torres, R. A. & Bruice, T. C. Theoretical investigation of the [1,2]-sigmatropic hydrogen migration in the mechanism of oxidation of 2-aminobenzoyl-CoA by 2-aminobenzoyl-CoA monooxygenase/reductase. *Proc. Natl. Acad. Sci. U. S. A.* **96**, 14748-14752 (1999).
24. Langkau, B., Ghisla, S., Buder, R., Ziegler, K. & Fuchs, G. 2-Aminobenzoyl-CoA monooxygenase/reductase, a novel type of flavoenzyme. Identification of the reaction products. *European Journal of Biochemistry* **191**, 365-371 (1990).

## Supplementary Figures



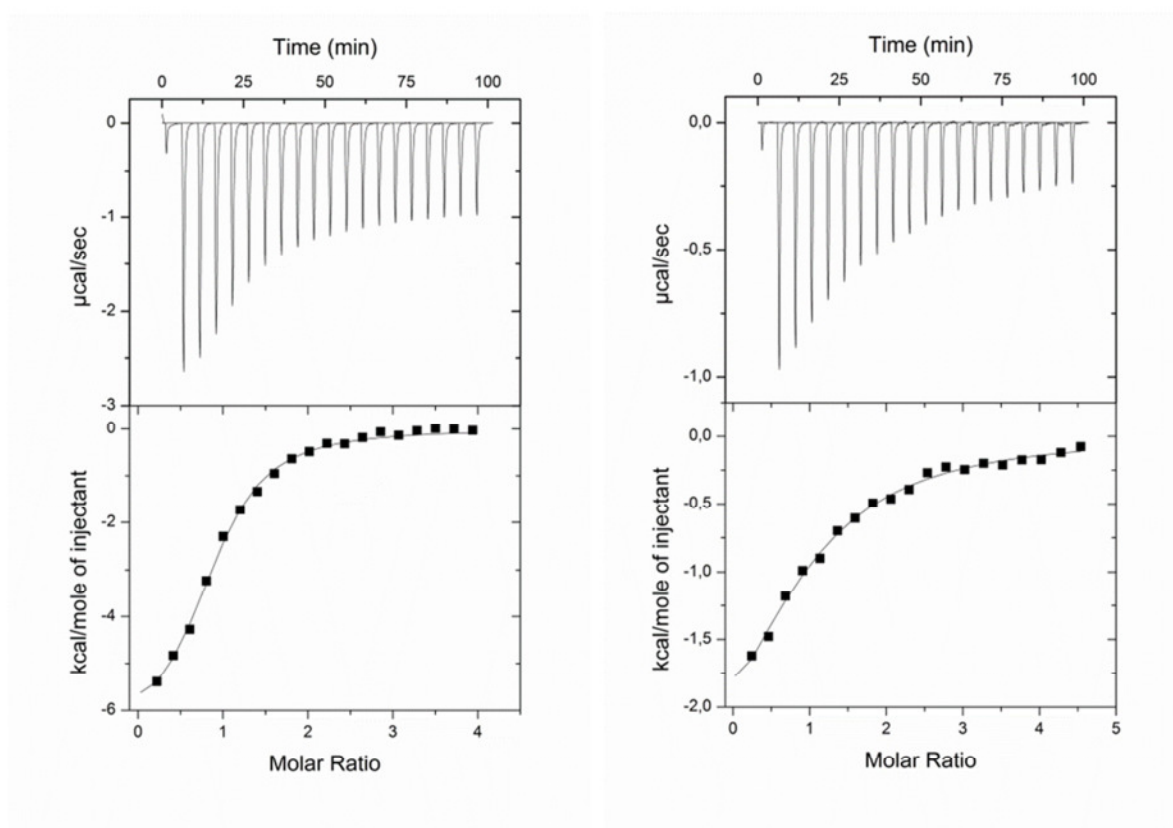
**Supplementary Figure 1:** Homology models performed using Swiss model. Both domains were modelled separately. The models for the reductase domain (left structure) and the monooxygenase domain (right structure) of ACMR were coloured by residue error (SwissModel): blue – more reliable regions, red – potentially unreliable regions. The structures of the OYE from *Thermus scotoductus* (PDB-entry: 3HGJ) and of VioD hydroxylase from *Chromobacterium violaceum* (PDB-entry: 3C4A) were used as templates.



**Supplementary Figure 2:** Titration of ACMR with AbCoA (left panel) and pHB (right panel) in the presence of the other substrate monitored by UV/Vis differential absorption spectroscopy:

Left panel: 15  $\mu\text{M}$  ACMR was saturated with pHB and titrated with a 1 mM AbCoA solution. The final pHB concentration in the sample was 500  $\mu\text{M}$ , absorption spectra were recorded after each addition from 300 to 600 nm. The fit shown in the insert was obtained from the data points and represents their hyperbolic fit, the observed  $K_D$  is 10  $\mu\text{M}$ .

Right Panel: 15  $\mu\text{M}$  ACMR was saturated with pHB and titrated with a 1 mM pHB solution. The final AbCoA concentration in the sample was 100  $\mu\text{M}$ , absorption spectra were recorded after each addition from 300 to 600 nm. The data points in the insert were fitted to a hyperbolic equation yielding a  $K_d$  of 61  $\mu\text{M}$ .



**Supplementary Figure 3:** Determination of dissociation constants when both substrates are present, using thermal titration calorimetry:

Left panel:  $44 \mu\text{M}$  ACMR saturated with pHB (final concentration of  $500 \mu\text{M}$ ) was titrated with a  $1 \text{ mM}$  AbCoA solution.

Right panel:  $49 \mu\text{M}$  ACMR saturated with AbCoA (final concentration of  $120 \mu\text{M}$ ) was titrated with a  $1 \text{ mM}$  solution of pHB.

## Supplementary Tables

**Supplementary Table 1:** Primers used for the application of the separated subunits, with and without linker.

Name	Sequence
ACR without linker fw	CCCCTCCGCCTCATATGTTTACCCCGTTTAAACTGC
ACR without linker rv	CGCAGTTTAAACGGGGTAAACATATGAGGCGGAGGGG
ACM without linker fw	GCATGCTGACCCGTCTCGAGCGTATTAGCCATGAAAATCTGC
ACM without linker rv	GCAGATTTTCATGGCTAATACGCTCGAGACGGGTCAGCATGC
ACM-Linker-fw	GGAATAACATATGCGCATTGTTTGTATTGGTGGTGGTCCGGC
ACM-Linker-rv	CCGCTCGAGCGGAGGCGGAGGGGTTTCATCATCACG
ACR-Linker-fw	GGAATAACATATGAGCCAGCGTATTAGCCATGAAAATCTGCG
ACR-Linker-rv	CCGCTCGAGTTACGGCCGTTAATGATGGTGGTGGTGGTCCGGC

# Curriculum vitae



## Contact Information and Personal Information

Name	Thomas Bergner
Address	Kärntnerlandstrasse 22/36 9360 Friesach
Mobil	0680/4004815
Email	<a href="mailto:thomasbergner.1983@gmail.com">thomasbergner.1983@gmail.com</a>
Date and place of birth	7 <sup>th</sup> August 1983 Klagenfurt, Austria
Citizenship	Austrian

## Education

1990 – 1994	Elementary School in Klagenfurt, Austria
1994 – 2002	Grammar School in St. Veit an der Glan, Austria
09/2002 – 04/2003	Basic military service
2003 – 2007	Studies of Technical Chemistry (F800) at Graz University of Technology
10/2007	First selection of the diploma completed
2007 – 2010	Studies of Biochemistry, Biotechnology and Food Chemistry (F809) at Graz University of Technology
02/2009 – 05/2010	Diploma thesis project at the Institute of Molecular Biotechnology / Applied Biocatalysis, TU Graz (Supervisor: Ao.Univ.-Prof. Anton Glieder)
17.05.2010	Defence of diploma thesis, diploma completed

---

---

10/2010 – 06/2014 PhD project at the Institute of Biochemistry, TU Graz  
(Supervisor: Univ.-Prof. Peter Macheroux)

### Research Activities

07/2008 Project at the Institute of Biochemistry, TU Graz, with Univ.-Prof. Peter Macheroux: “*Expression, purification and characterization of NikM*”

01/2010 Project at the the Institute of Molecular Biotechnology / Applied Biocatalysis, TU Graz, with Ao.Univ.-Prof. Anton Glieder: “*Activity enhancement of an `ene` reductase*”

02/2009 – 05/2010 Diploma thesis project entitled “*Enhancement of organic solvent stability of an `ene` reductase*” at the Institute of Molecular Biotechnology / Applied Biocatalysis, TU Graz

(Supervisor: Ao.Univ.-Prof. Anton Glieder)

10/2010 – 06/2014 Work on the PhD project entitled “*Characterisation of two flavin dependent monooxygenases*” at the Institute of Biochemistry, TU Graz

(Supervisor: Univ.-Prof. Peter Macheroux)

### Other Qualifications

Language Skills German as mother tongue

fluent in English, basics in Italian

Computer Skills Microsoft Office, skills in Bioinformatics (databases, sequence alignments, Pymol, etc.), Origin